Earth-Science Reviews 185 (2018) 806–846

Contents lists available at ScienceDirect

Earth-Science Reviews

journal homepage: www.elsevier.com/locate/earscirev

Glacial geomorphological mapping: A review of approaches and frameworks for best practice

Benjamin M.P. Chandler[a,*], Harold Lovell[b], Clare M. Boston[b], Sven Lukas[c], Iestyn D. Barr[d], Ívar Örn Benediktsson[e], Douglas I. Benn[f], Chris D. Clark[g], Christopher M. Darvill[h], David J.A. Evans[i], Marek W. Ewertowski[j], David Loibl[k], Martin Margold[l], Jan-Christoph Otto[m], David H. Roberts[i], Chris R. Stokes[i], Robert D. Storrar[n], Arjen P. Stroeven[o,p]

[a] School of Geography, Queen Mary University of London, Mile End Road, London E1 4NS, UK
[b] Department of Geography, University of Portsmouth, Portsmouth, UK
[c] Department of Geology, Lund University, Lund, Sweden
[d] School of Science and the Environment, Manchester Metropolitan University, Manchester, UK
[e] Institute of Earth Sciences, University of Iceland, Reykjavík, Iceland
[f] Department of Geography and Sustainable Development, University of St Andrews, St Andrews, UK
[g] Department of Geography, University of Sheffield, Sheffield, UK
[h] Geography, School of Environment, Education and Development, University of Manchester, Manchester, UK
[i] Department of Geography, Durham University, Durham, UK
[j] Faculty of Geographical and Geological Sciences, Adam Mickiewicz University, Poznań, Poland
[k] Department of Geography, Humboldt University of Berlin, Berlin, Germany
[l] Department of Physical Geography and Geoecology, Charles University, Prague, Czech Republic
[m] Department of Geography and Geology, University of Salzburg, Salzburg, Austria
[n] Department of the Natural and Built Environment, Sheffield Hallam University, Sheffield, UK
[o] Geomorphology & Glaciology, Department of Physical Geography, Stockholm University, Stockholm, Sweden
[p] Bolin Centre for Climate Research, Stockholm University, Stockholm, Sweden

ARTICLE INFO

Keywords:
Glacial geomorphology
Geomorphological mapping
GIS
Remote sensing
Field mapping

ABSTRACT

Geomorphological mapping is a well-established method for examining earth surface processes and landscape evolution in a range of environmental contexts. In glacial research, it provides crucial data for a wide range of process-oriented studies and palaeoglaciological reconstructions; in the latter case providing an essential geomorphological framework for establishing glacial chronologies. In recent decades, there have been significant developments in remote sensing and Geographical Information Systems (GIS), with a plethora of high-quality remotely-sensed datasets now (often freely) available. Most recently, the emergence of unmanned aerial vehicle (UAV) technology has allowed sub-decimetre scale aerial images and Digital Elevation Models (DEMs) to be obtained. Traditional field mapping methods still have an important role in glacial geomorphology, particularly in cirque glacier, valley glacier and icefield/ice-cap outlet settings. Field mapping is also used in ice sheet settings, but often takes the form of necessarily highly-selective ground-truthing of remote mapping. Given the increasing abundance of datasets and methods available for mapping, effective approaches are necessary to enable assimilation of data and ensure robustness. This paper provides a review and assessment of the various glacial geomorphological methods and datasets currently available, with a focus on their applicability in particular glacial settings. We distinguish two overarching 'work streams' that recognise the different approaches typically used in mapping landforms produced by ice masses of different sizes: (i) mapping of ice sheet geomorphological imprints using a combined remote sensing approach, with some field checking (where feasible); and (ii) mapping of alpine and plateau-style ice mass (cirque glacier, valley glacier, icefield and ice-cap) geomorphological imprints using remote sensing and considerable field mapping. Key challenges to accurate and robust geomorphological mapping are highlighted, often necessitating compromises and pragmatic solutions. The importance of combining multiple datasets and/or mapping approaches is emphasised, akin to multi-proxy approaches used in many Earth Science disciplines. Based on our review, we provide idealised frameworks and general recommendations to ensure best practice in future studies and aid in accuracy assessment, comparison, and integration of geomorphological data. These will be of particular value where geomorphological data are

* Corresponding author.
E-mail address: b.m.p.chandler@qmul.ac.uk (B.M.P. Chandler).

https://doi.org/10.1016/j.earscirev.2018.07.015
Received 18 November 2017; Received in revised form 3 July 2018; Accepted 30 July 2018
Available online 01 August 2018
0012-8252/

incorporated in large compilations and subsequently used for palaeoglaciological reconstructions. Finally, we stress that robust interpretations of glacial landforms and landscapes invariably requires additional chronological and/or sedimentological evidence, and that such data should ideally be collected as part of a holistic assessment of the overall glacier system.

1. Introduction

1.1. Background and importance

Mapping the spatial distribution of landforms and features through remote sensing and/or field-based approaches is a well-established method in Earth Sciences to examine earth surface processes and landscape evolution (e.g. Kronberg, 1984; Hubbard and Glasser, 2005; Smith et al., 2011). Moreover, geomorphological mapping is utilised in numerous applied settings, such as natural hazard assessment, environmental planning, and civil engineering (e.g. Kienholz, 1977; Finke, 1980; Paron and Claessens, 2011; Marc and Hovius, 2015; Griffiths and Martin, 2017).

Two overarching traditions exist in geomorphological mapping: Firstly, the classical approach involves mapping all geomorphological features in multiple thematic layers (e.g. landforms, breaks of slope, slope angles, and drainage), regardless of the range of different processes responsible for forming the landscape. This approach to geomorphological mapping has been particularly widely used in mainland Europe and has resulted in the creation of national legends to record holistic geomorphological data that may be comparable across much larger areas or between studies (Demek, 1972; van Dorsser and Salomé, 1973; Leser and Stäblein, 1975; Klimaszewski, 1990; Schoeneich, 1993; Kneisel et al., 1998; Gustavsson et al., 2006; Rączkowska and Zwoliński, 2015). The second approach involves more detailed, thematic geomorphological mapping commensurate with particular research questions; for example, the map may have an emphasis on mass movements or glacial and periglacial landforms and processes. Such a reductionist approach is helpful in ensuring a map is not 'cluttered' with less relevant data that may in turn make a multi-layered map unreadable (e.g. Kuhle, 1990; Robinson et al., 1995; Kraak and Oremling, 2010). In recent years, the second approach has become much more widespread due to increasing specialisation and thus forms the basis for this review, which focuses on geomorphological mapping in glacial environments.

In glacial research, the production and analysis of geomorphological maps provide a wider context and basis for various process-oriented and palaeoglaciological studies, including:

(1) analysing glacial sediments and producing process-form models (e.g. Price, 1970; Benn, 1994; Lukas, 2005; Benediktsson et al., 2016);
(2) quantitatively capturing the pattern and characteristics ('metrics') of landforms to understand their formation and evolution (e.g. Spagnolo et al., 2014; Ojala et al., 2015; Ely et al., 2016a; Principato et al., 2016; Hillier et al., 2018);
(3) devising glacial landsystem models that can be used to elucidate former glaciation styles or inform engineering geology (e.g. Eyles, 1983; Evans et al., 1999; Evans, 2017; Bickerdike et al., 2018);
(4) reconstructing the extent and dimensions of former or formerly more extensive ice masses (e.g. Dyke and Prest, 1987a; Kleman et al., 1997; Houmark-Nielsen and Kjær, 2003; Benn and Ballantyne, 2005; Glasser et al., 2008; Clark et al., 2012);
(5) elucidating glacier and ice sheet dynamics, including advance/retreat cycles, flow patterns/velocities and thermal regime (e.g. Kjær et al., 2003; Kleman et al., 2008, 2010; Evans, 2011; Boston, 2012a; Hughes et al., 2014; Darvill et al., 2017);
(6) identifying sampling locations for targeted numerical dating programmes and ensuring robust chronological frameworks (e.g. Owen et al., 2005; Barrell et al., 2011, 2013; Garcia et al., 2012; Akçar et al., 2014; Kelley et al., 2014; Stroeven et al., 2014; Gribenski et al., 2016; Blomdin et al., 2018);
(7) calculating palaeoclimatic variables for glaciated regions, namely palaeotemperature and palaeoprecipitation (e.g. Kerschner et al., 2000; Bakke et al., 2005; Stansell et al., 2007; Mills et al., 2012; Boston et al., 2015); and
(8) providing parameters to constrain and test numerical simulations of ice masses (e.g. Kleman et al., 2002; Napieralski et al., 2007a; Golledge et al., 2008; Stokes and Tarasov, 2010; Livingstone et al., 2015; Seguinot et al., 2016; Patton et al., 2017a).

Thus, accurate representation of glacial and associated landforms is crucial to producing geomorphological maps of subsequent value in a wide range of glacial research. This is exemplified in glacial geochronological investigations, where a targeted radiometric dating programme first requires a clear geomorphological (and/or stratigraphic) framework and understanding of the relationships and likely relative ages of different sediment-landform assemblages. In studies that ignore this fundamental principle, it can be challenging to reconcile any scattered or anomalous numerical ages with a realistic geomorphological interpretation, as the samples have been obtained without a clear genetic understanding of the landforms being sampled (see Boston et al. (2015) and Winkler (2018) for further discussion).

The analysis of geomorphological evidence has been employed in the study of glaciers and ice sheets for over 150 years, with the techniques used in geomorphological mapping undergoing a number of significant developments in that time. The earliest geomorphological investigations involved intensive field surveys (e.g. Close, 1867; Penck and Brückner, 1901/1909; De Geer, 1910; Trotter, 1929; Caldenius, 1932; Raistrick, 1933), before greater efficiency was achieved through the development of aerial photograph interpretation from the late 1950s onwards (e.g. Lueder, 1959; Price, 1963; Welch, 1967; Howarth, 1968; Prest et al., 1968; Sugden, 1970; Sissons, 1977a; Prest, 1983; Kronberg, 1984; Mollard and Janes, 1984). Satellite imagery and digital elevation models (DEMs) have been in widespread usage since their development in the late 20th Century and have, in particular, helped revolutionise our understanding of palaeo-ice sheets (e.g. Barents-Kara Ice Sheet: Winsborrow et al., 2010; British Ice Sheet: Hughes et al., 2014; Cordilleran Ice Sheet: Kleman et al., 2010; Fennoscandian Ice Sheet: Stroeven et al., 2016; Laurentide Ice Sheet: Margold et al., 2018; Patagonian Ice Sheet: Glasser et al., 2008). In recent times, increasingly higher-resolution DEMs have become available due to the adoption of Light Detection and Ranging (LiDAR) technology (e.g. Salcher et al., 2010; Jónsson et al., 2014; Miller et al., 2014; Dowling et al., 2015; Hardt et al., 2015; Putniņš and Henriksen, 2017) and Unmanned Aerial Vehicles (UAVs) (e.g. Chandler et al., 2016a; Evans et al., 2016a; Ewertowski et al., 2016; Tonkin et al., 2016; Ely et al., 2017). Aside from improvements to remote sensing technologies, the last decade has seen a revolution in data accessibility, with the proliferation of freely available imagery (e.g. Landsat data), freeware mapping platforms (e.g. *Google Earth*) and open-source Geographical Information System (GIS) packages (e.g. *QGIS*). As a result, tools for glacial geomorphological mapping are becoming increasingly accessible, both practically and financially.

Field mapping remains a key component of the geomorphological mapping process, principally in the context of manageable study areas relating to alpine- and plateau-style ice masses, i.e. cirque glaciers, valley glaciers, icefields and ice-caps (e.g. Bendle and Glasser, 2012;

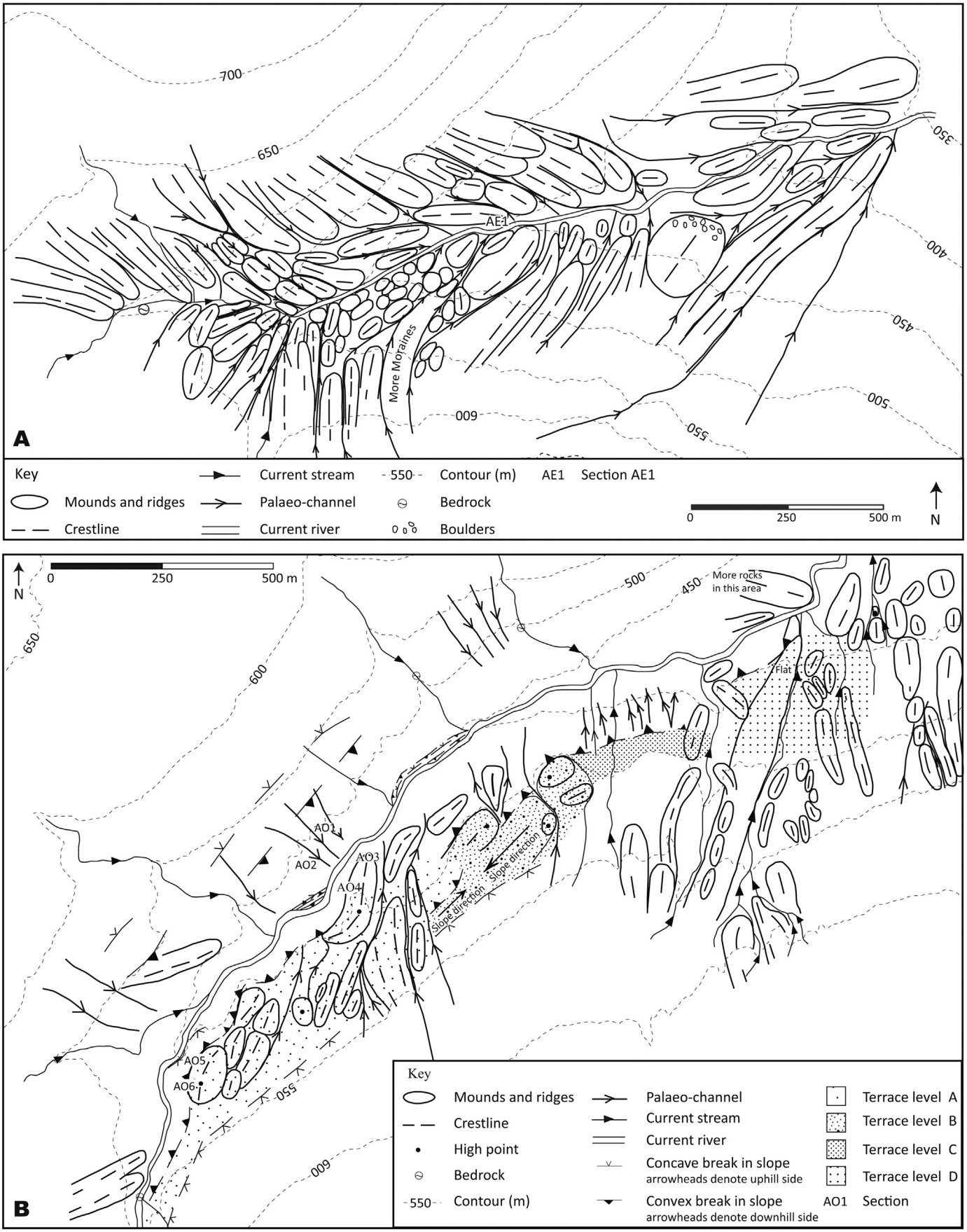

Fig. 1. Vectorised versions of two geomorphological maps drawn in the field for (A) Coire Easgainn and (B) Glen Odhar in the Monadhliath, Central Scottish Highlands. These field maps were used in the production of a 1: 57,500 geomorphological map for the entire region (Boston, 2012a, b).

Boston, 2012a, b; Jónsson et al., 2014; Gribenski et al., 2016; Lardeux et al., 2015; Brook and Kirkbride, 2018; Małecki et al., 2018). This approach is also employed in ice sheet settings, but typically in the form of selective ground checking of mapping from remotely-sensed data or focused mapping of regional sectors (e.g. Stokes et al., 2013; Bendle et al., 2017a; Pearce et al., 2018). Frequently, field mapping is conducted in tandem with sedimentological investigations (see Evans and Benn, 2004, for methods), providing a means of testing preliminary interpretations and identifying problems for specific (and more detailed) studies. This integrated approach is particularly powerful and enables robust interpretations of genetic processes, glaciation styles and/or glacier dynamics (e.g. Benn and Lukas, 2006; Evans, 2010; Benediktsson et al., 2010, 2016; Gribenski et al., 2016). In this context, it is worth highlighting the frequent use of the term 'sediment-landform assemblage' (or 'landform-sediment assemblage') as opposed to 'landform' in glacial geomorphology, underlining the importance of studying both surface form and internal composition (e.g. Evans, 2003a, 2017; Benn and Evans, 2010; Lukas et al., 2017).

Geomorphological mapping using a combination of field mapping and remotely-sensed data interpretation (hereafter 'remote mapping'), or a number of remote sensing methods, permits a holistic approach to mapping, wherein the advantages of each method/dataset can be combined to produce an accurate map with robust genetic interpretations (e.g. Boston, 2012a, b; Darvill et al., 2014; Storrar and Livingstone, 2017). As such, approaches are required that allow the accurate transfer and assimilation of data from these various sources, particularly where data are transferred from analogue (e.g. hard-copy aerial photographs) to digital format. Apart from a few recent exceptions for specific locations (e.g. the Scottish Highlands: Boston, 2012a, b; Pearce et al., 2014), there has been limited explicit discussion of the approaches used to integrate geomorphological data in map production (i.e. the relative contributions of different methods and/or datasets and their associated uncertainties), with many contributions simply stating that the maps were produced through fieldwork and/or remote sensing (e.g. Ballantyne, 1989; Lukas, 2007a; Evans et al., 2009a; McDougall, 2013). Given the diversity of scales, data sources and research questions inherent in glacial geomorphological research, and the increasing abundance of high-quality remotely-sensed datasets, finding the most cost- and time-effective approach is difficult, especially for researchers new to the field.

1.2. Aims and scope

In this contribution, we review the wide range of approaches and datasets available to practitioners and students for geomorphological mapping in glacial environments. The main aims of this review are to (i) synthesise scale-appropriate mapping approaches that are relevant to particular glacial settings, (ii) devise frameworks that will help ensure best practice when mapping, and (iii) encourage clear communication of details on mapping methods used in glacial geomorphological studies. This will ensure transparency and aid data transferability against a background of growing demand to collate geomorphological (and chronological) data in regional compilations (e.g. the BRITICE project: Clark et al., 2004, 2018a; the DATED-1 database: Hughes et al., 2016). A further aim of this contribution is to emphasise the continued and future importance of field mapping in geomorphological research, despite the advent of very high-resolution remotely-sensed datasets in recent years.

The following two sections of this review focus on field mapping (Section 2) and remote mapping (Section 3), respectively. We consider these methods in a broadly chronological order to provide historical context and illustrate the evolution of geomorphological mapping in glacial environments. Section 4 discusses the errors associated with each mapping method, an important issue that often receives limited attention within geomorphological mapping studies. Within this discussion, we highlight approaches that can help manage and minimise residual errors. Subsequently, we review the mapping methods used in particular glacial environments (Section 5) and synthesise frameworks to help ensure best practice when mapping (Section 6).

For the purposes of this review, we distinguish two overarching 'work streams': (i) mapping of palaeo-ice sheet geomorphological imprints using a combined remote sensing approach, with some field checking (where feasible); and (ii) mapping of alpine- and plateau-style ice mass geomorphological imprints using a combination of remote sensing and considerable field mapping/checking. The second workstream incorporates a spatial continuum of glacier morphologies, namely cirque glaciers, valley glaciers, icefields and ice-caps (cf. Sugden and John, 1976; Benn and Evans, 2010). The rationale for this subdivision is fourfold: Firstly, the approaches are governed by the size of the (former) glacial systems and thus feasibility of using particular mapping methods in certain settings (cf. Clark, 1997; Storrar et al., 2013). Secondly, there is a greater overlap of spatial and temporal scales (i.e. more detailed records are preserved) in areas glaciated by smaller ice masses that respond more rapidly to climate change (cf. Lukas, 2005, 2012; Bradwell et al., 2013; Boston et al., 2015; Chandler et al., 2016b). Thirdly, the different mapping methodologies reflect the difficulties in identifying vertical limits, thickness distribution and surface topography of palaeo-ice sheets (i.e. emphasis often on mapping bed imprints) (cf. Stokes et al., 2015). Lastly, the overarching methods employed to map glacial landforms in alpine and plateau settings do not differ fundamentally with ice mass morphology, i.e. most studies in these environments employ a combination of field mapping and remote sensing. In Section 5.3, we also specifically consider geomorphological mapping in modern glacial environments to highlight important issues relating to the temporal resolution of remotely-sensed data and landform preservation potential. We emphasise the importance of utilising multiple datasets and/or mapping approaches in an iterative process in all glacial settings (multiple remotely-sensed datasets in the case of ice-sheet-scale geomorphology) to increase accuracy and robustness, akin to multi-proxy methodologies used in many Earth Science disciplines.

2. Field mapping methods

2.1. Background and applicability of field mapping

Traditionally, glacial geomorphological mapping has been undertaken through extensive field surveys, an approach that dates back to the late 19th Century and early 20th Century (e.g. Close, 1867; Goodchild, 1875; Partsch, 1894; Sollas, 1896; Penck and Brückner, 1901/1909; Kendall, 1902; Wright, 1912; Hollingworth, 1931; Caldenius, 1932). Field mapping involves traversing the study area and recording pertinent landforms onto (enlarged) topographic base maps (Fig. 1). Typically, field mapping is conducted at cartographic scales of ~1: 10,000 (e.g. Leser and Stäblein, 1975; Rupke and De Jong, 1983; Thorp, 1986; Ballantyne, 1989; Evans, 1990; Benn et al., 1992; Mitchell and Riley, 2006; Rose and Smith, 2008; Boston, 2012a, b) or 1: 25,000 (e.g. Leser, 1983; Ballantyne, 2002, 2007a, b; Benn and Ballantyne, 2005; Lukas and Lukas, 2006). Occasionally, it is conducted at even larger scales, such as 1: 1,000 to 1: 5,000, but this is most appropriate for small areas or project-specific purposes (e.g. Kienholz, 1977; Leser, 1983; Lukas et al., 2005; Coray, 2007; Graf, 2007; Reinardy et al., 2013).

With improvements in technology, the widespread availability of remotely-sensed datasets, and a concomitant ease of access to high-quality printing facilities, alternative approaches to the traditional, *purely* field mapping method have also been employed, including (i) documenting sediment-landform assemblages during extensive field campaigns both prior to and after commencing remote mapping (e.g. Dyke et al., 1992; Krüger, 1994; Lukas and Lukas, 2006; Kjær et al., 2008; Boston, 2012a, b; Jónsson et al., 2014; Schomacker et al., 2014; Everest et al., 2017), (ii) mapping directly onto or annotating print-outs of imagery (e.g. aerial photographs) in the field (e.g. Lovell, 2014), (iii)

recording the locations of individual landforms using a (handheld) Global Navigation Satellite System (GNSS) device (e.g. Bradwell et al., 2013; Brynjólfsson et al., 2014; Lovell, 2014; Małecki et al., 2018), or (iv) digitally mapping landforms in the field using a ruggedised tablet PC with built-in GNSS and GIS software (e.g. Finlayson et al., 2011; Pearce et al., 2014). These approaches to field mapping are particularly useful where large-scale topographic maps are unavailable or out of date.

Detailed field mapping is typically restricted to alpine- and plateau-style ice masses due to logistical and financial constraints (Clark, 1997; Storrar et al., 2013). When conducted at the ice sheet scale, field mapping is (or historically was) undertaken either as part of long-term campaigns by national geological surveys in conjunction with surficial geology mapping programmes (e.g. Barrow et al., 1913; Flint et al., 1959; Krygowski, 1963; Campbell, 1967a, b; Hodgson et al., 1984; Klassen, 1993; Priamonosov et al., 2000; Follestad and Bergstrøm, 2004) or necessarily highly-selective ground-truthing of remote mapping (e.g. Kleman et al., 1997, 2010; Golledge and Stoker, 2006; Stokes et al., 2013; Darvill et al., 2014; Stroeven et al., 2016; Pearce et al., 2018).

2.2. The field mapping process

Field mapping should ideally begin with systematic traverses of the study area – sometimes referred to as a 'walk-over' (e.g. Demek, 1972; Otto and Smith, 2013) – to get a sense of the scale of the study area and ensure that subtle features of importance, such as the location and orientation of ice-flow directional indicators (e.g. flutes, striae, roches moutonnées and ice-moulded bedrock), are not missed. In a palaeo-ice sheet context, mapping the location and orientation of striae in the field may be of most interest as these can provide information on multiple (local) ice flow directions, of which not all are recorded in the pattern of elongated bedforms (e.g. drumlins) mappable from remotely-sensed data (cf. Kleman, 1990; Hättestrand and Stroeven, 1996; Smith and Knight, 2011). Similarly, in a contemporary outlet glacier context, flutes are an important indicator of ice flow direction – sometimes of annual ice flow trajectories of glacier margins (cf. Chandler et al., 2016b; Evans et al., 2017) – but due to their subtlety they may only be identifiable in the field (e.g. Jónsson et al., 2014).

Traversing should ideally start from higher ground, where an overview can be gained, and proceed by crossing a valley axis (or a cirque floor, for example) many times to enable the viewing and assessment of landforms from as many perspectives, angles and directions as possible (cf. Demek, 1972). In addition to systematic traverses, landform assemblages in, for example, individual valleys/basins should ideally be viewed from a high vantage point in low light (e.g. Benn, 1990). Depending on the location and orientation of landforms, it may be beneficial to see the same area either (i) early in the morning or late in the afternoon/evening due to longer shadows, or (ii) both in the morning and afternoon/evening due to the changing position of longer shadows. These procedures ensure that apparent dimensions and orientations, which are influenced by perception under different viewing angles and daylight conditions, can be taken into account in descriptions and interpretations. This approach circumvents potential complications relating to subtle features that may only be visible from one direction or certain angles.

The location of features should be recorded on field maps or imagery (e.g. aerial photograph) extracts with reference to 'landmarks' that are clearly identifiable both in the field and on the base maps/imagery, such as distinct changes in contour-line inflection, lakes, river bends, confluences, prominent bedrock exposures, and large ridges or mounds (Lukas and Lukas, 2006; Boston, 2012a, b). Where geomorphological features are small, background relief is low and/or conspicuous reference points are absent, a network of mapped reference points can be established by either taking a series of cross-bearings on prominent features using a compass (e.g. Benn, 1990) or by verifying locations using a handheld GNSS (e.g. Lukas and Lukas, 2006; Boston, 2012a, b; Brynjólfsson et al., 2014; Jónsson et al., 2014; Lovell, 2014; Pearce et al., 2014; van der Bilt et al., 2016). The latter is useful for recording the location of point-data such as striae, erratic or glacially-transported boulders, and sediment exposures (cf. Lukas and Lukas, 2006; Boston, 2012a, b; Pearce et al., 2014). Additional information between known reference points can then be interpolated and marked on the geomorphological map.

Establishing the size of landforms and features and plotting them on the map as accurately as possible is of crucial importance, and in addition to contour inflections (which may mark the location and boundaries of prominent ridges, for example), the mapper may pace out and/or estimate lengths, heights and widths. For larger landforms, or those masked by forest, walking around the perimeter of landforms and establishing a GNSS-marked 'waypoint-trail' is a good first approximation.

The strategy outlined above offers a broad perspective on the overall landform pattern and ensures accurate representation of landforms on field maps. To ensure accurate genetic interpretation of individual landforms, and the landscape as a whole, this field mapping strategy should ideally form part of an iterative process of observation and interpretation whilst still in the field (see Section 2.3).

2.3. Interpreting glacial landforms

In the preceding section, we focused on the technical aspects of field mapping and the means of recording glacial landforms. However, geomorphological mapping typically forms the foundation of process-oriented studies and palaeoglaciological reconstructions (see Section 1.1) and should, therefore, be embedded within a process of observation and interpretation. Definitive interpretation of glacial landforms, and glacial landscapes as a whole, can rarely be made on the basis of surface morphology alone. Additional strands of field evidence may become highly relevant, if not essential, depending on the objectives of the individual project: sedimentological data are crucial to interpreting processes of landform formation and glacier dynamics (e.g. Lukas, 2005; Benn and Lukas, 2006; Benediktsson et al., 2010, 2016; Chandler et al., 2016b; Gribenski et al., 2016), whilst chronological data are fundamental to robust palaeoglaciological reconstructions and related palaeoclimatic studies (e.g. Finlayson et al., 2011; Gribenski et al., 2016, 2018; Hughes et al., 2016; Stroeven et al., 2016; Bendle et al., 2017b; Darvill et al., 2017). Moreover, time and resources are limited and pragmatism necessary. Thus, observations must be targeted efficiently and effectively, in line with the research aims.

Much field-based research adopts an inductive approach, in which observations are collected and used to argue towards a particular conclusion. This is a valid approach at the exploratory stage of research, but deeper understanding of a landscape requires a more iterative process, in which data collection is conducted within a framework of hypothesis generation and testing. For this reason, it is useful to adopt a number of alternative working hypotheses (Chamberlin, 1897) that can be tested and gradually eliminated, following the principle of falsification (Popper, 1972). This process is best conducted in the field when it is possible to make key observations to test an interpretation, especially if the field site is remote and expensive to re-visit.

Following initial data collection, preliminary interpretations can be used to predict the outcome of new observations, which can then be used to test and refine the interpretation. Well-framed hypotheses allow an investigator to anticipate other characteristics of a glacial landscape and to test those predictions by targeted investigation of key localities (see Benn, 2006). For example, the presence of a certain group of landforms (e.g. moraines trending downslope into a side valley) can be used to formulate hypotheses (e.g. blockage of the side valley by glacier ice, and formation of a glacial lake), which in turn can be used to predict the presence of other sediment-landform associations in a particular locality (e.g. lacustrine sediments or shoreline terraces in the

side valley). Further detailed geomorphological mapping (and sedimentological analyses) in that area would then allow testing and falsification of the alternative working hypotheses. Iterations of this process during field mapping enable an increasingly detailed and robust understanding of the glacier system to be constructed. This coupled inductive-deductive approach is much more powerful than a purely inductive process: narratives that 'explain' a set of observations can appear very persuasive, even self-evident, but there may be other narratives that are also consistent with the same observations (cf. Popper, 1972).

Process-form models are useful tools in this inductive-deductive approach to landscape interpretation. In particular, *landsystem* or *facies models* make explicit links between landscape components and genetic processes, providing structure and context for data collection and interpretation (e.g. Eyles, 1983; Brodzikowski and van Loon, 1991; Evans, 2003a; Benn and Evans, 2010). At best, process-form models are not rigid templates or preconceived categories into which observations are forced, but a flexible set of possibilities that can guide, shape and enrich investigations (Benn and Lukas, 2006). For example, preliminary remote mapping may reveal features that suggest former glacier lobes may have surged (e.g. Lovell et al., 2012). Systematic study of sediment-landform assemblages, sediment exposures and other evidence, with reference to modern analogues (e.g. Evans and Rea, 2003), allows this idea to be rigorously evaluated in a holistic context (e.g. Darvill et al., 2017). This can open up new avenues for research in a creative and open-ended process.

This inductive-deductive approach to interpreting glacial landscapes and events should be embedded as part of the geomorphological mapping process (see Section 6). When dealing with palaeo-ice sheets, such field-based investigations may be guided by (existing) remote mapping. In alpine and plateau-style ice mass settings, sedimentological and chronological investigations should ideally form an integral part of field surveys.

3. Remote mapping methods

In the following sections, we review the principal remote mapping approaches employed in glacial geomorphological research, with analogue (or hard-copy) remote mapping (Section 3.1) and digital remote mapping (Section 3.2) considered separately. We give an overview of a number of datasets used for digital remote (i.e. GIS-based) mapping, namely satellite imagery (see Section 3.2.2.1), aerial photographs (see Section 3.2.2.2), digital elevation models (see Section 3.2.2.3), freeware virtual globes (see Section 3.2.2.4) and UAV-captured imagery (see Section 3.2.2.5). Each individual section provides a brief outline of the historical background and development of the methods, and we discuss the individual approaches in a broadly chronological order. Section 3.3 provides an overview of image processing techniques, highlighting that pragmatic solutions are often required.

We focus principally on remotely-sensed datasets relevant to terrestrial (onshore) glacial settings in the following sections because submarine (bathymetric) datasets and mapping of submarine glacial landforms have been subject to recent reviews elsewhere (see Dowdeswell et al., 2016; Batchelor et al., 2017). Nevertheless, we acknowledge that the emergence of geophysical techniques to investigate submarine (offshore) glacial geomorphology is a major development over the last two decades. Similarly, the emergence of geophysical datasets of sub-ice geomorphology in the last decade or so has been revolutionary, particularly in relation to subglacial bedforms (see Stokes, 2018). Many of the issues we discuss in relation to mapping from DEMs are transferable to those environments.

3.1. Analogue remote mapping

3.1.1. Background and applicability of analogue remote mapping

Geomorphological mapping from analogue (hard-copy) aerial photographs became a mainstream approach in glacial geomorphology in the 1960s and 1970s, with early proponents including, for example, the Geological Survey of Canada (e.g. Craig, 1961, 1964; Prest et al., 1968)

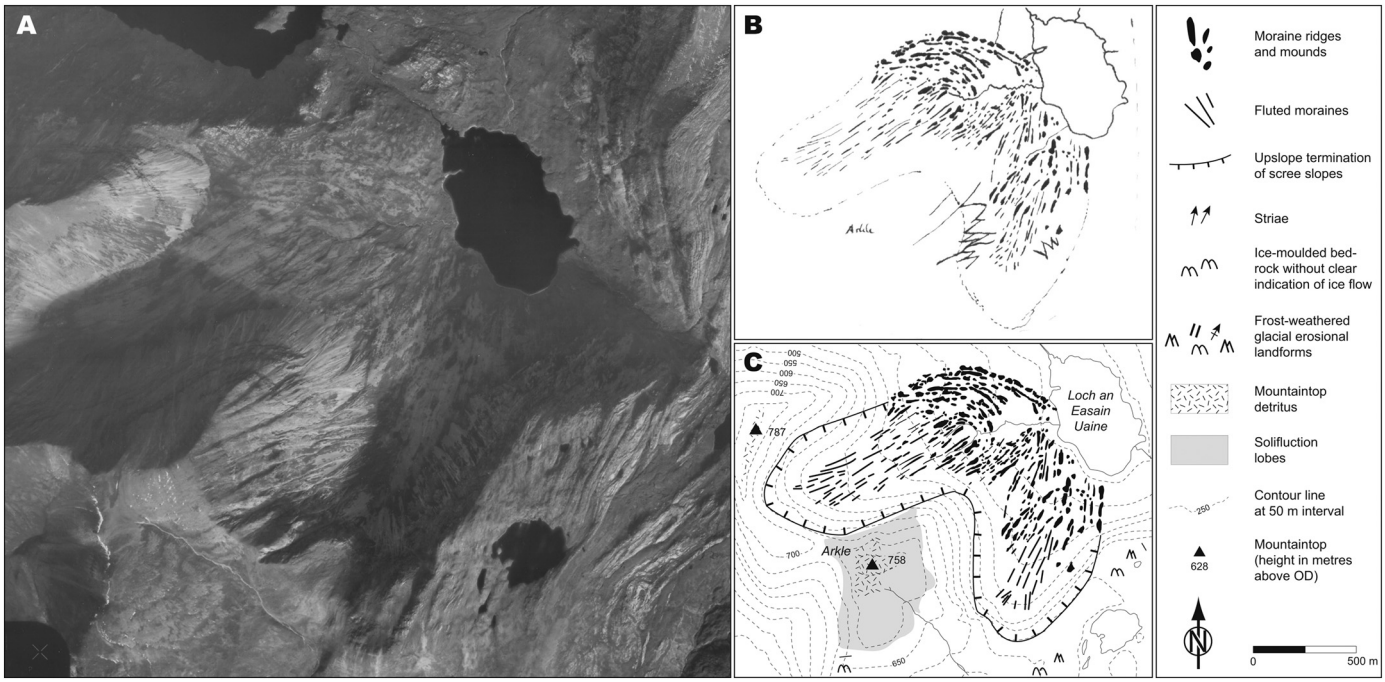

Fig. 2. The aerial photograph overlay-mapping process using an example from the mountain Arkle, NW Scotland. (A) aerial photograph at an average scale of ~1: 25,000 (extract from photo 38 88 087; ©RCAHMS 1988); (B) scan of original overlay mapped through a stereoscope from (A) (see Section 3.1.2 for method description), focusing on moraines, fluted moraines and the approximate upper limit of scree slopes as seen from the aerial photograph; (C) compiled, rectified geomorphological map, incorporating moraines and fluted moraines from (B) and additional data from field mapping, such as the exact upper limits of scree slopes, orientation of striae, solifluction lobes and mountaintop detritus. For description and interpretation of the geomorphology, see Lukas (2006).

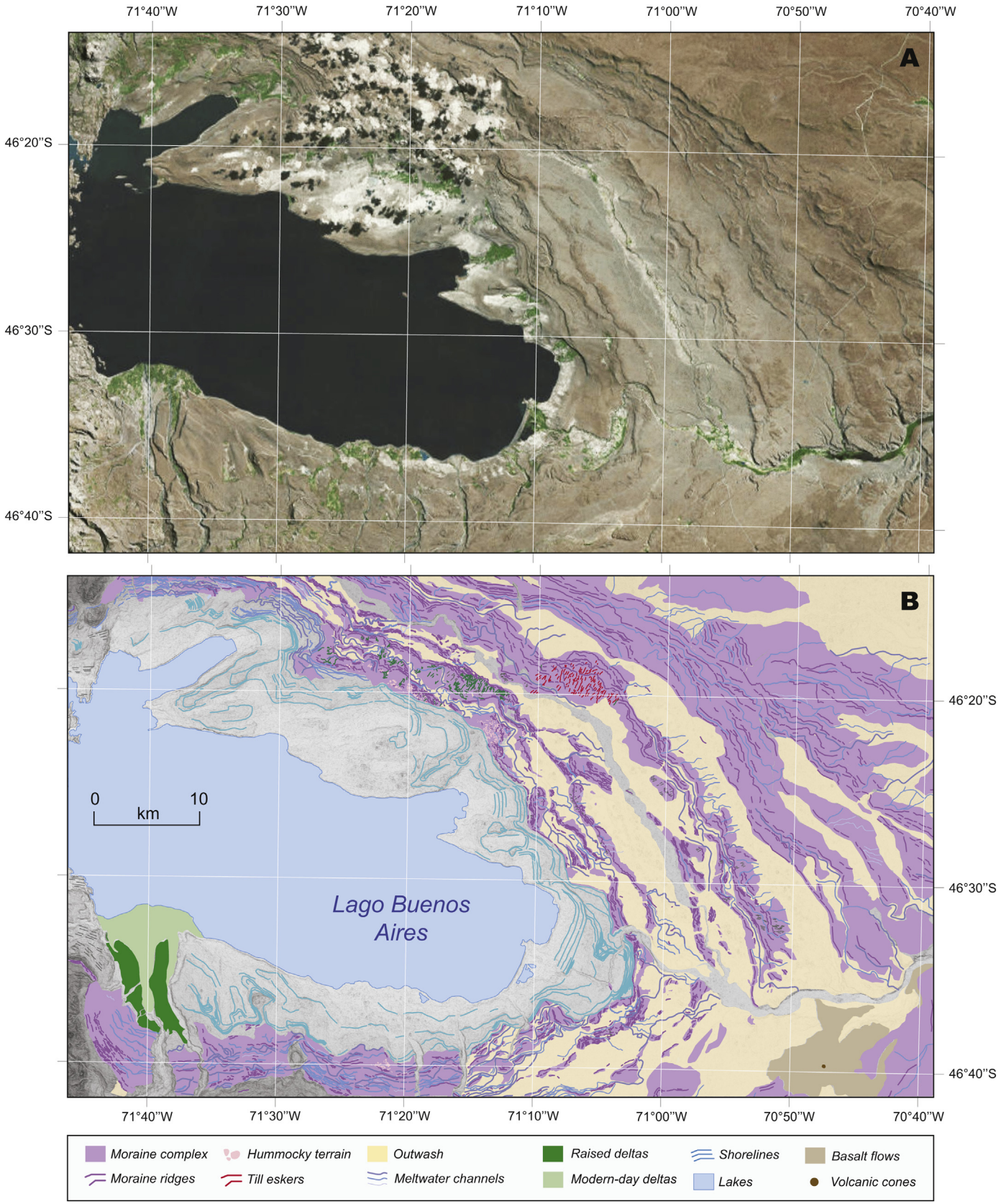

Fig. 3. Example of geomorphological mapping produced through on-screen vectorisation (tracing) in GIS software. Satellite image (A) and geomorphological mapping (B) showing suites of moraines formed by the Lago General Carrera–Buenos Aires ice lobe of the former Patagonian Ice Sheet, located to the east of the present-day Northern Patagonian Icefield. A combination of remotely-sensed datasets and field mapping were used to circumvent issues of localised cloud cover, as visible in (A). Where areas were obscured, SPOT-5 and DigitalGlobe images available in *Google Earth* were used. The geomorphological map extract is taken from Bendle et al. (2017a).

and UK-based researchers examining the Quaternary geomorphology of upland Britain (e.g. Price, 1961, 1963; Sissons, 1967, 1977a, b, 1979a, b; Sugden, 1970) and contemporary glacial landsystems (e.g. Petrie and Price, 1966; Price, 1966; Welch, 1966, 1967, 1968; Howarth, 1968; Howarth and Welch, 1969a, b). The latter research on landsystems in Alaska and Iceland was particularly pioneering in that it exploited a combination of aerial photograph interpretation, surveying techniques and early photogrammetry (see Evans, 2009, for further details).

Despite continued development of remote sensing technologies and the availability of digital aerial photographs (see Section 3.2.2.2), analogue stereoscopic aerial photographs are still used for glacial geomorphological mapping (e.g. Hättestrand, 1998; Benn and Ballantyne, 2005; Lukas et al., 2005; Hättestrand et al., 2007; Boston, 2012a, b; Evans and Orton, 2015). Additionally, the availability of high-quality photogrammetric scanners means that archival, hard-copy aerial photographs can be scanned at high resolutions, processed using digital photogrammetric methods and subsequently used for on-screen vectorisation (Section 3.2; e.g. Bennett et al., 2010; Jónsson et al., 2014).

As with field mapping, the interpretation of analogue aerial photographs is primarily used for mapping alpine- and plateau-style ice mass geomorphological imprints. Historically, analogue aerial photograph interpretation was extensively used for mapping palaeo-ice sheet geomorphological imprints, particularly by the Geological Survey of Canada, who combined aerial photograph interpretation with detailed ground-checking and helicopter-based surveys (e.g. Craig, 1961, 1964; Hodgson et al., 1984; Aylsworth and Shilts, 1989; Dyke et al., 1992; Klassen, 1993; Dyke and Hooper, 2001). Similarly, panchromatic and/or infrared vertical aerial photographs were used extensively to map glacial landforms relating to the Fennoscandian Ice Sheet (e.g. Sollid et al., 1973; Kleman, 1992; Hättestrand, 1998; Hättestrand et al., 1999). Aerial photograph interpretation has largely been superseded by satellite imagery and DEM interpretation in palaeo-ice sheet settings (see Section 5.1) but is applied for more detailed mapping of selected and/or complex areas (e.g. Dyke, 1990; Hättestrand and Clark, 2006; Kleman et al., 2010; Stokes et al., 2013; Storrar et al., 2013; Darvill et al., 2014; Evans et al., 2014).

3.1.2. Mapping from analogue datasets

For glacial geomorphological mapping purposes, vertical panchromatic aerial photographs have traditionally been employed, with pairs of photographs (stereopairs) viewed in stereo using a stereoscope (with magnification) (e.g. Karlén, 1973; Melander, 1975; Horsfield, 1983; Krüger, 1994; Kleman et al., 1997; Hättestrand, 1998; Evans and Twigg, 2002; Jansson, 2003; Benn and Ballantyne, 2005; Lukas and Lukas, 2006; Boston, 2012a, b; Chandler and Lukas, 2017). During aerial surveys, longitudinally-overlapping photographs along the flight path (endlap $\geq$ 60%) are captured in a series of laterally-overlapping parallel strips (sidelap $\geq$ 30%), with the two different viewing angles of the same area resulting in the stereoscopic effect (due to the principle of parallax; see Lillesand et al., 2015, for further details). This form of aerial photograph interpretation has been demonstrated to be a particularly valuable tool for determining the exact location, shape and planform of small features in glaciated terrain (e.g. Ballantyne, 1989, 2002, 2007a, b; Bickerton and Matthews, 1992, 1993; Lukas and Lukas, 2006; Boston, 2012a, b), provided the photographs are of appropriate scale, quality and tonal contrast (cf. Benn, 1990; Benn et al., 1992).

Mapping from hard-copy aerial photographs is undertaken by drawing onto acetate sheets (transparency films) whilst viewing the aerial photographs through a stereoscope, with the acetate overlain on one photograph of a stereopair (Fig. 2). Ideally, mapping should be conducted using a super-fine pigment liner with a nib size of 0.05 mm to enable small features to be mapped. Even so, it may still be necessary to compromise on the level of detail mapped; for example, meltwater channels between ice-marginal moraines have been left off maps in some studies due to map scale, with the associated text describing chains of moraines interspersed with meltwater channels (e.g. Benn and Ballantyne, 2005; Lukas, 2005).

Examining stereopairs from multiple sorties ('flight missions') in parallel or in combination with digital aerial photographs may be beneficial and help alleviate issues such as localised cloud cover, snow cover, poor tonal contrast, afforestation, and anthropogenic developments (e.g. Horsfield, 1983; Bennett, 1991; McDougall, 2001). Additionally, it is advantageous to examine stereopairs multiple times – preferably before and after field mapping – to increase feature identification and improve the accuracy of genetic interpretations (Lukas and Lukas, 2006; Sahlin and Glasser, 2008). When conducting mapping over a large area with multiple stereopairs, examining stereopairs from a sortie 'out of sequence' (i.e. not mapping from consecutive pairs of photographs) may provide a means of internal corroboration and ensure objectivity and robustness (Bennett, 1991).

In order to reduce geometric distortion, which increases towards the edges of aerial photographs due to the central perspective (Lillesand et al., 2015), it is advisable to keep the areas mapped onto the acetate as close as possible to the centre of one aerial photograph of a stereopair (Kronberg, 1984; Lukas, 2002; Lukas and Lukas, 2006; Evans and Orton, 2015). These hand-drawn overlays can subsequently be scanned at high resolutions and then georeferenced and vectorised using GIS software (see Section 3.3.1).

3.2. Digital remote mapping

3.2.1. Background and applicability of digital remote mapping

The development of GIS software packages (e.g. commercial: *ArcGIS*; open source: *QGIS*) and the proliferation of digital imagery, particularly freely available satellite imagery, have undoubtedly been the most significant developments in glacial geomorphological mapping in the last fifteen years or so. GIS packages have provided platforms and tools for visualising, maintaining, manipulating and analysing vast quantities of remotely-sensed and geomorphological data (cf. Gustavsson et al., 2006, 2008; Napieralski et al., 2007b). Their use in combination with digital imagery allows geomorphological features to be mapped directly in GIS software (Fig. 3), with individual vector layers created for each geomorphological feature. Moreover, the availability of digital imagery enables the mapper to alter the viewing scale instantaneously and switch between various datasets, allowing for a flexible but systematic approach.

Digital mapping (on-screen vectorisation/tracing) also provides georeferenced geomorphological data, which has two important benefits: Firstly, these data can easily be used to extract landform metrics (e.g. Hättestrand et al., 2004; Clark et al., 2009; Spagnolo et al., 2010, 2014; Storrar et al., 2014; Ojala et al., 2015; Dowling et al., 2016; Ely et al., 2016a, 2017); and, secondly, these data can be seamlessly incorporated into wider, regional-scale GIS compilations (e.g. Bickerdike et al., 2016; Stroeven et al., 2016; Clark et al., 2018a). Additionally, digital remote mapping allows the user to record attribute data (e.g. data source) tied to individual map (vector) layers, which can be useful for large compilations of previously published mapping (e.g. Bickerdike et al., 2016; Clark et al., 2018a). Such compendia help to circumvent issues relating to the often-fragmented nature of geomorphological evidence (i.e. numerous spatially separate studies) and identify gaps in the mapping record. Once assembled across large areas, they also enable evidence-based reconstructions of entire ice sheets and regional ice sheet sectors (see Clark et al., 2004, 2018a). Indeed, the ongoing open access data revolution in academia and the increasing publication/availability of mapping output (in the form of GIS files; e.g. Finlayson et al., 2011; Fu et al., 2012; Darvill et al., 2014; Bickerdike et al., 2016; Bendle et al., 2017a), means that geomorphological mapping can have wider impact beyond individual local to regional studies.

3.2.2. Datasets for digital remote mapping

There is now a plethora of remotely-sensed datasets covering a wide

range of horizontal resolutions (10^{-2} to 10^{2} m), enabling the application of digital mapping (in some form) to all glacial settings. We provide an overview of the principal datasets used in digital mapping below, with mapping approaches in specific glacial settings reviewed in Section 5.

3.2.2.1. Satellite imagery. The development of satellite-based remote sensing in the 1970s and subsequent advances in technology have revolutionised understanding of glaciated terrain, particularly with respect to palaeo-ice sheet geomorphology and dynamics (see Section 5.1; Clark, 1997; Stokes, 2002; Stokes et al., 2015). The potential of satellite imagery was first demonstrated by the pioneering work of Sugden (1978), Andrews and Miller (1979) and Punkari (1980), with the availability of large-area view (185 km x 185 km) Landsat Multi-Spectral Scanner (MSS) images affording a new perspective of glaciated regions. These allowed a single analyst to systematically map ice-sheet-scale (1: 45,000 to 1: 1,000,000) glacial geomorphology (e.g. Boulton and Clark, 1990a, b) in a way that previously would have required the painstaking mosaicking of thousands of aerial photographs (e.g. Prest et al., 1968).

Since the 1980s, there has been an explosion in the use of satellite imagery for glacial geomorphological mapping and there is now a profusion of datasets available (Table 1). Importantly, many of these sensors capture multispectral data, which can enhance landform detection through image processing and the use of different band combinations (see Section 3.3.3). The uptake of satellite imagery has coincided with improvements in the availability and spatial and spectral resolution of satellite datasets globally, with Landsat (multispectral: 30 m; panchromatic: 15 m), ASTER (15 m), Sentinel-2 (10 m) and SPOT (up to 1.5 m) images proving the most popular. More recently, satellite sensor advancements have enabled the capture of satellite images with resolutions comparable to aerial photographs (Fig. 4; e.g. QuickBird, SPOT6-7, WorldView-2 and later). These datasets are also suitable for mapping typically smaller and/or complex glacial landforms produced by cirque glaciers, valley glaciers and icefield/ice-cap outlets (e.g. Chandler et al., 2016a; Evans et al., 2016b; Ewertowski et al., 2016; Gribenski et al., 2016; Małecki et al., 2018).

In general, as better-resolution imagery has become more widely available at low to no cost, older, coarser-resolution datasets (e.g. Landsat MSS: 60 m) have largely become obsolete. Nevertheless, Landsat data (TM, ETM+, and OLI: 15 to 30 m) are still the standard data source for ice-sheet-scale mapping, with the uptake of high-resolution commercial satellite imagery still relatively slow in such studies. This is primarily driven by the cost of purchasing high-resolution commercial datasets, making freely-available imagery such as Landsat a

Table 1
Satellite imagery types that have been used in glacial geomorphological mapping and example applications. The satellites are broadly ordered in terms of the spatial resolution of the captured imagery. Note, we also anticipate imagery from the Planet (RapidEye, PlanetScope and SkySat) and Sentinel constellations being widely used in future.

Satellite	Sensor	Temporal coverage	Spectral bands	Spatial resolution (m)	Source	Example studies
Landsat 1–5	MSS	1972–2013	4	60	USGS Earth Explorer (earthexplorer.usgs.gov)	Clark and Stokes (2001); Stokes and Clark (2002, 2003); Jansson et al. (2003); see also Clark (1997, Table 1)
Landsat 4–5	TM	1982–2013	1	120	Global Land Cover Facility (landcover.org)	Punkari (1995); Alexanderson et al. (2002); De Angelis (2007); Storrar et al. (2013); Orkhonselenge (2016)
			6	30		
Landsat 7	ETM+	1999–	1	60		Kassab et al. (2013); Stroeven et al. (2013); Darvill et al. (2014); Blomdin et al. (2016a); Ely et al. (2016b); Ercolano et al. (2016); Lindholm and Heyman (2016); Storrar and Livingstone (2017); see also Clark (1997, Table 1)
			6	30		
			1	15		
Landsat 8	OLI/TIRS	2013–	2	100		Espinoza (2016); Carrivick et al. (2017); Storrar and Livingstone (2017)
			8	30		
			1	15		
Terra	ASTER	2000–	5	90	LP DAAC (LPDAAC.usgs.gov)	Glasser and Jansson (2005, 2008); Glasser et al. (2005); Lovell et al. (2011); Sagredo et al. (2011); Darvill et al. (2014); Ercolano et al. (2016)
			6	20		
			5	15		
ERS 1	SAR	1991–2000	1	30	European Space Agency (earth.esa.int)	Clark et al. (2000); Clark and Stokes (2001); Heiser and Roush (2001); see also Clark (1997, Table 1)
SPOT 1–3	HRV	1986–2009	3	20	Airbus Defence and Space (intelligence-airbusds.com)	Smith et al. (2000); Coronato et al. (2009)
			1	20		
			1	10		
SPOT 4	HRVIR	1998–2013	1	10		Trommelen and Ross (2010, 2014); Ercolano et al. (2016) [viewed in Google Earth™]; McHenry and Dunlop (2016); Principato et al. (2016)
			3	20		
			1	20		
SPOT 5	HRG/HRS	2002–2015	1	2.5, 5		Trommelen and Ross (2010, 2014); Ercolano et al. (2016) [viewed in Google Earth™]; McHenry and Dunlop (2016); Principato et al. (2016); Bendle et al. (2017a)
			3	10		
			1	20		
SPOT 6–7	NAOMI	2012–	1	1.5		Gribenski et al. (2016)
			4	6		
CORONA/ARGON/ LANYARD	KH1–KH6	1959–1972	1	1.8–140	USGS Earth Explorer (earthexplorer.usgs.gov)	Alexanderson et al. (2002); Zech et al. (2005); Lifton et al. (2014)
IKONOS	HRG	1999–2015	1	1	DigitalGlobe (digitalglobe.com)	Juyal et al. (2011); Kłapyta (2013); Zasadni and Kłapyta (2016)
			4	4		
COSMO-Skymed	SAR	2008–	1/3/15/16/ 20	1	e-GEOS (e-geos.it)	da Rosa et al. (2013)
Quickbird	HRG	2001–2014	1	0.61	DigitalGlobe (digitalglobe.com)	da Rosa et al. (2011, 2013); May et al. (2011); Lovell et al. (2011)
			4	2.44		
GeoEye-1		2008–	1	0.46	European Space Imaging (euspaceimaging.com)	Westoby et al. (2014)
			4	1.84		
WorldView-2		2009–	1	0.46		Jamieson et al. (2015); Chandler et al. (2016a); Evans et al. (2016e); Ewertowski et al. (2016)
			8	1.84		
Google Earth™ (specific image details not given)	n/a	n/a	n/a	n/a	Google Earth	Margold and Jansson (2011); Margold et al. (2011); Kassab et al. (2013); Stroeven et al. (2013); Darvill et al. (2014); Blomdin et al. (2016a); Evans et al. (2016d); Li et al. (2016); Lindholm and Heyman (2016); Orkhonselenge (2016)

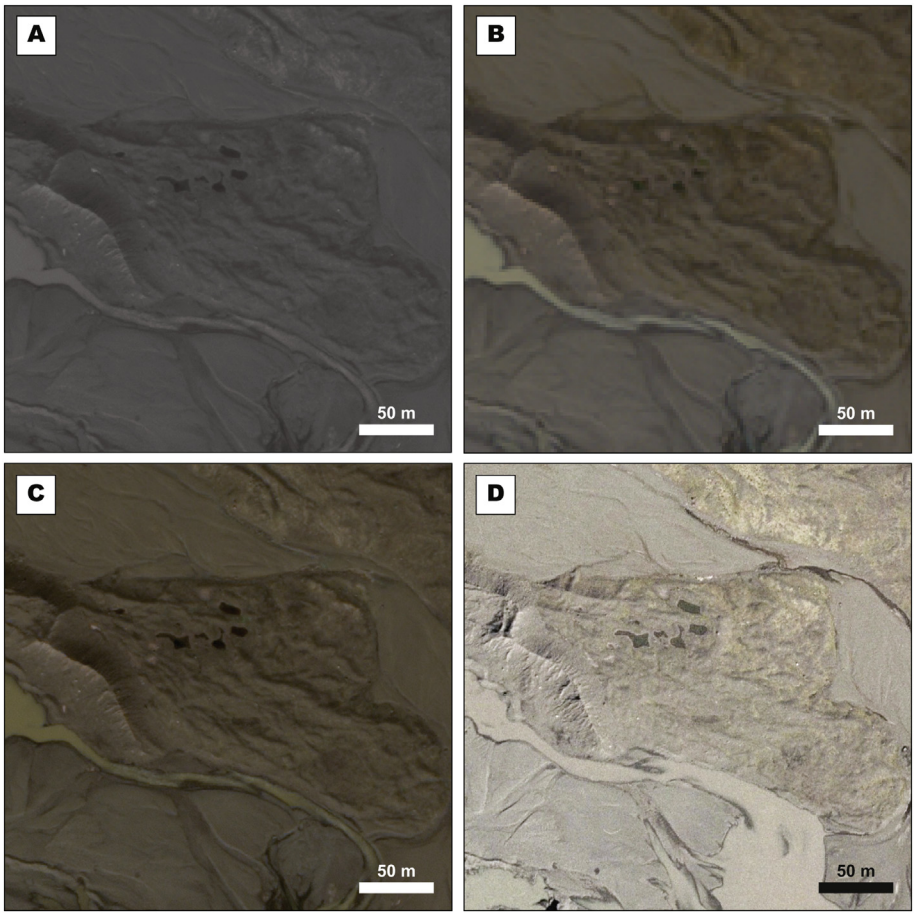

Fig. 4. Comparison of WorldView-2 satellite imagery (June 2012, European Space Imaging) with digital colour aerial photographs (2006, Loftmyndir ehf) for the Skálafellsjökull foreland, SE Iceland. (A) Panchromatic satellite image (0.5 m ground sampled distance, GSD). (B) Multispectral satellite image (2.0 m GSD). (C) Pansharpened three-band natural colour satellite image (0.5 m GSD). (D) Digital colour aerial photographs (0.41 m GSD). The satellite imagery is of sufficient resolution to allow mapping of small-scale (< 2 m in height) annual moraines (see Chandler et al., 2016a, b).

valuable resource. In addition, archival satellite data afford time-series of multi-spectral images that may facilitate assessments of geomorphological changes through time; for example, fluctuations in highly dynamic (surging or rapidly retreating) glacial systems (e.g. Flink et al., 2015; Jamieson et al., 2015). Conversely, for smaller research areas (e.g. for a single valley or foreland), high-resolution satellite imagery is becoming an increasingly viable option, with prices for georeferenced and orthorectified products comparable to those for digital aerial photographs (see Section 3.2.2.2). This also has the benefit of saving time on photogrammetric processing, with many vendors providing consumers with various processing options. Consequently, on-demand, high-resolution (commercial) satellite imagery will inevitably come into widespread usage, where costs are not prohibitive. Alternatively, freeware virtual globes and web mapping services (e.g. *Bing Maps*, *Google Earth*) offer valuable resources for free visualisation of such high-resolution imagery (see Section 3.2.2.4).

3.2.2.2. Digital aerial photographs. With improvements in technology, high-resolution (ground resolution < 0.5 m per pixel) digital copies of aerial photographs have become widely available and used for glacial geomorphological mapping (e.g. Brown et al., 2011a; Bradwell et al., 2013; Brynjólfsson et al., 2014; Jónsson et al., 2014; Pearce et al., 2014; Schomacker et al., 2014; Chandler et al., 2016a; Evans et al., 2016c; Lardeux et al., 2015; Lønne, 2016; Allaart et al., 2018). Indeed, digital aerial photographs, along with scanned copies of archival aerial photographs, are now more widely used than hard-copy stereoscopic aerial photographs, particularly in modern glacial settings. Additionally, the introduction of UAV technology in recent years has allowed sub-decimetre resolution aerial photographs to be captured on demand (see Section 3.2.2.5). A further key advantage of aerial photographs in digital format is the ability to produce orthorectified aerial photograph mosaics (or 'orthophotographs') and DEMs with low root mean square errors (RMSEs < 1 m; see Section 4.4), when combined with ground control points (GCPs) collected using surveying equipment (e.g. Kjær et al. 2008; Bennett et al., 2010; Schomacker et al., 2014; Chandler et al., 2016a; Evans et al., 2017). These photogrammetric products can then be used for on-screen vectorisation (tracing) and the generation of georeferenced geomorphological mapping (Fig. 5), as outlined above.

Digital aerial photographs are commonly captured by commercial surveying companies (e.g. Loftmyndir ehf, Iceland; Getmapping, UK), meaning that they may be expensive to purchase and costs may be prohibitive for large study areas. This is in contrast to hard-copy (archival) aerial photographs that are often freely available for viewing in national collections. Additionally, digital aerial photographs are not readily viewable in stereo with a standard desktop setup, although on-screen mapping in stereoscopic view is possible on workstations equipped with stereo display and software such as *BAE Systems SOCET SET* (e.g. Kjær et al., 2008; Benediktsson et al., 2009). However, this approach is not applicable to orthophotographs. An alternative approach is to visualise orthophotographs in 3D by draping them over a DEM (see Section 3.2.2.3) in GIS software such as *ESRI ArcScene* or similar (Fig. 6; e.g. Benediktsson et al., 2010; Jónsson et al., 2014; Schomacker et al., 2014; van der Bilt et al., 2016). Three-dimensional assessment in *ArcScene*, parallel to mapping in *ArcMap*, may aid in landform detection, delineation and interpretation.

3.2.2.3. Digital Elevation Models (DEMs). Over the last ~15 years there has been increasing use of DEMs in glacial geomorphology, particularly for mapping at the ice sheet scale (e.g. Glasser and Jansson, 2008; Hughes et al., 2010; Ó Cofaigh et al., 2010; Evans et al., 2014, 2016d; Ojala, 2016; Principato et al., 2016; Stokes et al., 2016a; Mäkinen et al.,

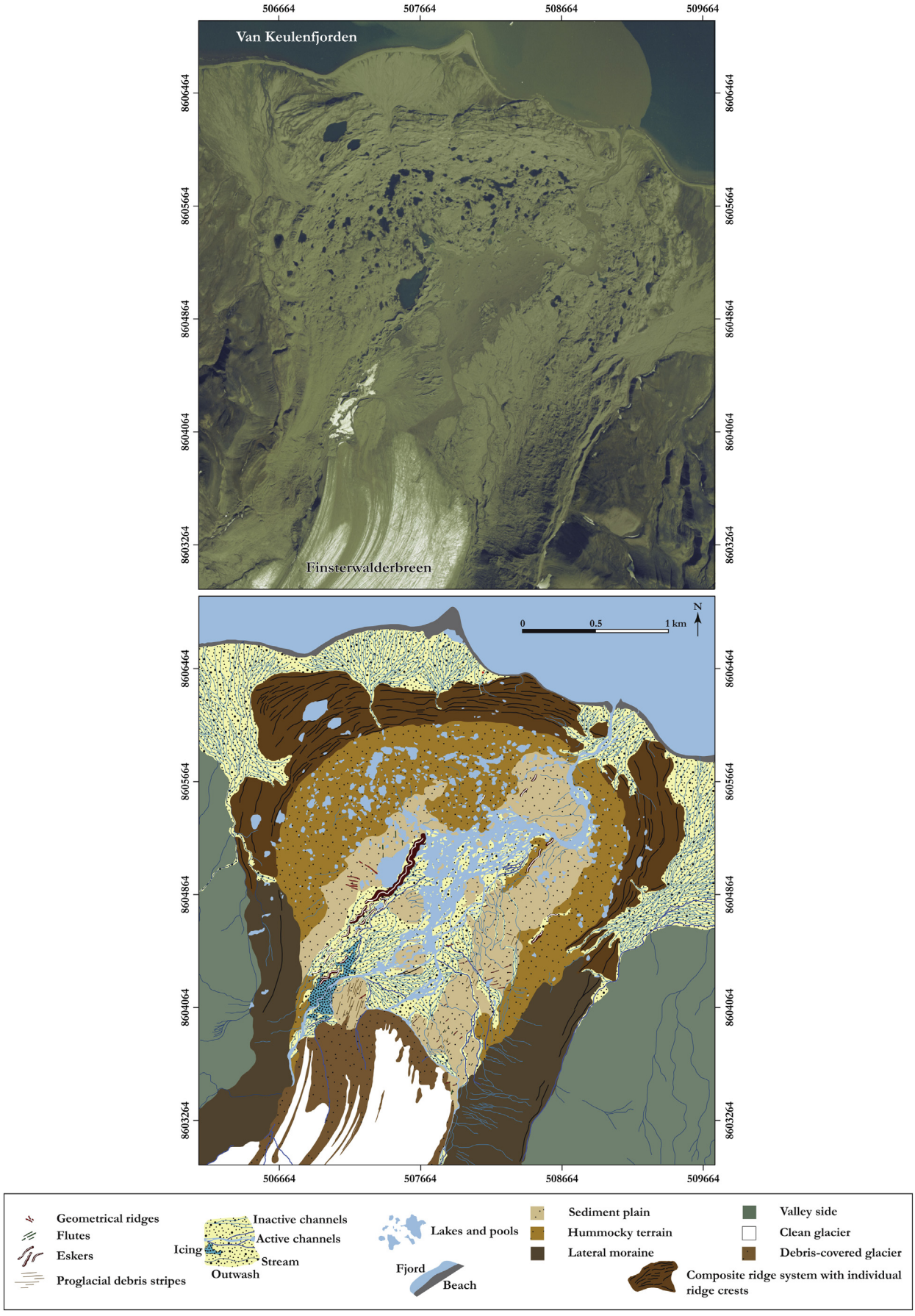

(caption on next page)

Fig. 5. Geomorphological map of the Finsterwalderbreen foreland, Svalbard, produced digitally in GIS software through mapping from a digital aerial photograph (captured in 2004). Field mapping was also conducted and incorporated in the final map. Aerial photograph provided by the NERC Earth Observation Data Centre. Modified from Lovell et al. (2018).

2017; Norris et al., 2017). DEMs are raster-based models of topography that record absolute elevation, with each grid cell in a DEM representing the average height for the area it covers (Clark, 1997; Smith et al., 2006). Terrestrial DEMs can be generated by a variety of means, including from surveyed contour data, directly from stereo imagery (aerial photographs, satellite and UAV-captured imagery), or from air- and space-borne radar and LiDAR systems (Smith and Clark, 2005). An important recent development in this regard has been the 'Surface Extraction with TIN-based Search-space Minimization' (SETSM) algorithm for automated extraction of DEMs from stereo satellite imagery (Noh and Howat, 2015), which has been used to generate the ArcticDEM dataset (https://www.pgc.umn.edu/data/arcticdem/). However, SETSM DEMs may contain systematic vertical errors that require correction (e.g. Carrivick et al., 2017; Storrar et al., 2017).

The majority of DEMs with national- to international-scale coverage (Table 2) typically have a coarser spatial resolution than aerial photographs and satellite imagery and represent surface elevations rather than surface reflectance. As a result, it may be difficult to identify glacial landforms produced by relatively small ice masses (cirque glaciers, valley glaciers and icefield outlets), precluding detailed mapping of their planforms (cf. Smith et al., 2006; Hughes et al., 2010; Brown et al., 2011a; Boston, 2012a, b; Pearce et al., 2014). Conversely, these DEMs can be particularly valuable for mapping glacial erosional features (e.g. glacial valleys, meltwater channels), as well as major glacial depositional landforms produced by larger ice masses (e.g. Greenwood and Clark, 2008; Heyman et al., 2008; Livingstone et al., 2008; Hughes et al., 2010; Morén et al., 2011; Barr and Clark, 2012; Stroeven et al., 2013; Turner et al., 2014a; Margold et al., 2015a; Blomdin et al., 2016a, b; Lindholm and Heyman, 2016; Mäkinen et al., 2017; Storrar and Livingstone, 2017). However, the recent development of UAV (see Section 3.2.2.5) and LiDAR technologies have allowed the generation of very high resolution DEMs (< 0.1 m), enabling the application of DEMs to map small glacial landforms (e.g. Evans et al., 2016a; Ewertowski et al., 2016; Ely et al., 2017). We anticipate national-scale LiDAR DEMs becoming widely-used in the future, with a number of nations recently releasing or currently capturing/processing high horizontal resolution (≤2 m) LiDAR data (Table 2; e.g. Dowling et al. 2013; Johnson et al.

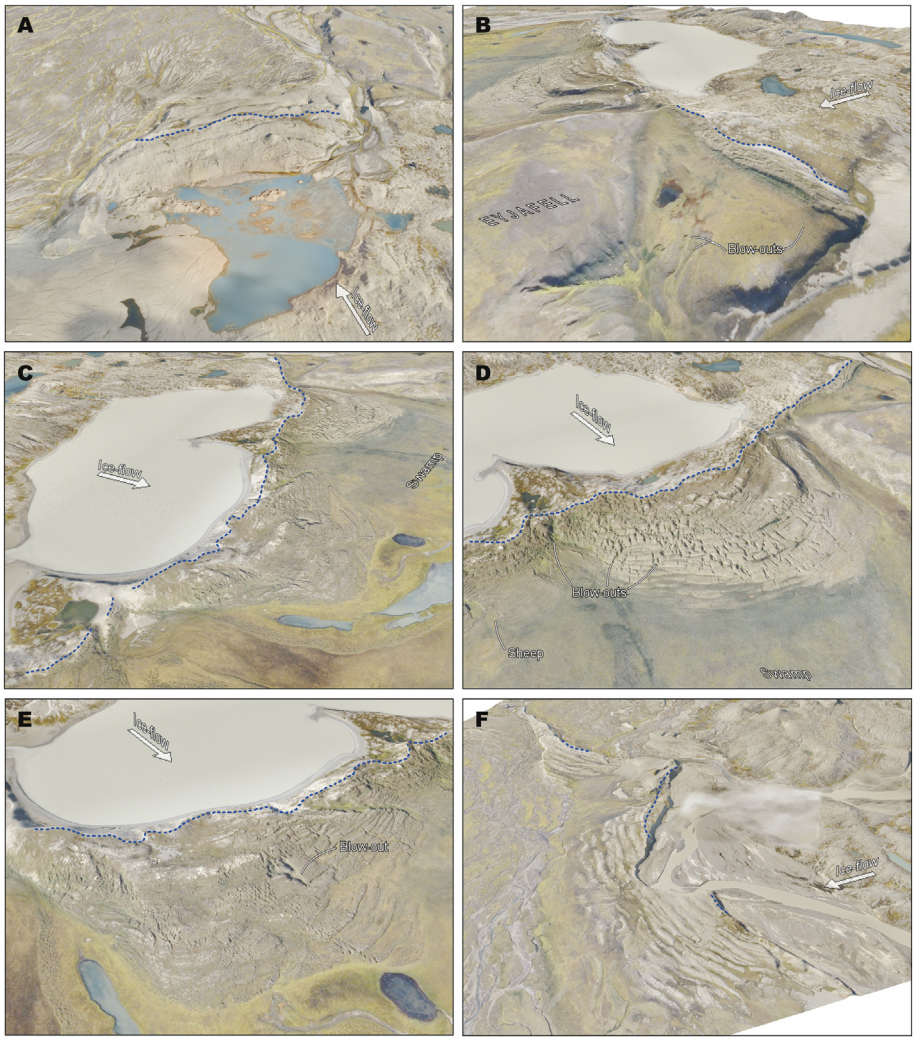

Fig. 6. Views at various points along the length of the 1890 surge end moraine at Eyjabakkajökull, Iceland, visualised in 3D within *ESRI ArcScene* (Benediktsson et al., 2010). Aerial orthophotographs from 2008 are draped over a 3 m grid DEM with 1.5x vertical exaggeration. For reference to the individual image panels, readers are directed to the original publication.

Table 2
Examples of DEM datasets with national- to international-coverage that have been employed in glacial geomorphological map production.

Dataset	Coverage	Spatial resolution (m)	RMSE or CE90 (m)		Data source(s)	Example studies
			Vertical	Horizontal		
SRTM[a]	Global	~90 (3 arc-second) ~30 (1 arc-second)	~5–13	-	Global Land Cover Facility (landcover.org) USGS Earth Resources and Science Center (eros.usgs.gov)	Glasser and Jansson (2008); Barr and Clark (2009); Ó Cofaigh et al. (2010); Morén et al. (2011); Stroeven et al. (2013); Darvill et al. (2014); Evans et al. (2014, 2016d); Trommelen and Ross (2014); Stokes et al. (2016a); Ely et al. (2016b); Lindholm and Heyman (2016)
ASTER GDEM (V2)	Global	~30 (1 arc-second)	~8.7	-	LP DAAC Global Data Explorer (gdex.cr.usgs.gov/gdex) NASA Reverb (reverb.echo.nasa.gov/reverb)	Barr and Clark (2012); Blomdin et al. (2016a, b); Lindholm and Heyman (2016)
Canadian Digital Elevation Dataset (CDED)	Canada	~20 (0.75 arc-second)	-	-	Natural Resources Canada (geogratis.gc.ca)	Margold et al. (2011, 2015a); Evans et al. (2016c); Storrar and Livingstone (2017)
USGS National Elevation Dataset (NED)[b]	US	~30 (1 arc-second) ~10 (1/3 arc-second)	~2.4	-	US Geological Survey (ned.usgs.gov)	Hess and Briner (2009); Margold et al. (2015a); Ely et al. (2016a)
TanDEM-X	Global	~12 (0.4 arc-second)	< 10	< 10	German Aerospace Center (DLR) (tandemx-science.dlr.de)	Pipaud et al. (2015)
NEXTMap Britain™	UK	5	~1	2.5	NERC Earth Observation Data Centre[c] (ceda.ac.uk)	Livingstone et al. (2008); Finlayson et al. (2010, 2011); Hughes et al. (2010); Brown et al. (2011a); Boston (2012a, b); Pearce et al. (2014); Turner et al. (2014a)
ArcticDEM	Arctic	2	2.0	3.8	Polar Geospatial Center (pgc.umn.edu/data/arcticdem)	Levy et al. (2017)
Maanmittauslaitos LiDAR DEM	Finland	2	~0.3	-	National Land Survey of Finland (maanmittauslaitos.fi)	Ojala et al. (2015); Ojala (2016); Mäkinen et al. (2017)
Ny Nationell Höjdmodell	Sweden	2	~0.1	-	Lantmäteriet (lantmateriet.se)	Dowling et al. (2015, 2016); Greenwood et al. (2015); Möller and Dowling (2016); Peterson et al. (2017)
Environment Agency LiDAR DEM	UK (partial)	2, 1, 0.5 and 0.25	0.05 – 0.15	0.4	DEFRA Environment Data (environment.data.gov.uk)	Miller et al. (2014)
Iceland Met Office and Institute of Earth Sciences, University of Iceland, LiDAR DEM[d]	Iceland (partial)	< 5	< 0.5	-	Iceland Meteorological Office (en.vedur.is)	Brynjólfsson et al. (2014, 2016); Benediktsson et al. (2016); Jónsson et al. (2016)

[a] SRTM data was only freely available with a spatial resolution of ~90 m (3 arc-seconds) outside of the United States until late 2015 when the highest resolution data were thereafter made available globally (see http://www2.jpl.nasa.gov/srtm/)
[b] The USGS NED dataset has been superseded by the 3D Elevation Program (3DEP), with this data available as seamless 1/3 arc-second, 1 arc-second and 2 arc-second DEMs (see https://nationalmap.gov/3DEP/3dep_prodserv.html)
[c] NEXTMap Britain™ data is freely available to NERC staff and NERC-funded researchers, though subsets can be applied for by non-NERC-funded researchers under a Demonstrator User License Agreement (DULA)
[d] The Icelandic LiDAR DEM data are available at 5 m resolution, but it is possible to derive higher-resolution DEMs (e.g. 2 m) from the point clouds using denser interpolation.

2015).

Although the principal focus of this contribution is terrestrial/onshore glacial geomorphological mapping, it is worth highlighting here that the availability of spatially-extensive bathymetric charts, such as the General Bathymetric Chart of the Oceans (GEBCO) and International Bathymetric Chart of the Arctic Ocean (IBCAO: Jakobsson et al., 2012), and high-resolution, regional (often industry-acquired) bathymetric data has been an important development in submarine/offshore glacial geomorphological mapping. This has enabled the gridding of DEMs to map submarine glacial geomorphological imprints (see Dowdeswell et al., 2016), markedly enhancing understanding of palaeo-ice sheets in marine sectors (e.g. Ottesen et al., 2005, 2008a, 2016; Bradwell et al., 2008; Winsborrow et al., 2010, 2012; Livingstone et al., 2012; Ó Cofaigh et al., 2013; Hodgson et al., 2014; Stokes et al., 2014; Margold et al., 2015a, b; Greenwood et al., 2017) and modern tidewater (often surging) glaciers (e.g. Ottesen and Dowdeswell, 2006a, b; Ottesen et al., 2008b, 2017; Robinson and Dowdeswell, 2011; Dowdeswell and Vazquez, 2013; Flink et al., 2015; Streuff et al., 2015; Allaart et al., 2018). In addition, recent years have seen the production of DEMs of sub-ice topography from geophysical datasets (radar and seismics) at spatial resolutions suitable for identifying and mapping bedforms (see King et al., 2007, 2009, 2016a; Smith et al., 2007; Smith and Murray, 2009). This work has advanced understanding of the evolution of bedforms beneath Antarctic ice streams, providing important genetic links between the formation of landforms beneath modern ice sheets and those left-behind by palaeo-ice masses (Stokes, 2018). The interested reader is directed to recent reviews for further discussion on the importance of geophysical evidence for understanding ice sheet extent and dynamics (Livingstone et al., 2012; Ó Cofaigh, 2012; Stokes et al., 2015; Dowdeswell et al., 2016; Batchelor and Dowdeswell, 2017; Stokes, 2018).

3.2.2.4. Freeware virtual globes. The advent of freeware virtual globes (e.g. *Google Earth*, *NASA Worldwind*) and web mapping services (e.g. *Bing Maps*, *Google Earth Engine, Google Maps*) has provided platforms for free visualisation of imagery from various sources and low-cost mapping resources. A key benefit of virtual globes is the ability to visualise imagery and terrain in 3D and from multiple viewing angles, which may aid landform detection when used in conjunction with other datasets and software (e.g. Heyman et al., 2008; Bendle et al., 2017a). Moreover, a number of virtual globes and web mapping services have the ability to link with other freeware and open-source programmes; for example, free plugins are available to import *Google Earth* and *Bing Maps* imagery into the open-source GIS software package *QGIS*. Thus, a mapper can combine freely available, often high-resolution (e.g. QuickBird, SPOT6-7, WorldView-2 and later), imagery and the capabilities of GIS technology without the expense associated with commercial imagery and software (see Sections 3.2.2.1 and 3.2.2.2).

The most widely-used virtual globe is *Google Earth*, with a 'professional' version (*Google Earth Pro*) freely available since 2015 (see Mather et al., 2015, for a review). An increasing number of glacial geomorphological studies are noting the use of *Google Earth* (but not necessarily the imagery type) as a mapping tool (see Table 1), principally to cross-check mapping conducted from other imagery. However, some studies have also utilised the built-in vectorising tools for mapping (e.g. Margold and Jansson, 2011; Margold et al., 2011; Fu et al., 2012). There is a compromise on the functionality of freeware virtual globes and vectorisation tools are often not as flexible and/or user-friendly, but these can be overcome by importing imagery into GIS software. In the case of *Google Earth*, it is also possible to export Keyhole Markup Language (KML) files that can be used for subsequent analyses and map production in GIS software (following file conversion). Open access remotely-sensed datasets are also available through commercial GIS software, with high resolution satellite imagery (e.g. GeoEye-1, SPOT-5, WorldView) available for mapping through the in-built 'World Imagery' service in *ESRI ArcGIS* (e.g. Bendle et al., 2017a).

Despite the benefits, some caution is necessary when using freeware virtual globes as there may be substantial errors in georeferencing of imagery, which users cannot account for and/or correct. Moreover, dating of imagery is not necessarily clear or accurate (Mather et al., 2015; Wyshnytzky, 2017). The latter may not be a concern if mapping in a palaeoglaciological setting, whilst any georeferencing errors may not be as significant if mapping broad patterns at the ice sheet scale. Conversely, errors associated with freeware mapping may be significant when comparing imagery from different times and/or when mapping in highly dynamic, contemporary glacial environments. Aside from these potential issues, limitations are imposed by pre-processing of imagery, with no option to, for example, modify band combinations to enhance landform detection (see Section 3.3.3).

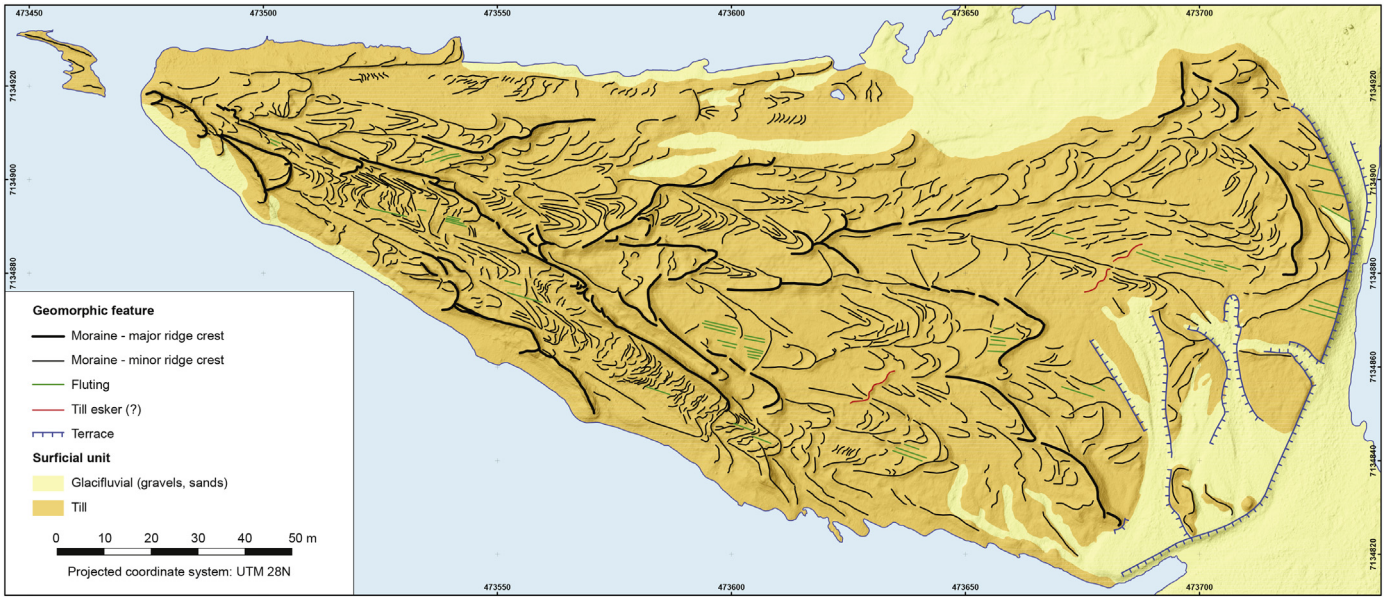

Fig. 7. High-resolution geomorphological mapping of part of the Fláajökull foreland, Iceland, based on UAV-derived imagery (Evans et al., 2016a). A 1: 350 scale version of this map is freely available for download from *Journal of Maps*: https://doi.org/10.1080/17445647.2015.1073185.

3.2.2.5. UAV-captured imagery. The recent emergence of UAV technology provides an alternative method for the acquisition of very high-resolution (< 0.1 m per pixel) geospatial data that circumvents some of the issues associated with more established approaches, particularly in relation to temporal resolution and the high cost of acquiring commercial remotely-sensed data (see also Smith et al., 2016a). Following the initial acquisition of the UAV and associated software, this method provides a rapid, flexible and relatively inexpensive means of acquiring up-to-date imagery at an unprecedented spatial resolution, and it is becoming increasingly employed in glacial research (Fig. 7; Rippin et al., 2015; Ryan et al., 2015; Chandler et al., 2016a; Ewertowski et al., 2016; Tonkin et al., 2016; Westoby et al., 2016; Ely et al., 2017; Allaart et al., 2018). UAV-captured images are processed using Structure-from-Motion (SfM) photogrammetry techniques, with *Agisoft Photoscan* being the most common software in use at present (e.g. Chandler et al., 2016a; Evans et al., 2016a; Ely et al., 2017; Allaart et al., 2018). This methodology has enabled the production of sub-decimetre resolution orthophotographs and DEMs with centimetre-scale error values (RMSEs < 0.1 m; see Section 4.4) for glacial geomorphological mapping (e.g. Evans et al., 2016a; Ely et al., 2017). Although surveying of GCPs is still preferable for processing UAV-captured imagery, a direct georeferencing workflow (see Turner et al., 2014b, for further details) is capable of producing reliable geospatial datasets from imagery captured using consumer-grade UAVs and cameras, without the need for expensive survey equipment (see Carbonneau and Dietrich, 2017).

The use of UAVs will be valuable in future glacial geomorphological research due to their flexibility and low-cost. In particular, UAVs open up the exciting possibility of undertaking repeat surveys at high temporal (sub-annual to annual) resolutions in modern glacial settings (Immerzeel et al., 2014; Chandler et al., 2016b; Ely et al., 2017). Multi-temporal UAV imagery will enable innovative geomorphological studies on issues such as (i) the modification and preservation potential of landforms over short timescales (Ely et al., 2017), (ii) the frequency of ice-marginal landform formation, particularly debates on sub-annual to annual landform formation (Chandler et al., 2016b), and (iii) changes in process-form regimes at contemporary ice-margins (Evans et al., 2016a).

Using UAVs to capture aerial imagery is not without challenges, particularly in relation to the challenge of intersecting suitable weather conditions in modern glacial environments: many UAVs are unable to fly in high windspeeds, whilst rain can infiltrate electrical components and create hazy imagery (Ely et al., 2017). Flight times and areal coverage are also limited by battery life, with some battery packs permitting as little as 10 minutes per flight. There are also legal considerations, with the use of UAVs prohibited in some localities/countries or requiring licenses/permits. Moreover, there may be restrictions on flying heights and UAVs may need to be flown in visual line of sight, further limiting areal coverage. Nevertheless, we envisage UAV technology becoming more widespread and a key tool in high-resolution glacial geomorphological investigations, especially if future technological developments can increase the range of conditions in which UAVs can be flown. In future, it is likely that UAV technology will be primarily used for investigating short-term changes across relatively small areas.

3.3. Image processing for mapping

An important part of geomorphological mapping is processing remotely-sensed datasets in preparation for mapping, but this is often given limited prominence in glacial geomorphological studies. Crucially, processing of remotely-sensed data aids the identification of glacial landforms and ensures accurate transfer of geomorphological data from the imagery. In the sections below, we provide a brief overview of image processing solutions for aerial photographs (Section 3.3.1), satellite imagery (Section 3.3.2) and DEMs (Section 3.3.3). Reference is made to common processing techniques used to remove distortion and displacement evident in aerially-captured imagery (see Campbell and Wynne (2011) and Lillesand et al. (2015) for further details), but these are not discussed in detail for reasons of brevity and clarity. However, a detailed workflow diagram outlining the potential procedures for a range of scenarios (depending on data, resources and time) is available as Supplementary Material. We emphasise that compromises and pragmatic solutions are necessary, particularly in the case of aerial photographs, as the 'idealised' scenario is frequently not an option due to data limitations or logistical constraints.

3.3.1. Aerial photograph processing

Aerial photographs contain varying degrees of distortion and displacement owing to their central (or perspective) projection. Geometric distortion is related to radial lens distortion and refraction of light rays in the atmosphere. Additional displacement occurs as a result of the deviation of the camera from a vertical position (caused by roll, pitch and yaw of the aircraft), and the relief and curvature of the Earth. Non-corrected aerial photographs are therefore characterised by relief displacement and scale variations, which increase towards the edges of the photograph (see Campbell and Wynne (2011) and Lillesand et al. (2015) for further details). Thus, it is necessary to apply geometric corrections to aerial photographs before geomorphological mapping.

Ideally, aerial photographs should be corrected using stereoscopic (or conventional) photogrammetric processing in software packages such as *Imagine Photogrammetry* (formerly *Leica Photogrammetry Suite*, or *LPS*). This approach involves the extraction of quantitative elevation data from stereoscopic (overlapping) imagery to generate DEMs and orthorectified imagery (see also Section 3.2). Internal and external parameters, along with the location of GCPs, are used to establish the relationship between the position of the images and a ground co-ordinate system (e.g. Kjær et al., 2008; Bennett et al., 2010). However, this approach may be impractical and unsuitable in many glacial settings. For example, it is unrealistic to collect GCPs using (heavy) survey equipment (e.g. RTK-GPS) in former plateau icefield and ice-cap settings due to their location (remote, upland environments) and the size of the study area (and thus quantity of aerial photographs and GCPs required). Moreover, camera calibration data (focal length, fiducial marks, principal point coordinates and lens distortion) are frequently unavailable or incomplete for archive datasets, and the process is not applicable to acetate overlays. Thus, orthorectification of imagery – three-dimensional correction of geometric distortions – is typically precluded over larger areas, although it may be possible to employ this approach for individual cirque basins, valleys, and glacier forelands (e.g. Wilson, 2005; Bennett et al., 2010; Chandler et al., 2016a). Consequently, pragmatic solutions are required for georectification of imagery, i.e. the process of transforming and projecting imagery to a (local) planar coordinate system. Several approaches have been used to overcome this and we briefly outline these below in relation to analogue aerial photographs (Section 3.3.1.1) and digital aerial photographs (Section 3.3.1.2).

3.3.1.1. Analogue aerial photograph processing. A pragmatic solution to correcting analogue (hard-copy) aerial photographs is to georeference scanned copies of acetate overlays or the original aerial photographs to reference points on other forms of (coarser) georeferenced digital imagery (if available; e.g. DEMs, orthorectified radar images, satellite images). The scanned images can then be georectified and resampled using the georeferencing functions within GIS and remote sensing programmes such as *ArcGIS* or *Erdas Imagine* (cf. Boston, 2012a, for further details). This approach is particularly useful when hard-copy aerial photographs are used in combination with (coarser) digital imagery. Using this procedure, georeferenced acetate overlays of Quaternary features in the Scottish Highlands have been produced with RMSE values ranging between 2.71 m and 7.82 m (Boston, 2012a),

comparable to archival aerial photographs that have been processed using stereoscopic photogrammetric techniques (e.g. Bennett et al., 2010).

The above georectification method works best if relatively small areas are mapped on one acetate. This is because radial distortion increases towards the edges of aerial photographs, which presents a significant problem for matching reference points when large areas have been mapped. From our experience, we estimate the maximum effective area that can be corrected without the danger of mismatches is ~6 km^2. However, this figure depends on the terrain conditions and would have to be smaller in high mountain areas where relief distortion is increased due to greater differences between valleys and adjacent peaks (Lillesand et al., 2015). The mapped area could, conversely, be somewhat larger in low-relief terrain because objects are roughly equally as far away from the camera lens over larger areas and thus subject to less distortion (Kronberg, 1984; Lillesand et al., 2015). The aforementioned constraints might seem to make georectification from hard-copy aerial photographs a laborious process, but this is counterbalanced by being able to record small landforms in great detail due to the high-resolution 3D visualisation allowed by stereopairs.

3.3.1.2. Digital aerial photograph processing. Digital aerial photographs can be georeferenced within GIS and remote sensing software following a similar process to that outlined in Section 3.3.1.1, i.e. digital aerial photographs can be georeferenced to other forms of (coarser) georeferenced imagery. Alternatively, SfM photogrammetry can be used to produce orthophotographs and DEMs from digital aerial photographs, which partly circumvents issues relating to incomplete or absent camera calibration data (e.g. Chandler et al., 2016a; Evans et al., 2016e, 2017; Tonkin et al., 2016; Mertes et al., 2017; Midgley and Tonkin, 2017). SfM photogrammetry functions under the same basic principles as stereoscopic photogrammetry, but there are some fundamental differences: the geometry of the 'scene', camera positions and orientation are solved automatically in an arbitrary 'image-space' coordinate system without the need to specify either the 3D location of the camera or a network of GCPs with known 'object-space' coordinates (cf. Westoby et al., 2012; Carrivick et al., 2016; Smith et al., 2016a, for further details). However, positional data (GCPs) are still required to process the digital photographs for geomorphological mapping, i.e. to assign the SfM models to an 'object-space' coordinate system. Ideally, this should be conducted through ground control surveys (see above), but a potential pragmatic solution is to utilise coordinate data from freeware virtual globes such as *Bing Maps* (see also Supplementary Material). Position information ('object-space' coordinates) is introduced after model production, with the benefit that errors in GCPs will not propagate in the DEM.

3.3.2. Satellite imagery processing

Satellite imagery products are typically available in georectified form as standard and therefore do not require geometric correction prior to geomorphological mapping. With respect to high-resolution, commercial satellite imagery (e.g. WorldView-4 captured imagery; 0.31 m Ground Sampled Distance), these products are often available for purchase as either georeferenced and orthorectified products (with consumers able to define the processing technique used) at comparable prices to commercial aerial photographs, thereby removing the need for photogrammetric processing. Alternatively, it is possible to purchase less expensive 'ortho-ready' imagery and perform orthorectification (where DEM or GCP data are available), thus providing greater end-user control on image processing (e.g. Chandler et al., 2016a; Ewertowski et al., 2016).

Although satellite imagery does not typically require geometric correction for mapping, it is important to consider the choice of band combinations when using multispectral satellite imagery (e.g. Landsat, ASTER; Table 1). Since the detection of glacial landforms from optical satellite imagery relies on the interaction of reflected radiation with topography, different combinations of spectral bands can be employed to optimise landform identification (see Jansson and Glasser, 2005). Manipulating the order of bands with different spectral wavelengths allows the generation of various visualisations, or false-colour composites, of the terrain. For example, specific band combinations may be particularly useful for detecting moraine ridges (7, 5, 2 and 5, 4, 2), mega-scale glacial lineations (4, 5, 6) and meltwater channels (4, 3, 2) from Landsat TM and ETM+ imagery (Jansson and Glasser, 2005;

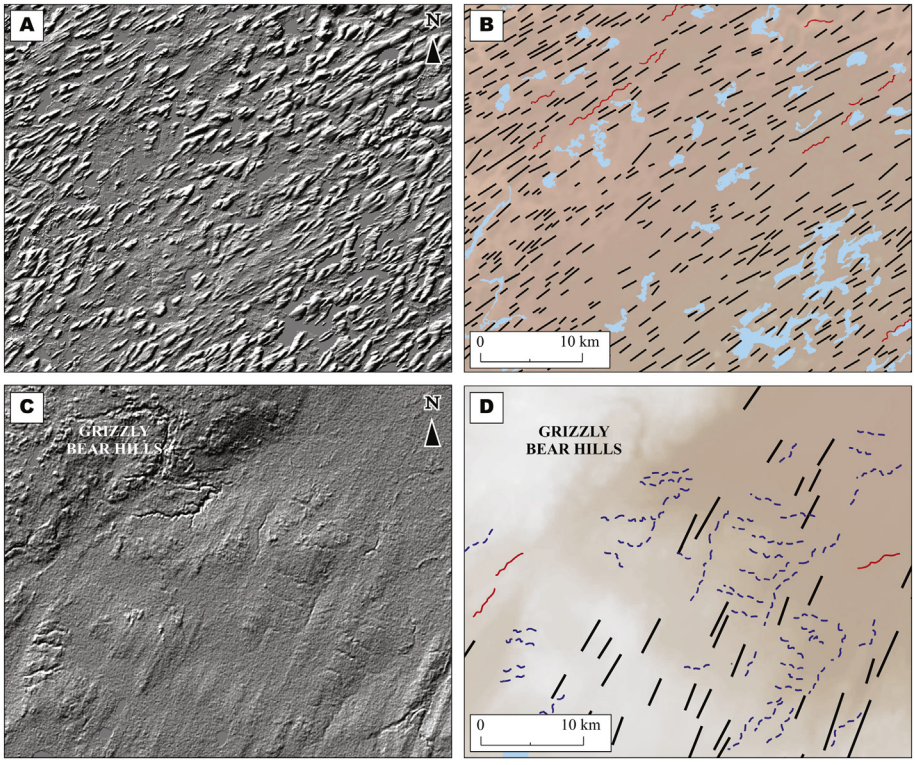

Fig. 8. Example of geomorphological mapping conducted from hillshaded relief models (modified from Norris et al., 2017). (A) Densely spaced drumlins and (B) highly elongated flutings in northwest Saskatchewan, Canada, visualised in hillshaded relief models generated from SRTM DEM data. Geomorphological map extracts in (C) and (D) show lineations (black lines), eskers (red lines) and meltwater channels (dashed blue lines).

Heyman et al., 2008; Lovell et al., 2011; Morén et al., 2011). This is principally due to the change in surface vegetation characteristics (e.g. type, density, and degree of development) between different landforms, and between landforms and the surrounding terrain. For example, moraine ridges or the crests of glacial lineations are typically better drained and therefore less densely vegetated than intervening low-relief areas. In contrast, former meltwater channels typically appear as overly-wide corridors (relative to any modern drainage) of lush green vegetation and stand out clearly as bright red when using a near-infrared false-colour composites (bands 4, 3, 2: Landsat TM and ETM+), since the chlorophyll content of surface vegetation is strongly reflected in near-infrared bands (band 4: Landsat TM and ETM+). In addition to the manipulation of band combinations during the mapping process, it can also be beneficial to use satellite image derivatives based on ratios of band combinations, such as vegetation indices (see Walker et al., 1995) and semi-automated image classification techniques (e.g. Smith et al., 2000, 2016b).

Aside from manipulating spectral band combinations, it may also be beneficial to use the higher-resolution panchromatic band as a semi-transparent layer alongside the multispectral bands to aid landform detection (e.g. Morén et al., 2011; Stroeven et al., 2013; Lindholm and Heyman, 2016), or to merge the pixel resolutions of a higher resolution panchromatic band with lower resolution multispectral bands through 'pan-sharpening' techniques (e.g. Glasser and Jansson, 2008; Greenwood and Clark, 2008; Storrar et al., 2014; Chandler et al., 2016a; Ewertowski et al., 2016). Pan-sharpening can be particularly valuable when it is desirable to have both multispectral capabilities (e.g. different band combinations to differentiate between features with varying surface characteristics) and higher-spatial resolutions to help determine the extent and morphology of individual landforms.

3.3.3. Digital Elevation Model processing

Various processing techniques are available that can be beneficial when identifying and mapping glacial landforms from DEMs (Bolch and Loibl, 2017). DEM data are typically converted into 'hillshaded relief models' for mapping (Fig. 8), whereby different solar illumination angles and azimuths are simulated within GIS software to produce the shaded DEMs. This rendition provides a visually realistic representation of the land surface, with shadows improving detection of surface features. Ideally, hillshaded relief models should be generated using a variety of illumination azimuths (direction of light source) and angles (elevation of light source) to alleviate the issue of 'azimuth bias', the notion that some linear landforms are less visible when shaded from certain azimuths (see Lidmar-Bergström et al., 1991; Smith and Clark, 2005). An illumination angle of 30° and azimuths set at orthogonal positions of 45° and 315° have been suggested as optimal settings for visualisation (Smith and Clark, 2005; Hughes et al., 2010). Vertical exaggeration of these products (e.g. three to four times) can also aid landform identification (e.g. Hughes et al., 2010). Semi-transparent DEMs can be draped over shaded-relief images to accentuate topographic contrasts (Fig. 9), or a semi-transparent satellite image can be draped over a DEM to achieve both a multispectral and topographic assessment of a landscape (e.g. Jansson and Glasser, 2005). First- and second-order DEM-derivatives, including surface gradient (slope) and curvature, have also been found to be useful for mapping (e.g. Smith and Clark, 2005; Evans, 2012; Storrar and Livingstone, 2017).

4. Assessment of mapping errors and uncertainties

In this section, we provide an overview of the main sources of error and uncertainty associated with the various geomorphological mapping methods introduced in the preceding sections. Consideration and

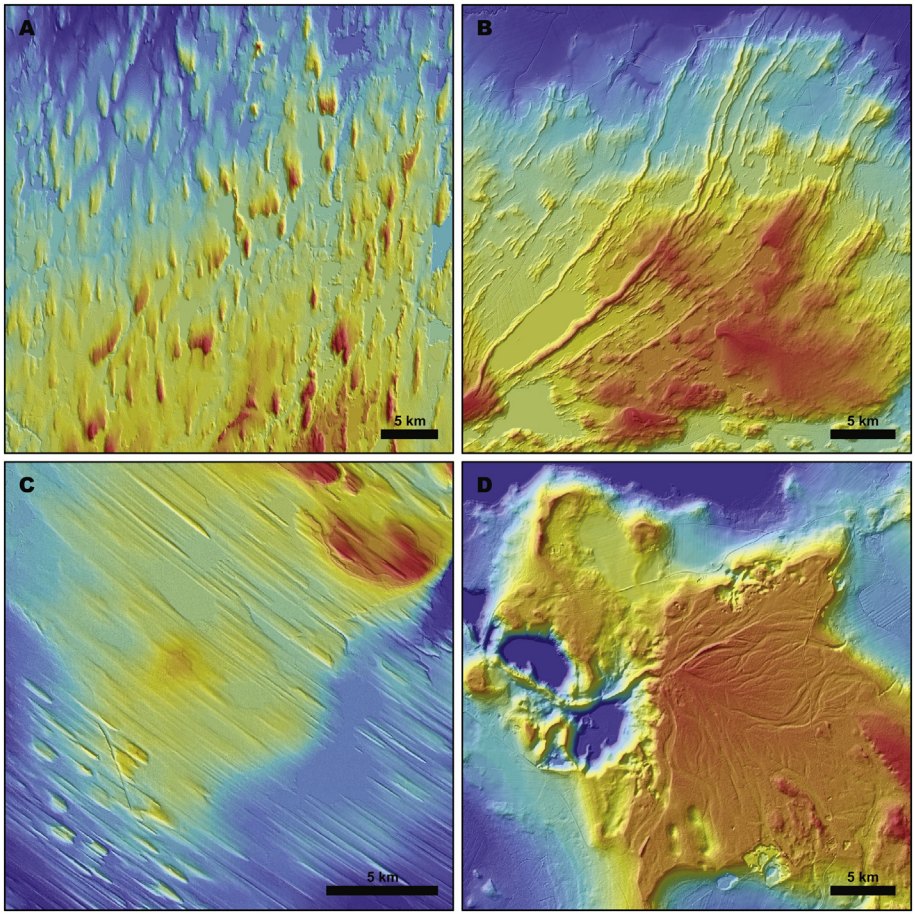

Fig. 9. Examples of landforms in relief-shaded DEMs. Red indicates higher elevations and blue lower elevations. (A) Lineations in N Canada shown in 16 m resolution CDED data. (B) De Geer moraines in SW Finland shown in 2 m resolution LiDAR data. (C) Lineations of the Dubawnt Lake Ice Stream shown in 5 m resolution ArcticDEM mosaic data. (D) Esker-fed ice-contact outwash fan in SW Finland shown in 2 m resolution LiDAR data. See Table 2 for DEM data sources.

management of mapping errors should be an important part of glacial geomorphological mapping studies because any errors/uncertainties incorporated in the geomorphological map may propagate into subsequent palaeoglaciological and palaeoclimatic reconstructions. This is of most relevance to small ice masses (cirque glaciers, valley glaciers, outlet glaciers), e.g. metre-scale geolocation errors would have significant implications for studies aiming to establish ice-margin retreat rates of the order of tens of metres (e.g. Krüger, 1995; Lukas and Benn, 2006; Lukas, 2012; Bradwell et al., 2013; Chandler et al., 2016b). Conversely, any mapping errors might be negligible in the context of continental-scale ice sheet reconstructions (e.g. Hughes et al., 2016; Stroeven et al., 2016; Margold et al., 2018).

The overall 'quality' of a geomorphological map is a function of three interlinked factors: mapping resolution, accuracy, and precision. It is important to highlight that, irrespective of the mapping method employed (field or remote-based), the accuracy and precision of the mapping reflects two related factors: (i) the skill, philosophy, and experience of the mapper; and (ii) the detectability of the landforms (Smith and Wise, 2007; Otto and Smith, 2013; Hillier et al., 2015). Mapper philosophy concerns issues such as how landforms are mapped (e.g. generalised mapping vs. mapping the intricate details of individual landforms) and interpreted (e.g. differences in terminology and landform classification), which will partly vary with study objectives and mapper background and training. The significance of skill, philosophy and experience in mapping is exemplified by the stark differences across boundaries of British Geological Survey (BGS) map sheets that have been mapped by different surveyors (cf. Clark et al., 2004).

A key determinant of landform detectability is resolution, generally defined as the finest element that can be distinguished during survey/observation (Lam and Quattrochi, 1992). In geomorphological mapping it may be, for example, the smallest distinguishable landform that is visible from remotely-sensed data or that can be drawn on a field map. The accuracy of geomorphological mapping relates to positional accuracy (i.e. difference between 'true' and mapped location of the landform), geometric accuracy (i.e. difference between 'true' and mapped shape of the landform), and attribute accuracy (i.e. deviation between 'true' and mapped landform types) (Smith et al., 2006). For spatial data, it is usually not possible to obtain absolute 'true' data, due to limitations such as the 'resolution' of remotely-sensed data and the accuracy of instruments/surveying equipment. Precision is often used to express the reproducibility of surveys, which is controlled by random errors. These are errors that are innate in the survey/observation process and cannot be removed (Butler et al., 1998). We now outline the specific uncertainties associated with field mapping (Section 4.1), analogue remote mapping (Section 4.2) and digital remote mapping (Section 4.3).

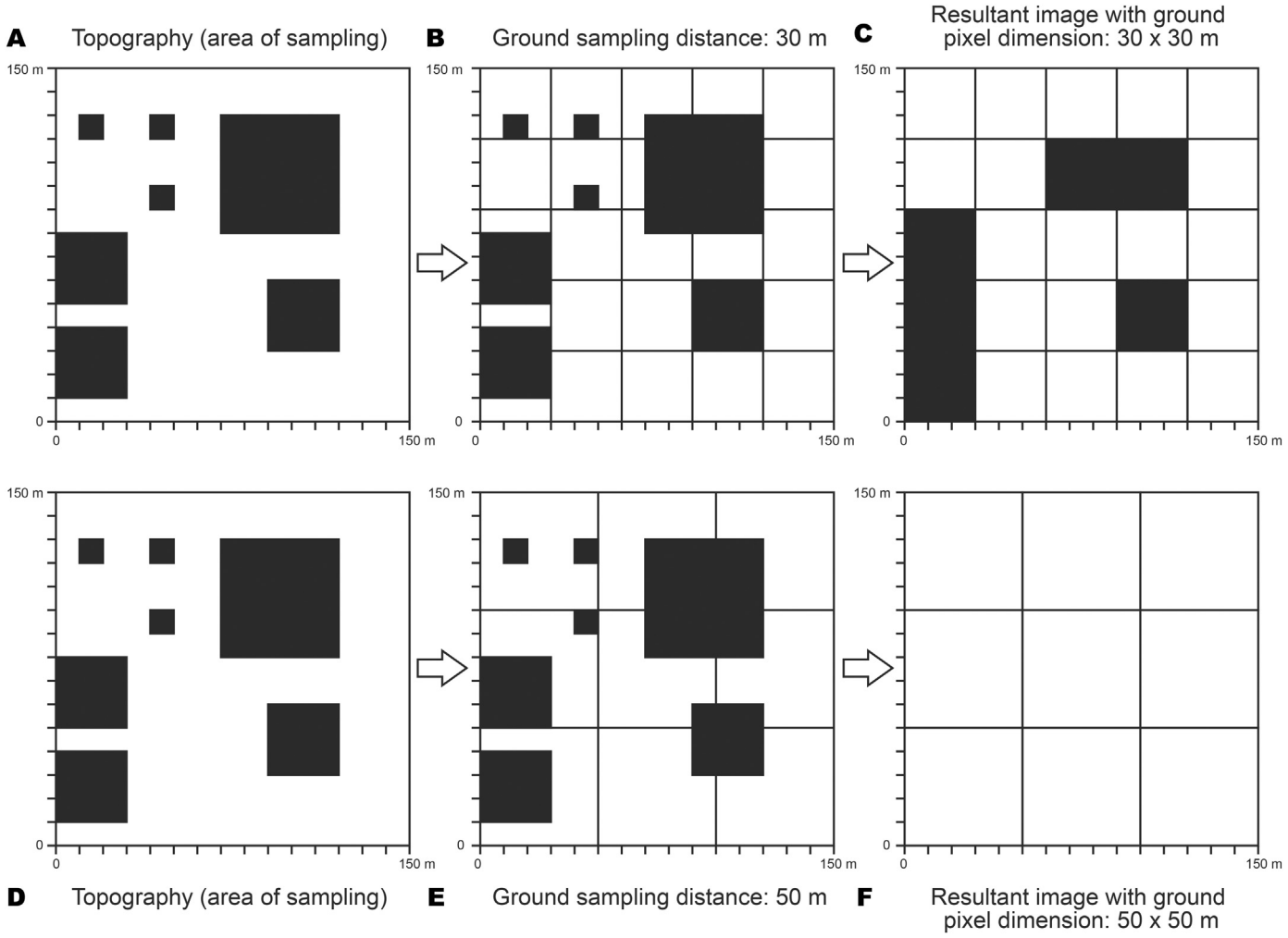

Fig. 10. Conceptual diagrams illustrating the distinction between Ground Sampled Distance (B and E) and pixel size (C and F). The ground distances between two measurements by the detector (i.e. the Ground Sampled Distances) are 30 m and 50 m in (B) and (E), respectively. These Ground Sample Distances are then assigned to pixels in the resulting 30 x 30 m (C) and 50 x 50 m (F) digital images. Note, resultant images may fail to accurately represent the shape of the objects (upper row) or may even fail to reproduce them (lower row), even where the size of the object is the same or larger than the sampling distance.

4.1. Field mapping errors and uncertainty

The correct positioning, orientation and scale of individual geomorphological features on field maps is dependent on the skill of the mapper and the ability to correctly interpret and record landforms. If a handheld GNSS device is used to locate landforms in the field, the positional accuracy is usually restricted to several metres and related to three factors: (i) the quality of the device (e.g. antenna, number of channels, ability to use more than one GNSS); (ii) the position of satellites; and (iii) the characteristics of the surrounding landscapes and space weather (solar activity can affect signal quality). Higher accuracy (cm- or even mm-scale) can only be achieved when supplemented by measurements using additional surveying (e.g. differential Global Positioning Systems (dGPS), real time kinematic (RTK-) GPS or total station). Alongside positioning errors, the horizontal resolution (and, consequently, accuracy) of the field map is related to line thickness on the field map (Knight et al., 2011; Boston, 2012a, b; Otto and Smith, 2013). A pencil line has a thickness of between 0.20 and 0.50 mm on a field map; therefore, individual lines represent a thickness of between 2 and 5 m on 1: 10,000 scale maps, rendering the maps accurate to this level at best (Raisz, 1962; Robinson et al., 1995; Boston, 2012a). This necessitates some element of selection during field mapping of relatively small landforms formed by alpine- and plateau-style ice masses, as not all the information that can be seen in the field can be mapped, even at a large scale such as 1: 10,000. In terms of the vertical accuracy of field maps, it should be recognised that the mapping is only as accurate as the resolution of the source elevation data: if the topographic base map has contours at 10 m intervals, the mapping has a vertical resolution, and thus accuracy, of 10 m at best, irrespective of the (perceived) skill of the cartographer. As with positional accuracy, higher vertical accuracy necessitates the use of geodetic-grade surveying equipment.

4.2. Analogue remote mapping errors and uncertainty

Accurate detection and mapping of individual landforms from analogue (hard-copy) aerial photographs is influenced by factors such as the scale or resolution of the photographs, shadow length (shadows may obscure the 'true' planform or landforms altogether), the presence/absence of vegetation, cloud cover, and tonal contrast (photographs may appear 'flat', thus limiting landform detection). The resolution of analogue remotely-sensed datasets is associated with scale, which results from the altitude of the plane, camera lens focal length, and the optical resolution of the lens and sensor (Wolf et al., 2013). The accuracy of the (non-rectified) mapping, as with field mapping, is also limited by the thickness of the pen used for drawing on the acetate sheets. Super-fine pens typically have a nib size of 0.05–0.20 mm; thus, lines on an acetate overlay typically represent thicknesses between ~1.25 m and 5.00 m at a common aerial photograph average scale of 1: 25,000. Despite being particularly useful for detailed mapping of small features and complex landform patterns, the level of accuracy achievable using this method is therefore ~1.25 m at best. However, further errors will be introduced to the geomorphological mapping once the raw, non-rectified acetates are georectified (see Section 3.3.1).

4.3. Digital remote mapping errors and uncertainty

A key influence on landform detectability from digital remotely-sensed data is the scale of the feature relative to the resolution of the digital dataset, with a particular challenge being the mapping of features with a scale close to or smaller than the resolution of the imagery. Conversely, mapping exceptionally large ('mega-scale') glacial landforms can be challenging, depending on the remotely-sensed dataset employed (e.g. Greenwood and Kleman, 2010). Unlike analogue mapping (both in the field and remotely), the thickness of digital lines is not typically a problem for digital mapping, so landform detection and recording are fundamentally linked to spatial resolution. Spatial resolution of digital remotely-sensed data refers to the capability to

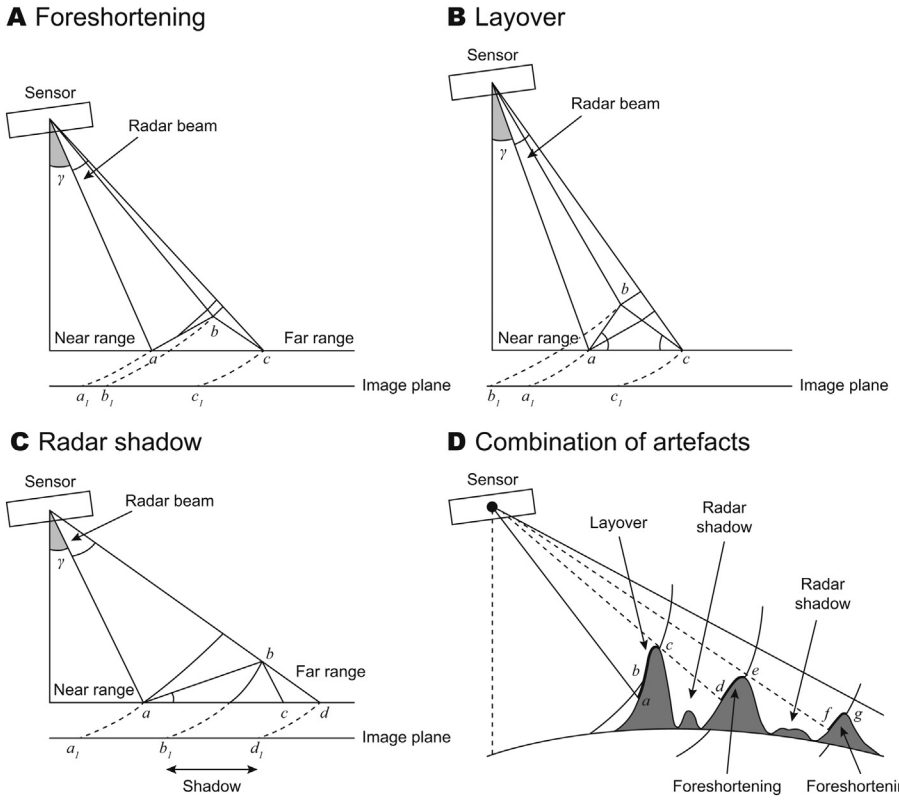

Fig. 11. Geometric artefacts that may be present in space- and air-borne radar captured imagery, resulting from the effects of relief. (A) Foreshortening, occurring where the slope of the local terrain is less than the incidence angle (γ). The facing slope, $a - b$, becomes compressed to $a_1 - b_1$ in the resulting image. (B) Layover, occurring in steep terrain when the slope angle is greater than the incidence angle. As a mountain-top, b, is closer to the sensor than the base, a, this causes layover in the imagery (an incorrect positioning of b_1 relative to a_1). (C) Radar shadow in areas of rugged terrain as the illumination is from an oblique source. No data is recorded for the region $b_1 - d_1$. (D) In regions of varying topography, a combination of artefacts may be present: points b and c will be impacted by layover and will be positioned incorrectly relative to a; no data will be recorded for the region between c and d due to radar shadow; foreshortening occurs at slope facet $d - e$; further radar shadow occurs at $e - f$; and foreshortening at f and g. After Clark (1997).

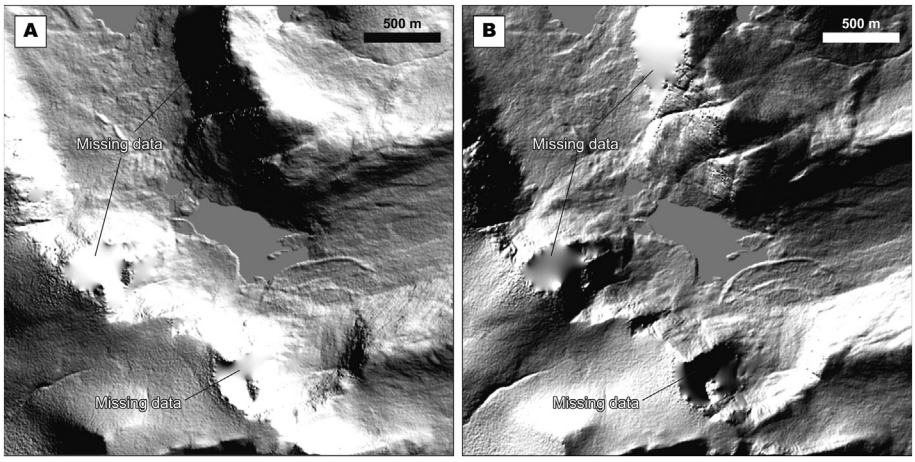

Fig. 12. Extracts from hillshaded relief models of Ben More Coigach, NW Scottish Highlands, showing the effect of geometric artefacts on the models. The hillshades were generated with azimuths of 45° (A) and 315° (B). Stretching of upland terrain during processing of the DEM data results in blurred regions on the hillshaded relief models. NEXTMap DSM from Intermap Technologies Inc. provided by NERC via the NERC Earth Observation Data Centre.

distinguish between two objects, typically expressed as either (i) pixel size or grid cell size or (ii) Ground Sampled Distance. Pixel/grid size refers to the projected ground dimension of the smallest element of the digital image (Fig. 10), whilst Ground Sampled Distance (GSD) refers to the ground distance between two measurements made by the detector (the value of measurement is subsequently assigned to a pixel) (Fig. 10; Duveiller and Defourny, 2010). In practice, the spatial resolution of digital imagery is lower than the pixel size (Fig. 10).

Landform detectability from raster images (i.e. remotely-sensed data) can be considered with reference to the Nyquist-Shannon sampling theorem, since they comprise discrete sampled values. According to this theorem, the *intrinsic resolution* is twice the sampling distance of the measured values, whereas the *nominal resolution* is twice the pixel/grid size (cf. Pipaud et al., 2015, and references therein). The *effective resolution* and, consequently, the minimum landform footprint/planform that can be unambiguously sampled are defined by the smaller of these two values (cf. Pike, 1988). Where the Nyquist–Shannon criterion is not satisfied for either the intrinsic or nominal resolution, landforms with footprints below the critical value may be visible but are rendered ambiguously in digital imagery, i.e. their boundaries are not clearly definable and mappable (cf. Cumming and Wong, 2005). Further factors that influence landform identification from digital imagery include the strength of the landform signal relative to background terrain, and the azimuth bias introduced by differences in the orientation of linear features and the illumination angle of the sun (Smith and Wise, 2007), along with localised issues such as cloud cover, snow cover, areas in shadow, and vegetation. The timing of data collection is also a key factor, particularly in the case of modern glacial environments (see Section 5.3).

Aside from the factors outlined above, (raw) remotely-sensed data will contain distortion and/or geometric artefacts of varying degrees. Distortions inherent in raw aerial photographs can be partially or almost fully removed during georeferencing of acetate sheets or photogrammetric processing of aerial photographs (see Section 3.3.1). Raw satellite imagery will contain biases related to attitude, ephemeris and drift errors, as well as displacements related to the relief, which, similarly to aerial photographs, is more visible in mountainous areas than in lowland settings (Grodecki and Dial, 2003; Shean et al., 2016). With respect to DEMs, some datasets captured using air- and space-borne radar approaches may contain a number of artefacts (Clark, 1997; Fig. 11), with geometric artefacts particularly significant in upland settings. Geometric artefacts, such as foreshortening and layover, are corrected during image processing by stretching high terrain into the correct position, which can result in a smoothed region on steep slopes (Fig. 12). In other parts of upland terrain, information will be lost on the leeside of slopes, away from the sensor, where high ground prevents the radar beam from reaching the lower ground beneath it (Fig. 11). Such issues can be alleviated, at least partly, by examining multiple complementary remotely-sensed datasets and mapping at a variety of scales.

4.4. Assessment and mitigation of uncertainties

Due to the subjective nature of geomorphological mapping, assessing mapping precision is not an easy task. One possible approach is to compare results of mapping using different datasets/methods with a dataset perceived to be more 'truthful' (i.e. field-based survey) (Smith et al., 2006). The number, size and shape of mapped landforms in comparison with a 'true' dataset can be used as an approximation of mapping reliability. Precision and accuracy of the produced geomorphological map can also be estimated based on the quality of the source data. Most of the datasets are delivered with at least some assessment of uncertainties, often expressed as accuracy, e.g. the SRTM DEM has a horizontal accuracy of ± 20 m and a vertical accuracy of ± 16 m (Rabus et al., 2003). Alternatively, some remotely-sensed datasets have an associated *total root mean square error* (RMSE), which indicates displacement between 'true' control points and corresponding points on the remotely-sensed data (Wolf et al., 2013). However, both are

Table 3
Summary of the glacial settings where the main geomorphological mapping methods and remotely-sensed data types are *most* appropriate. ✓ = the method/dataset is appropriate and should be used (where the dataset is available). ● = the method is applicable in certain cases, depending on factors such as the resolution of the *specific* dataset, the size of the study area and landforms, and the accessibility of the study area.

Glacial setting	DEMs	Coarse satellite imagery	LiDAR DEMs	High-resolution satellite imagery	Aerial photographs	UAV imagery	Field mapping
Ice sheets	✓	✓	✓				
Ice sheet sectors/lobes	✓	✓	✓	●	●		●
Ice-caps	●	●	●	✓	✓		✓
Icefields			●	✓	✓		✓
Valley (outlet) glaciers			●	✓	✓	●	✓
Cirque glaciers			●	✓	✓	●	✓
Modern glacier forelands			●	✓	✓	✓	✓

measures of the overall ('global') quality of the dataset. Thus, these errors may be deceptive because such 'global' measures ignore spatial patterns of errors and local terrain characteristics (cf. Lane et al., 2005; James et al., 2017). For example, DEM errors will typically be more pronounced on steep slopes, where even a small horizontal shift will incur large differences in elevation.

Ideally, remotely-sensed datasets should be evaluated independently by the mapper to establish their geolocation accuracy (accuracy of *x*, *y* and *z* coordinates). If feasible, surveys of GCPs should be conducted using geodetic-grade surveying equipment (e.g. RTK-GPS, total station). A sub-sample of this GCP dataset can be used for photogrammetric processing and allow RMSEs to be calculated. Subsequently, the remaining GCPs (i.e. those not used for photogrammetric processing) can be used to perform a further quality check, by quantifying deviations from the coordinates of the GCPs and the corresponding points on the generated DEM (e.g. Carrivick et al., 2017). An additional approach, in geomorphologically stable areas, is to compare the location of individual data points from the DEM (or raw point cloud) being used for mapping with those on a reference DEM (or raw point cloud) (e.g. King et al., 2016b; Carrivick et al., 2017; James et al., 2017; Mertes et al., 2017; Midgley and Tonkin, 2017). Parameters such as the mean deviation, standard deviation and relative standard

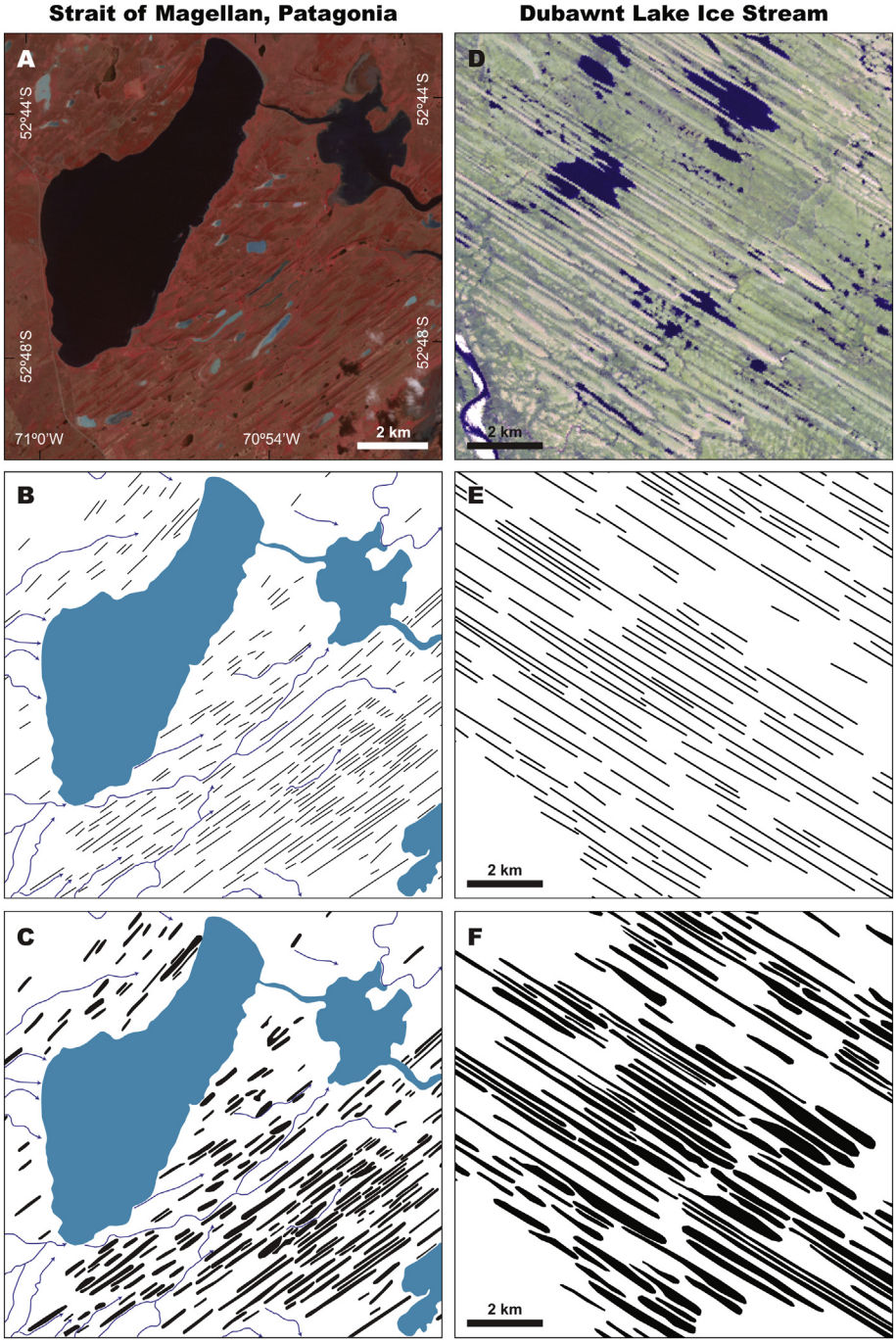

Fig. 13. Example mapping of subglacial bedforms from the Strait of Magellan, Patagonia (A–C), and the Dubawnt Lake Ice Stream (D–F). The bedforms are mapped as polylines along landform crests in (B) and (E), and they are mapped as polygons delineating lower-break-of-slope in (C) and (F). The Dubawnt Lake Ice Stream polylines (Stokes and Clark, 2003) and polygons (Dunstone, 2014) were mapped by different mappers at different times, which may account for small inconsistencies. For further details on the bedform examples from the Strait of Magellan, see Lovell et al. (2011) and Darvill et al. (2014).

deviation between the two datasets can then be calculated to perform a quantitative assessment of quality and accuracy of the DEM (e.g. King et al., 2016b; Mertes et al., 2017). Performing these assessments may then facilitate correction of the processed datasets (e.g. Nuth and Kääb, 2011; Carrivick et al., 2017; King et al., 2017).

To some extent, residual uncertainties relating to the skill, philosophy and experience of the mapper may be reduced by developing a set of clear criteria for identifying and mapping particular landforms (e.g. Barrell et al., 2011; Darvill et al., 2014; Bendle et al., 2017a; Lovell and Boston, 2017). That said, there are currently no 'agreed' genetic classification schemes for interpreting glacial sediment-landform assemblages, despite the development of facies and landsystem models for particular glacial environments (e.g. Eyles, 1983; Brodzikowski and van Loon, 1991; Evans, 2003a; Benn and Evans, 2010). Indeed, terminologies are inconsistently used in glacial geomorphological research, as different 'schools' or traditions still exist. Thus, it is probably most appropriate to select a scheme that has been in frequent use in a given area (to enable ready comparison) or to develop one suited for a particular area or problem. Notwithstanding potential discrepancies relating to genetic classification or terminology, this will at least ensure transparency in future use and analysis of the geomorphological mapping.

Given the influence of the individual mapper on accuracy and precision, it may be beneficial and desirable for multiple mappers to complete (initially) independent field surveys and examination of remotely-sensed datasets to enhance reliability and reproducibility (cf. Hillier et al., 2015; Ewertowski et al., 2017). However, this approach would only be applicable in collaborative efforts and may be impractical due to various factors (e.g. study area size, data access restrictions). The level of detection of individual landforms might be improved by employing multiple methods to enhance landform detectability, whilst the genetic interpretation of landforms (landform classification) can be tested by detailed sedimentological investigations (see Section 2.3). Some uncertainties associated with the quality of the data source (e.g. shadows, artefacts) can be alleviated, at least partly, by examining multiple complementary remotely-sensed datasets and mapping at a variety of scales.

5. Scale-appropriate mapping approaches

The following sections place the presented geomorphological mapping methods (see Sections 2 and 3) in the spatial and temporal context of the glacial settings in which they are commonly used, demonstrating that particular methods are employed depending on factors such as the size of the study area, former glacial system, and landform assemblages (Table 3). We focus on three broad glacial settings for the purposes of this discussion: palaeo-ice sheets (Section 5.1), alpine- and plateau-style ice masses (Section 5.2), and the forelands of modern cirque, valley and outlet glaciers (Section 5.3). Although geomorphological mapping in modern glacial settings follows the same general procedures as in former alpine and plateau-style ice mass settings (see Section 6.2), specific consideration of contemporary glacier forelands is warranted due to important issues relating to the temporal resolution of remotely-sensed data and landform preservation potential, which are not as significant in palaeoglaciological settings.

5.1. Palaeo-ice sheet settings

The continental-scale of palaeo-ice sheets typically necessitates a mapping approach that enables systematic mapping of a large area in a time- and cost-effective manner while still allowing accurate identification of landform assemblages at a variety of scales. The nature of the approach will differ depending on the aim of the investigation, as this fundamentally determines *what* needs to be mapped and *how* it should be mapped. Palaeo-ice sheet reconstructions have been produced at a range of scales, from entire ice sheets (e.g. Dyke and Prest, 1987a, b, c; Kleman et al., 1997, 2010; Boulton et al., 2001; Glasser et al., 2008; Clark et al., 2012; Livingstone et al., 2015; Stroeven et al., 2016) to regional/local sectors (e.g. Hättestrand, 1998; Jansson et al., 2003; Stokes and Clark, 2003; Ó Cofaigh et al., 2010; Astakhov et al., 2016; Darvill et al., 2017). Depending on the aim of the study, some investigations may focus specifically on mapping particular landforms. For example, studies of ice-sheet flow patterns frequently focus on mapping subglacial bedforms, such as drumlins (e.g. Boulton and Clark, 1990a, b; Kleman et al., 1997, 2010; Stokes and Clark, 2003; Hughes et al., 2010). Nonetheless, cartographic reduction is often still required to manage the volume of information, resulting in the grouping of similarly-orientated bedforms into flow-sets (occasionally termed fans or swarms) (e.g. Jansson et al., 2002, 2003; De Angelis and Kleman, 2007; Greenwood and Clark, 2009a, b; Stokes et al., 2009; Hughes et al., 2014; Atkinson et al., 2016).

In many cases, studies attempt to incorporate all or most of the common landform types across ice sheet scales to derive palaeoglaciological reconstructions (e.g. Kleman et al., 1997, 2010; Stroeven et al., 2016). The rationale for this is that glaciation styles and processes (e.g. ice-marginal, subglacial) can be inferred from particular combinations of landforms in landform assemblages (e.g. Clayton et al., 1985; Stokes and Clark, 1999; Evans, 2003b; Kleman et al., 2006; Evans et al., 2008, 2014; Darvill et al., 2017; Norris et al., 2018). Establishing relationships between landforms is therefore valuable, not only in understanding glaciation styles, but also in helping decipher the relative sequence of formation (e.g. Clark, 1993; Kleman and Borgström, 1996) that may lay the foundations for absolute dating. Typically, ice sheet investigations are focused on the spatial and temporal evolution of these various aspects, requiring the robust integration of geomorphological mapping with absolute dating techniques (see Stokes et al., 2015). For example, following pioneering palaeoglaciological studies of the Fennoscandian ice sheet (e.g. Kleman, 1990, 1992; Kleman and Stroeven, 1997; Kleman et al., 1997), cosmogenic nuclide exposure dating offered a means to quantify dates of glaciation and rates of deglaciation (e.g. Fabel et al., 2002, 2006; Stroeven et al., 2002a, b, 2006; Harbor et al., 2006). Such data are crucial to tune and validate numerical models used to reconstruct evolving ice sheet limits, flow configurations and subglacial processes (e.g. Boulton and Clark, 1990a, b; Näslund et al., 2003; Evans et al., 2009b; Hubbard et al., 2009; Stokes and Tarasov, 2010; Kirchner et al., 2011; Livingstone et al., 2015; Stokes et al., 2016b; Patton et al., 2017a, b).

5.1.1. Manual mapping of palaeo-ice sheet geomorphological imprints

Satellite imagery and DEMs are the prevailing remotely-sensed datasets used for mapping ice-sheet-scale landforms, and these datasets have been at the forefront of key developments in the understanding of palaeo-ice sheets (cf. Stokes, 2002; Stokes et al., 2015). Notably, the use of satellite imagery resulted in the identification of hitherto-unrecognised mega-scale glacial lineations (MSGLs; Boulton and Clark, 1990a, b; Clark, 1993), which are now recognised as diagnostic geomorphological evidence of ice streams within palaeo-ice sheets (see Stokes and Clark, 1999, 2001, and references therein). This has allowed tangible links to be made between the behaviours of former Quaternary ice sheets and present-day ice sheets (e.g. King et al., 2009; Stokes and Tarasov, 2010; Stokes et al., 2016b). Aerial photograph interpretation and field mapping are also used in some studies (e.g. Hättestrand and Clark, 2006; Kleman et al., 2010; Darvill et al., 2014), but satellite imagery and DEMs are in wider usage for practical reasons (see also Section 3.2). In recent years, the development of LiDAR datasets has led to their increasing application for high-resolution mapping of landforms formed by palaeo-ice sheets, particularly in Scandinavia (e.g. Dowling et al., 2015; Greenwood et al., 2015; Ojala et al., 2015; Ojala, 2016; Mäkinen et al., 2017; Peterson et al., 2017). We expect this to be a major area of growth in future mapping studies of former ice sheets.

Mapping glacial landforms from remotely-sensed data typically involves manual on-screen vectorisation (tracing) using one of two main

approaches: (i) creating polylines along the crestline or thalweg of landforms or (ii) digitally tracing polygons that delineate the breaks of slope around landform margins (i.e. vectorising the planform). The approach employed will depend on the requirements of the study; for example, flow-parallel bedforms (e.g. drumlins and MSGLs) have variously been mapped as polylines (e.g. Kleman et al., 1997, 2010; Stokes and Clark, 2003; De Angelis and Kleman, 2007; Storrar and Stokes, 2007; Livingstone et al., 2008; Brown et al., 2011b) and polygons (e.g. Hättestrand and Stroeven, 2002; Hättestrand et al., 2004; Hughes et al., 2010; Spagnolo et al., 2010, 2014; Stokes et al., 2013; Ely et al., 2016a; Bendle et al., 2017a) (Fig. 13). The rationale behind mapping flow-parallel bedforms as linear features is that dominant orientations of a population provide sufficient information when investigating ice-sheet-scale flow patterns and organisation, although image resolution may also be a determining factor. Mapping polygons allows the extraction of individual landform metrics (e.g. elongation ratios) that can provide insights into subglacial processes (e.g. Ely et al., 2016a) and regional variations in ice sheet flow dynamics (e.g. Stokes and Clark, 2002, 2003; Hättestrand et al., 2004; Spagnolo et al., 2014), but it is far more time-consuming than vectorising linear features. Increasingly, it is being recognised that the population metrics and spectral characteristics of the subglacial bedform 'field' as a whole are most important for

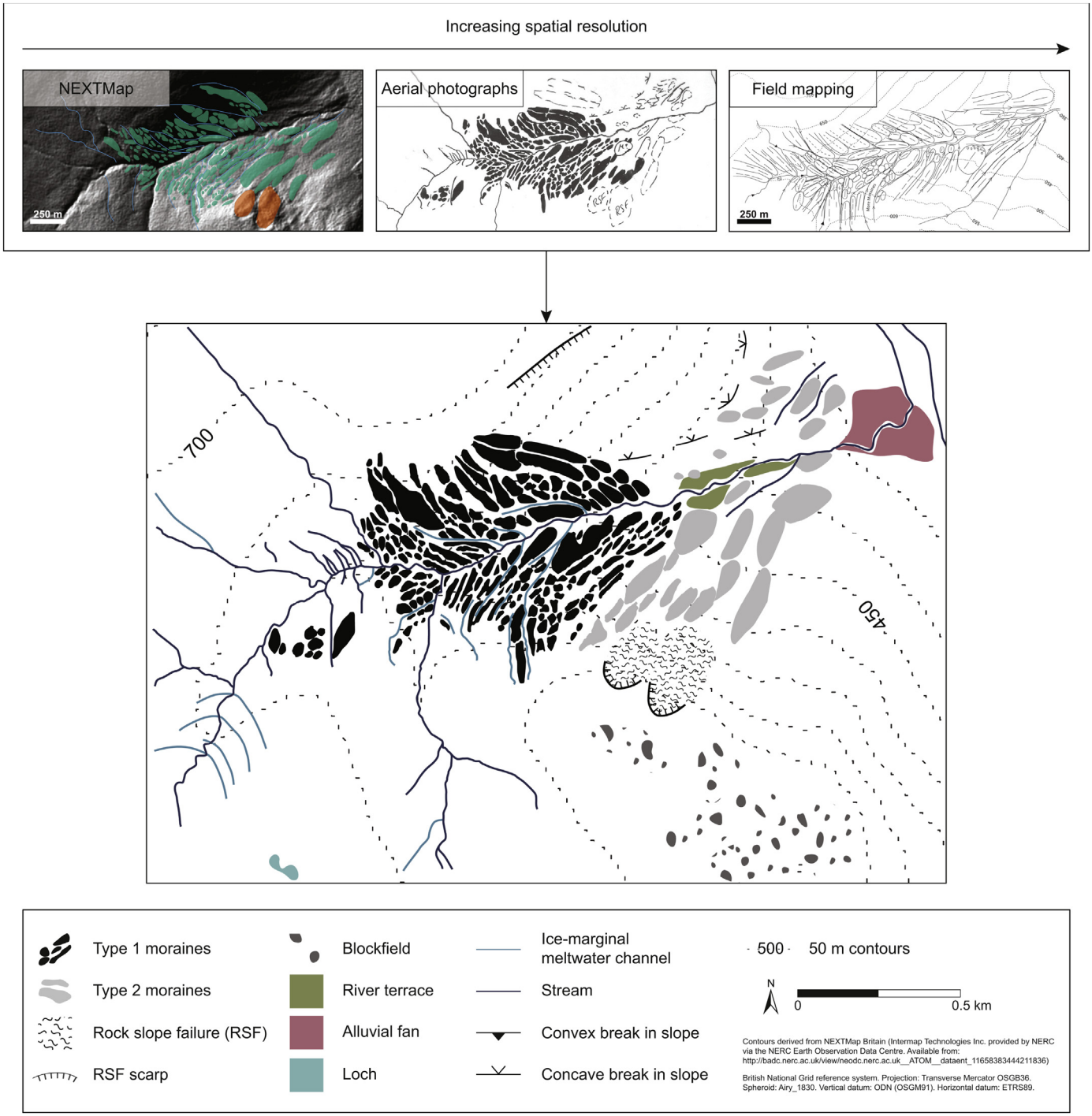

Fig. 14. Geomorphological mapping of Coire Easgainn, Monadhliath, Scotland, using a combination of NEXTMap DSMs, analogue aerial photographs and field mapping. Modified from Boston (2012a, b).

quantifying bedforms and deciphering subglacial processes and conditions (see Hillier et al., 2013, 2016; Spagnolo et al., 2017; Clark et al., 2018b; Ely et al., 2018; Stokes, 2018).

5.1.2. Automated mapping of palaeo-ice sheet geomorphological imprints

Comprehensive mapping of palaeo-ice sheet geomorphological imprints, and particularly of bedforms, typically entails the identification and mapping of large numbers (in some cases > 10,000) of the same, or very similar, types of features (e.g. Hättestrand et al., 2004; Clark et al., 2009; Kleman et al., 2010; Storrar et al., 2013). The manual vectorisation of such large numbers of landforms is a time-consuming process. Consequently, semi-automated and automated mapping techniques are increasingly being applied to glacial geomorphology (e.g. Napieralski et al., 2007b; Saha et al., 2011; Maclachlan and Eyles, 2013; Eisank et al., 2014; Robb et al., 2015; Yu et al., 2015; Jorge and Brennand, 2017a, b), particularly given that features of a single landform type (e.g. drumlins or MSGLs) will have fairly uniform characteristics (orientation, dimensions, and morphology). Automated and semi-automated mapping techniques typically use either a pixel- or an object-based approach (see Robb et al., 2015, and references therein). Thus far, automated and semi-automated approaches have primarily focused on mapping drumlins or MSGLs from medium- to high-resolution DEMs. Several methods have been used, including multi-resolution segmentation (MRS) algorithms (Eisank et al., 2014), a Curvature Based Relief Separation (CBRS) technique (Yu et al., 2015), Object Based Image Analysis (OBIA) (Saha et al., 2011; Robb et al., 2015), and clustering algorithms (Smith et al., 2016b).

Most recently, 2D discrete Fourier transformations have been applied to automatically quantify the characteristics of MSGLs (see Spagnolo et al., 2017). In contrast to traditional mapping approaches, this new method analyses all of the topography (rather than simply focusing on the landforms) to identify the wavelength and amplitude of periodic features (i.e. waves or ripples across the topography) without the need to manually vectorise (trace) them. This automated approach is in its infancy but is likely to provide quantitative data that are useful for (i) testing and parameterising models of subglacial processes and landforms (e.g. Barchyn et al., 2016; Stokes, 2018) and (ii) facilitating comparison between subglacial bedforms and other bedforms (e.g. Fourrière et al., 2010; Kocurek et al., 2010; Murray et al., 2014).

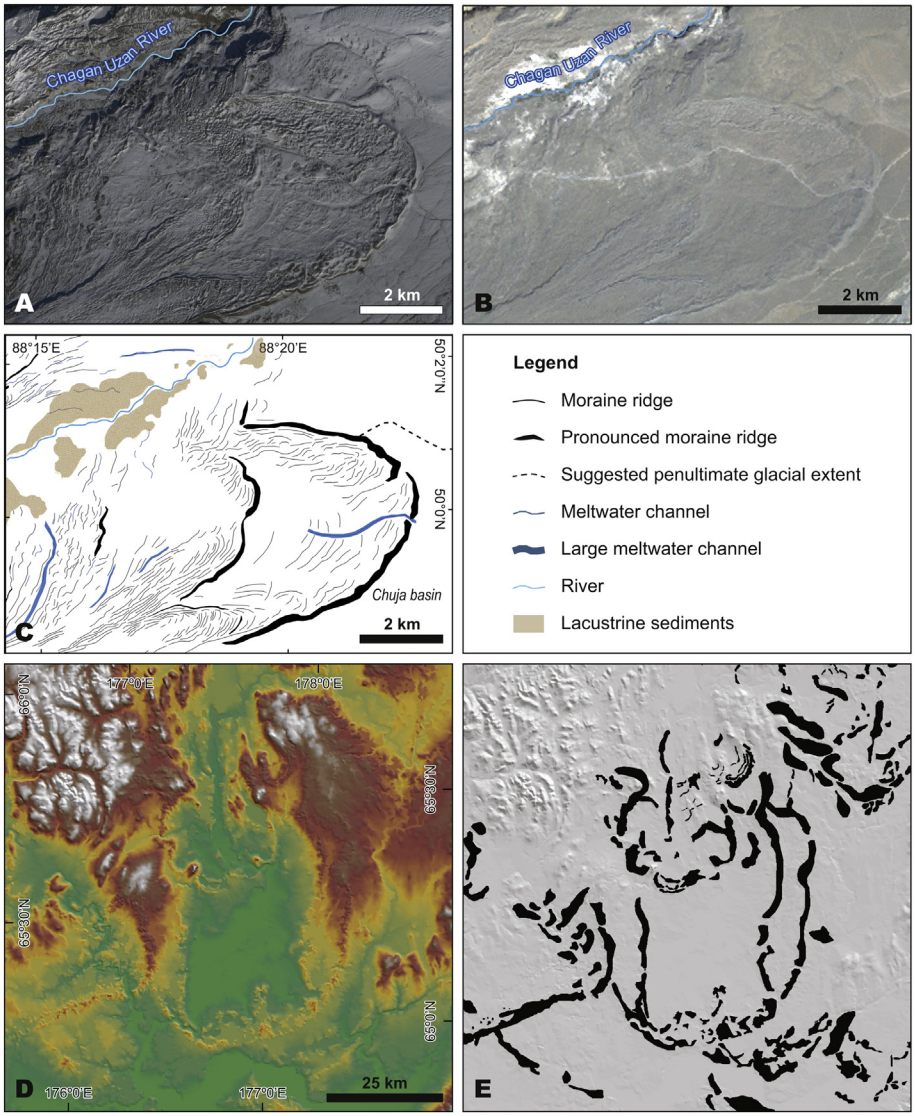

Fig. 15. Examples of landforms in icefield and valley glacier settings mapped on medium to coarse resolution imagery. Landforms observed in the Chagan Uzun Valley, Russian Altai, displayed on (A) SPOT image and (B) Landsat 7 ETM+ image. (C) Associated geomorphological map extract from Gribenski et al. (2016). Moraines in the Anadyr Lowlands, Far NE Russia, displayed on (D) semi-transparent shaded ViewFinder Panorama (VFP) DEM data (NE solar azimuth) draped over the raw VFP DEM. (E) Associated mapping of moraines (black polygons) from Barr and Clark (2012).

5.2. Alpine and plateau glacial settings

Mapping the geomorphological imprints of former alpine- and plateau-style ice masses (cirque glaciers, valley glaciers, icefields, and ice-caps) is particularly important because the geomorphological imprints of these discrete ice masses can facilitate reconstructions of their three-dimensional form (extent, morphology, and thickness). By contrast, establishing the vertical limits, thickness distribution, and surface topography of palaeo-ice sheets is challenging (cf. Stokes et al., 2015). Importantly, three-dimensional glacier reconstructions permit the calculation of palaeoclimatic boundary conditions for glaciated regions (e.g. Kerschner et al., 2000; Bakke et al., 2005; Stansell et al., 2007; Mills et al., 2012; Boston et al., 2015), data that cannot be obtained from point-source palaeoenvironmental records in distal settings (e.g. lacustrine archives). Empirical palaeoclimatic data derived from glacier reconstructions are important for three reasons. Firstly, these data facilitate analyses of wind patterns across loci of former glaciers and, in a wider context, regional precipitation gradients and atmospheric circulation patterns (e.g. Ballantyne, 2007a, b). Secondly, the data allow glaciodynamic conditions reconstructed from sediment-landform assemblages (e.g. moraines) to be directly linked to climatic regimes, thereby providing insights into glacier-climate interactions at long-term timescales (e.g. Benn and Lukas, 2006; Lukas, 2007a). Finally, independent, empirical information on climatic boundary conditions is fundamental to parameterising and testing numerical models used to simulate past glacier-climate interactions (e.g. Golledge et al., 2008). Thus, the geomorphological records of alpine and plateau-style ice masses are powerful proxies for understanding the interactions of such ice masses with climate.

Alpine- and plateau-style ice masses encompass a broad spatial spectrum of glacier morphologies (cf. Sugden and John, 1976; Benn and Evans, 2010), but geomorphological mapping of glacial landforms in alpine and plateau settings generally follows a similar approach that combines remote sensing and considerable field mapping/checking (Fig. 14; e.g. Federici et al., 2003, 2017; Bakke et al., 2005; Lukas and Lukas, 2006; Reuther et al., 2007; Hyatt, 2010; Bendle and Glasser, 2012; Pearce et al., 2014; Blomdin et al., 2016a; Gribenski et al., 2016; Borsellino et al., 2017). Hence, alpine- and plateau-style ice masses are considered collectively here. The similarities in mapping approaches across a wider range of spatial scales partly reflect the fact that, in both alpine and plateau settings, the majority of (preserved) glacial landforms are confined to spatially- and/or topographically-restricted areas (e.g. cirques, glaciated valleys), i.e. glacial landforms relating to plateau-style ice masses (plateau icefields, ice-caps) are dominantly formed by outlet glaciers. Conversely, an important component of mapping in upland environments is often assessing any glacial geomorphological evidence for connections between supposed valley glaciers and plateau surfaces/rounded summits, i.e. alpine vs. plateau styles of glaciation (e.g. McDougall, 2001; Boston et al., 2015). The recognition of any plateau-based ice has significant implications for studies aiming to assess glacier dynamics and regional palaeoclimate (see Rea et al., 1999; Boston, 2012a, and references therein). Consequently, it is important to deploy a versatile mapping approach in alpine and plateau settings that allows mapping of glacial landforms at a wide range of spatial scales and potentially across very large areas ($> 500\ km^2$), whilst also providing sufficiently high resolution imagery to map planforms of individual, small landforms (e.g. moraines).

5.2.1. Remote mapping of alpine and plateau settings

Glacial geomorphological mapping from remotely-sensed data in alpine and plateau ice mass settings typically involves interpretation of either analogue or digital aerial photographs (see Sections 3.1 and 3.2.2.2; e.g. Bickerton and Matthews, 1993; Boston, 2012b; Finlayson et al., 2011; Lukas, 2012; Izagirre et al., 2018). This reflects the superior resolution required to map in detail the frequently smaller glacial landforms produced by alpine and plateau-style ice masses, by contrast to the coarser resolution satellite imagery and DEMs predominantly used in ice sheet settings (see Section 5.1). The use of analogue (hard-copy) and digital aerial photographs varies in alpine and plateau settings, depending on data availability and the preference of individual mappers. For example, hard-copy, panchromatic aerial photographs have been widely used in conjunction with stereoscopes (see Section 3.1) for mapping Younger Dryas glacial landforms in Scotland, owing to their excellent tonal contrast (e.g. Benn and Ballantyne, 2005; Lukas and Lukas, 2006; Boston, 2012a, b). Indeed, depending on the environment and quality/resolution of available remotely-sensed imagery, panchromatic, stereoscopic aerial photographs can provide the most accurate approach (in terms of landform identification), with photographs of this format having superior tonal contrast than their digital (colour) counterparts. Digital colour aerial photographs may appear 'flat' (i.e. shadows are absent or less pronounced) making it more difficult to pick out subtle features, particularly in the absence of *SOCET SET* stereo display software and equipment (see Section 3.2.2.2). Nevertheless, mapping from digital aerial photographs has the advantage of providing georeferenced data and avoiding the duplication of effort, with hand-drawing on acetate overlays necessitating subsequent vectorisation (see Sections 3.1 and 3.2). Although panchromatic aerial photographs are invariably older, temporality usually presents no issue in palaeoglaciological (non-glacierised) settings, with the critical factor being image quality.

Irrespective of the type of aerial photographs used for geomorphological mapping, georectification is required to ensure accurate depiction of glacial landforms on the final maps (Section 3.3). This is important for minimising potential geospatial errors that will propagate into any subsequent glacier reconstructions and analyses of glacier-climate interactions. Ideally, georectification would involve stereoscopic photogrammetry, as discussed in Section 3.3, but this approach is impractical for larger ice masses (i.e. plateau icefields and plateau ice-caps). Thus, it is necessary to apply the pragmatic solutions described in Section 3.3.1.1, namely georectifying the aerial photographs or acetate overlays to other (coarser) georeferenced digital imagery or topographic data. Conversely, geomorphological studies at the scale of individual cirque basins, valley glaciers or glacier forelands would be appropriate for topographic surveys and hence stereoscopic photogrammetry, provided (i) the accessibility of the study area permits the use of surveying equipment and (ii) camera calibration data are available (see Section 3.3).

In some locations, coarse to medium resolution satellite imagery may be the only source of imagery available, yet sufficiently detailed to map the geomorphological imprint of former or formerly more extensive valley glaciers, icefields and ice-caps (Fig. 15; e.g. Glasser et al., 2005; Heyman et al., 2008; Barr and Clark, 2009, 2012; Morén et al., 2011; Hochreuther et al., 2015; Loibl et al., 2015; Blomdin et al., 2016a, b; Gribenski et al., 2016, 2018). However, these coarse remotely-sensed datasets may only allow for mapping of broad landform arrangements and patterns, rather than the intricate details of individual landforms, and preclude mapping of small features (cf. Barr and Clark, 2012; Fu et al., 2012; Stroeven et al., 2013; Blomdin et al., 2016b). The emergence of high-resolution (commercial) satellite imagery may result in more widespread use of satellite imagery for mapping in alpine and plateau settings, although the benefits of increased resolution may be counteracted by prohibitive costs for large study areas (see Section 3.2.2.1).

5.2.2. Field mapping in alpine and plateau settings

Detailed field mapping, following the procedures outlined in Section 2.2, has been widely applied as part of geomorphological studies focused on alpine- and plateau-style ice masses (e.g. Benn, 1992; Federici et al., 2003, 2017; Lukas, 2007a; Reuther et al., 2007; Boston, 2012b; Małecki et al., 2018; Brook and Kirkbride, 2018). Although field mapping is widely used in such settings, many studies do not explicitly report whether this entails field mapping *sensu stricto* (i.e. the procedure

outlined in Section 2.2), or verification of landforms mapped from remotely-sensed data by direct ground observations ('ground truthing'). We reaffirm the points raised in Sections 2.2 and 2.3 that, whenever possible, field mapping should be combined with remote mapping in cirque glacier, valley glacier, icefield and ice-cap settings in order to identify subtle glacial landforms and test interpretations of ambiguous features. While we advocate the application of detailed field mapping, we recognise that logistical and/or financial issues may preclude this and that it may only be possible to 'ground truth' selected areas. Nevertheless, some form of field survey is important in alpine and plateau settings to (i) circumvent potential issues with the quality/resolution of remotely-sensed data (e.g. poor tonal contrast) and (ii) arrive at definitive interpretations of glacial landforms and landscapes (see also Section 2.3).

5.3. Modern glacial settings

Many contemporary glacier forelands are rapidly evolving and new landscapes are emerging. This is largely due to changes resulting from the current retreat of ice masses and exposure of previously-glacierised terrain, leading to destabilisation of some landforms (e.g. Krüger and Kjær, 2000; Kjær and Krüger, 2001; Lukas et al., 2005; Lukas, 2011), erosion by changing meltwater routes, and remoulding or complete obliteration of extant landforms in areas following a glacier re-advance or surge (e.g. Evans et al., 1999; Evans and Twigg, 2002; Evans, 2003b; Evans and Rea, 2003; Benediktsson et al., 2008). Glaciofluvial processes on active temperate glacier forelands (e.g. Iceland) often make these environments unfavourable for preservation of (small) landforms (e.g. Evans and Twigg, 2002; Evans, 2003b, Kirkbride and Winkler, 2012; Evans and Orton, 2015; Evans et al., 2016a). In addition, de-icing and sediment re-working processes prevalent in many modern glacial environments (e.g. Iceland, Svalbard) typically result in substantial ice-

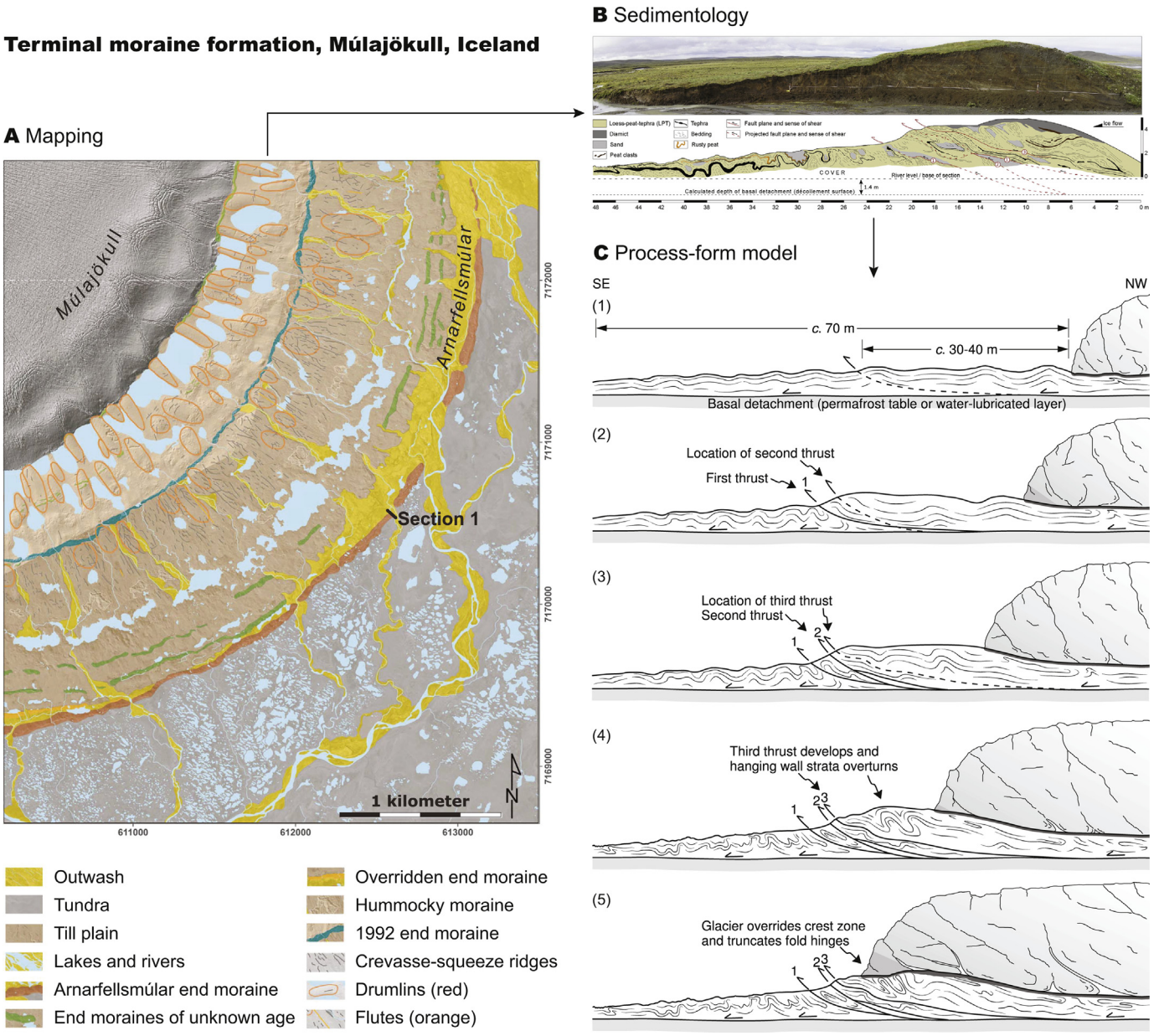

Fig. 16. Geomorphological mapping (A) from the Múlajökull foreland, Iceland, completed as part of a process-oriented study examining the internal architecture and structural evolution of a Little Ice Age terminal moraine at this surge-type glacier (Benediktsson et al., 2015). The mapping was combined with sedimentological investigations (B) to produce a process-form model of moraine formation and evolution (C).

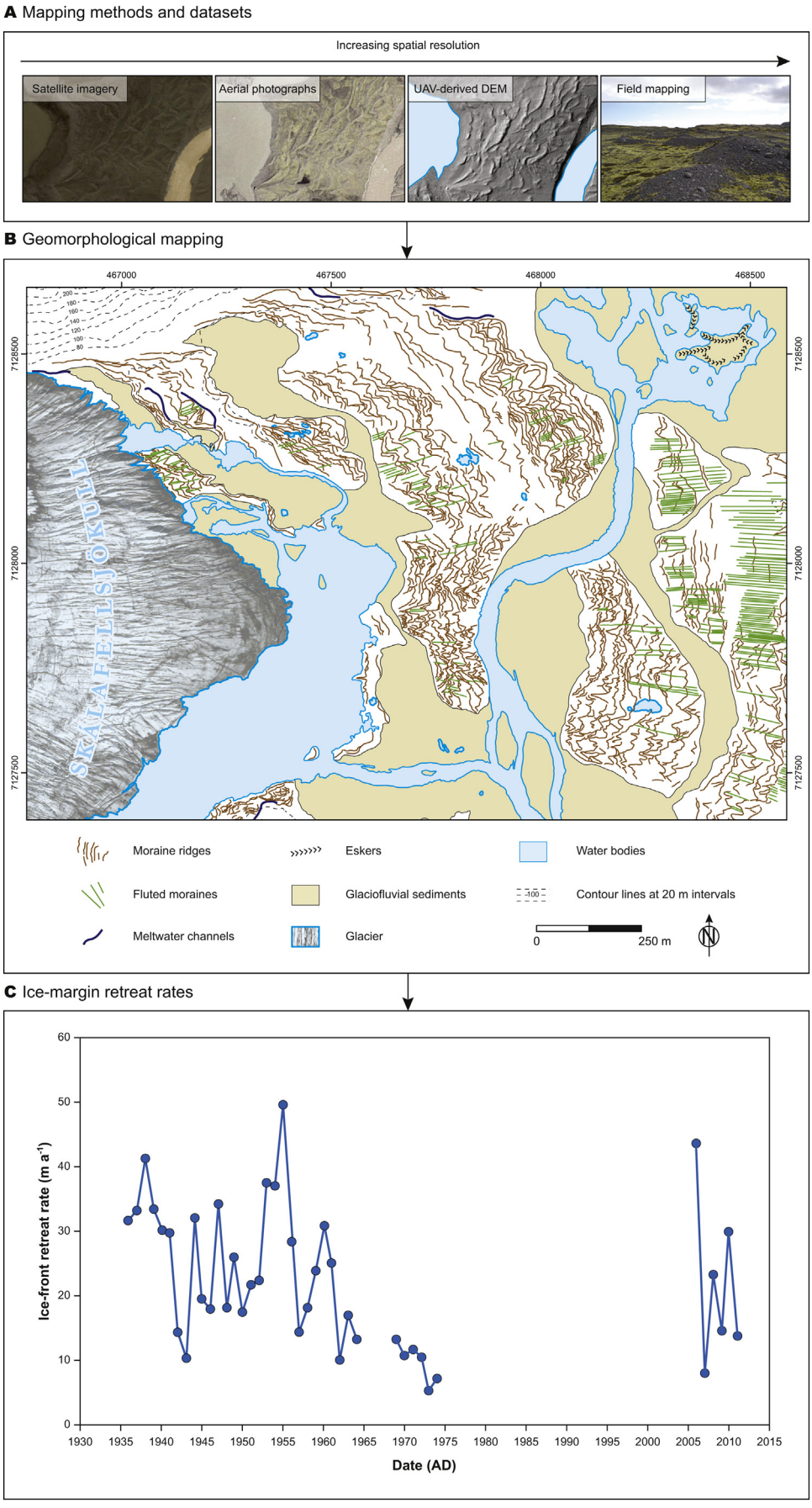

Fig. 17. Geomorphological mapping of the foreland of Skálafellsjökull, an active temperate outlet of Vatnajökull, SE Iceland. (A) Digital aerial photographs (2006; 0.41 m GSD; *Loftmyndir ehf*), pan-sharpened WorldView-2 multi-spectral satellite imagery (2012; 0.5 m GSD; *European Space Imaging*), a UAV-derived DEM (2013; 0.09 m GSD) and field mapping were employed to produce the mapping extract (B). A compromise on the level of detail was made, with annual moraines mapped along crestlines due to image resolution and map readability. This mapping detail was sufficient for calculating crest-to-crest moraine spacing (ice-margin retreat rates) shown in (C), which was the principal purpose of the study. Modified from Chandler et al. (2016a, b).

marginal landscape modification and topographic inversion (e.g. Etzelmüller et al., 1996; Krüger and Kjær, 2000; Kjær and Krüger, 2001; Lukas et al., 2005; Schomacker, 2008; Bennett and Evans, 2012; Ewertowski and Tomczyk, 2015). Anthropogenic activity can also have considerable implications for glacial systems (Jamieson et al., 2015; Evans et al., 2016b). The rapidity, ubiquity, and efficacy of these censoring processes (cf. Kirkbride and Winkler, 2012, for further details) in contemporary glacial environments should be key considerations in geomorphological mapping studies; in particular, the recognition that ice-cored features mapped at a given interval in time are not the 'final' geomorphological products (cf. Krüger and Kjær, 2000; Kjær and Krüger, 2001; Everest and Bradwell, 2003; Lukas et al., 2005, 2007; Lukas, 2007b).

In addition to landform preservation potential, spatial and temporal scales will be key determinants in the approaches used in mapping of ice-marginal landscapes, with studies in such settings often focused on the formation of small features (< 3 m in height) on recent, short timescales (0–30 years) (e.g. Beedle et al., 2009; Lukas, 2012; Bradwell et al., 2013; Reinardy et al., 2013; Chandler et al., 2016b) and/or evolution of the glacier foreland over a given time period (e.g. Bennett et al., 2010; Bennett and Evans, 2012; Ewertowski, 2014; Jamieson et al., 2015; Chandler et al., 2016a, b; Evans et al., 2016a). Thus, the approach to geomorphological mapping discussed in Section 5.2 requires some modification, as discussed below. It is also worth noting that geomorphological mapping usually forms part of process-oriented studies in modern glacial settings (Fig. 16), often with the intention of providing modern analogues for palaeo-ice masses and their geomorphological imprints (e.g. Evans et al., 1999; Evans, 2011; Schomacker et al., 2014; Benediktsson et al., 2016).

Geophysical surveying methods can also strengthen links between modern and ancient landform records through surveying of the internal architecture of landforms that can be directly linked to depositional processes, as well as glaciological and climatic conditions (e.g. Bennett et al., 2004; Benediktsson et al., 2009, 2010; Lukas and Sass, 2011; Midgley et al., 2013, 2018). Recent advances in geophysical imaging of sub-ice geomorphology have also allowed links to be made between modern and palaeo-ice sheets (see Section 3.2.2.3), and we expect this to be a growth area going forward (see also Stokes, 2018). More broadly, geophysical methods can be used to identify the extent of buried ice, allowing an assessment of the geomorphological stability of contemporary glacier forelands (e.g. Everest and Bradwell, 2003).

5.3.1. Remote mapping of modern glacial settings

The spatial resolution of remotely-sensed data is of critical importance in modern glacial settings: spatial resolutions commensurate with the size of the landforms being mapped and the scope of the research are required. Typically, aerial photographs or satellite imagery with GSDs of < 0.5 m are used in modern glacial settings to enable mapping of small features (e.g. Benediktsson et al., 2010; Lukas, 2012; Bradwell et al., 2013; Brynjólfsson et al., 2014; Lovell, 2014; Schomacker et al., 2014; Chandler et al., 2016a; Ewertowski et al., 2016; Lovell et al., 2018). LiDAR or UAV-derived DEMs are also becoming increasingly used for mapping in modern glacial environments (e.g. Brynjólfsson et al., 2014, 2016; Jónsson et al. 2014, 2016; Benediktsson et al., 2016; Chandler et al., 2016a; Ewertowski et al., 2016; Everest et al., 2017; Allaart et al., 2018; Lovell et al., 2018). Despite the high-resolution of the imagery, some compromise on the level of detail may be necessary, such as deciding on a maximum mapping scale (e.g. 1: 500–1: 1,000; Schomacker et al., 2014) to prevent too detailed mapping or by simplifying the mapping of certain features. In studies of low-amplitude (annual) moraines, the crestlines rather than the planforms are typically mapped, reflecting a combination of image resolution and data requirements: annual moraine sequences are often used to calculate ice-margin retreat rates and the position of crestlines offers sufficient detail for this purpose (Fig. 17; Krüger, 1995; Beedle et al., 2009; Lukas, 2012; Bradwell et al., 2013; Chandler et al., 2016a, b). Moreover, this approach can actually 'normalise' the data for subsequent analyses, removing the variability of, for example, moraine-base widths that result from gravitational processes during or after moraine formation.

The temporality (both month and year) of imagery takes on greater significance in modern glacial environments. Depending on the purpose of the research, either the most recent high-resolution remotely-sensed dataset available or a series of images from a number of intervals during a given time period are commonly required (e.g. Benediktsson et al., 2010; Bennett et al., 2010; Bradwell et al., 2013; Reinardy et al., 2013; Chandler et al., 2016a; Evans et al., 2016b; Ewertowski et al., 2016). In exceptional circumstances, the research may require an annual temporal resolution; for example, aerial photographs are commonly captured annually at the beginning and end of the ablation season in many forelands of the European Alps (cf. Lukas, 2012; Zemp et al., 2015). The increasing use of UAVs provides very high-resolution imagery (< 0.1 m GSD) of contemporary glacier forelands and the option to capture up-to-date imagery during every visit to the site, circumventing issues relating to temporal resolution. This approach is likely to come into greater usage for studies examining short-term ice-marginal landscape evolution and preservation potential.

Photogrammetric image processing (see Section 3.3) is arguably of most importance in contemporary glacial environments, particularly where the purpose of the mapping is to investigate small variations of the order of metres to tens of metres at short (0–30 years) timescales (cf. Evans, 2009). However, such constraints are not necessarily applicable where broader landsystem mapping is conducted (e.g. Evans, 2009; Evans and Orton, 2015; Evans et al., 2016a). Ideally, digital aerial photographs should be processed using stereoscopic photogrammetry techniques using GCPs collected during topographic surveys to enable the production of DEMs and orthorectified imagery with low error values (RMSEs < 2 m; see Section 3.3). It is preferable to survey GCPs and capture imagery contemporaneously, with surveyed GCPs appearing in the captured aerial imagery (e.g. Evans and Twigg, 2002; Evans et al., 2006, 2012; Schomacker et al., 2014), but imagery often pre-dates the geomorphological investigations and topographic surveys (e.g. Bennett et al., 2010; Bradwell et al., 2013; Chandler et al., 2016a). Alternatively, the digital aerial photographs could be processed using SfM photogrammetry methods (see Section 3.3.1.2).

5.3.2. Field mapping in modern glacial settings

The rapidly-changing nature of modern glacier forelands presents a number of challenges when using topographic base maps (see Section 2). Firstly, in relation to spatial limitations, topographic maps available in many settings (typically at scales of 1: 25,000 or 1: 50,000) may offer insufficient spatial resolution for mapping due to two factors: (i) the relief of the small geomorphological features ubiquitous in contemporary glacial environments is often less than the contour intervals depicted on the maps; and (ii) many forelands, such as those of southeast Iceland, have limited elevation changes across the foreland (cf. Evans and Twigg, 2002; Evans et al., 2016a).

Publicly-available topographic maps are rarely updated frequently enough to be useful for mapping the often rapid (annual to decadal-scale) changes taking place at modern glacier margins and in proglacial landscapes. Instead, it is desirable to undertake geodetic-grade surveying (i.e. using an RTK-GPS) of landforms and measurement of high-resolution topographic profiles, where conditions allow a safe approach towards the glacier margin (e.g. Benediktsson et al., 2008; Bradwell et al., 2013). Indeed, conducting detailed surveying with geodetic-grade equipment is essential for quantifying small changes in ice-marginal/proglacial landscapes (e.g. Schomacker and Kjær, 2008; Ewertowski and Tomczyk, 2015; Korsgaard et al., 2015) and obtaining metre-scale ice-margin retreat rates from the geomorphological record (e.g. Bradwell et al., 2013; Chandler et al., 2016b). This level of detail and accuracy may be unnecessary for some glacial geomorphological studies (e.g. those focused on the overall glacial landsystem), and

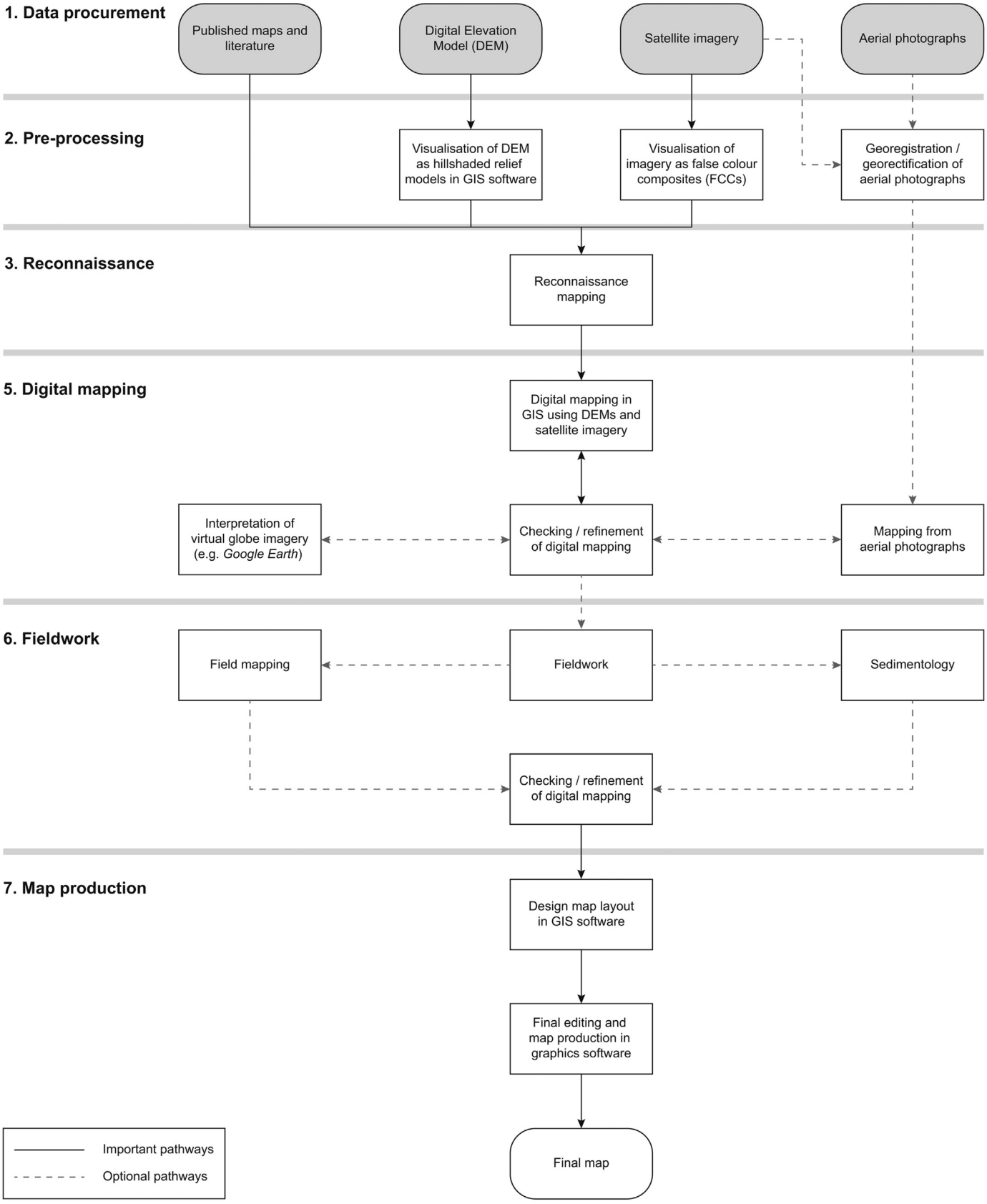

Fig. 18. Idealised workflow for mapping palaeo-ice sheet geomorphological imprints. Some pathways in the workflow are optional (grey dashed lines) depending on data availability and the feasibility and applicability of particular methods. Note, where analogue (hard-copy) aerial photographs are used for mapping, processing of acetate overlays would be undertaken after mapping from the aerial photographs. Further details on image processing are shown on the processing workflow available as Supplementary Material.

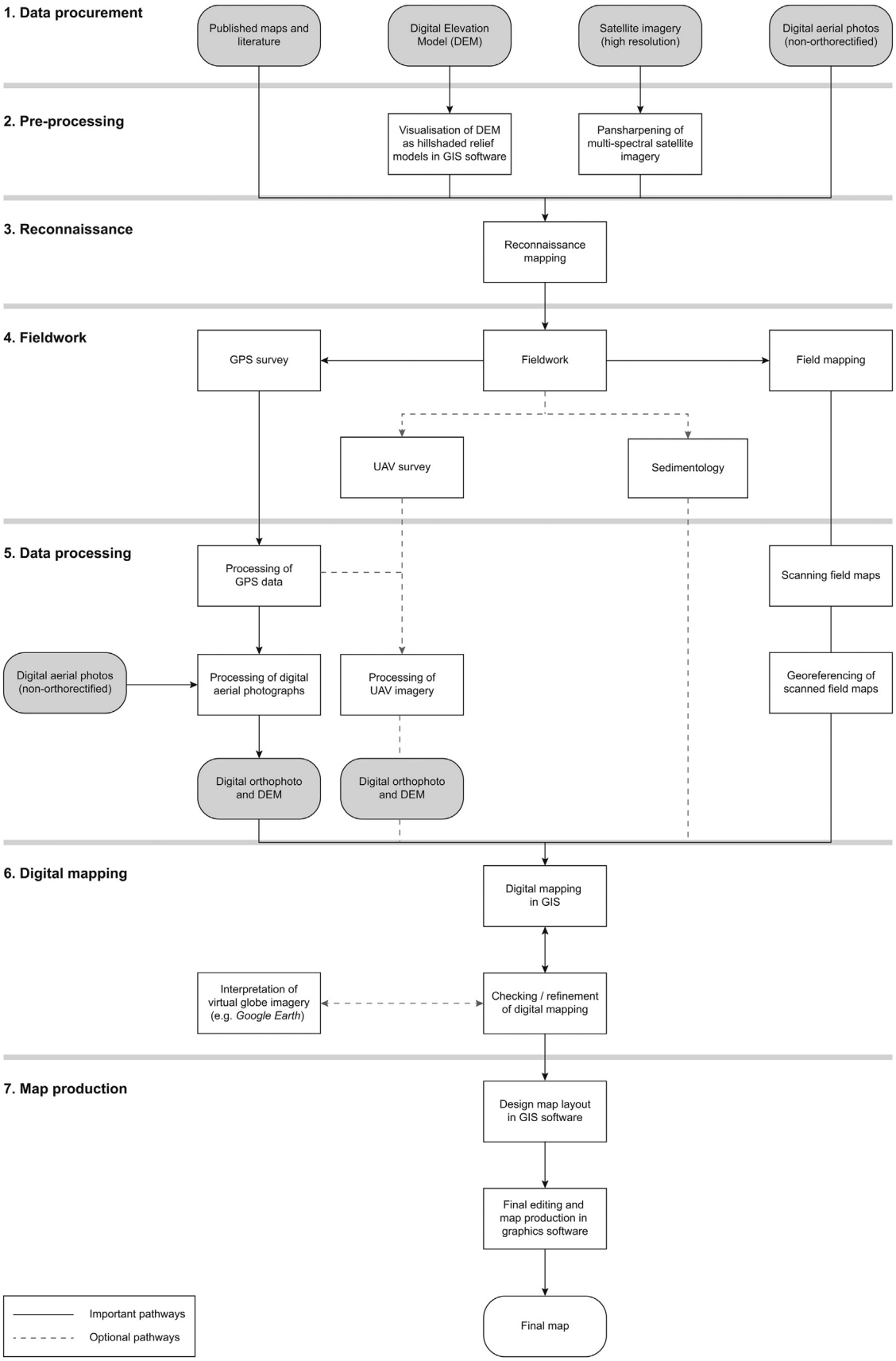

Fig. 19. Idealised workflow for mapping alpine- and plateau-style ice mass geomorphological imprints. In this scenario, digital remotely-sensed datasets are used and this necessitates image processing before mapping is undertaken. Ideally, GNSS surveys would be conducted in order to process digital aerial photographs, as depicted in the workflow. Some pathways are optional (grey dashed lines) depending on data availability and the feasibility and applicability of particular methods. Although sedimentology is shown as 'optional', it is highly desirable to undertake sedimentological investigations, wherever possible. Alternative image processing solutions are available and readers should consult with the detailed processing workflow which is available as Supplementary Material.

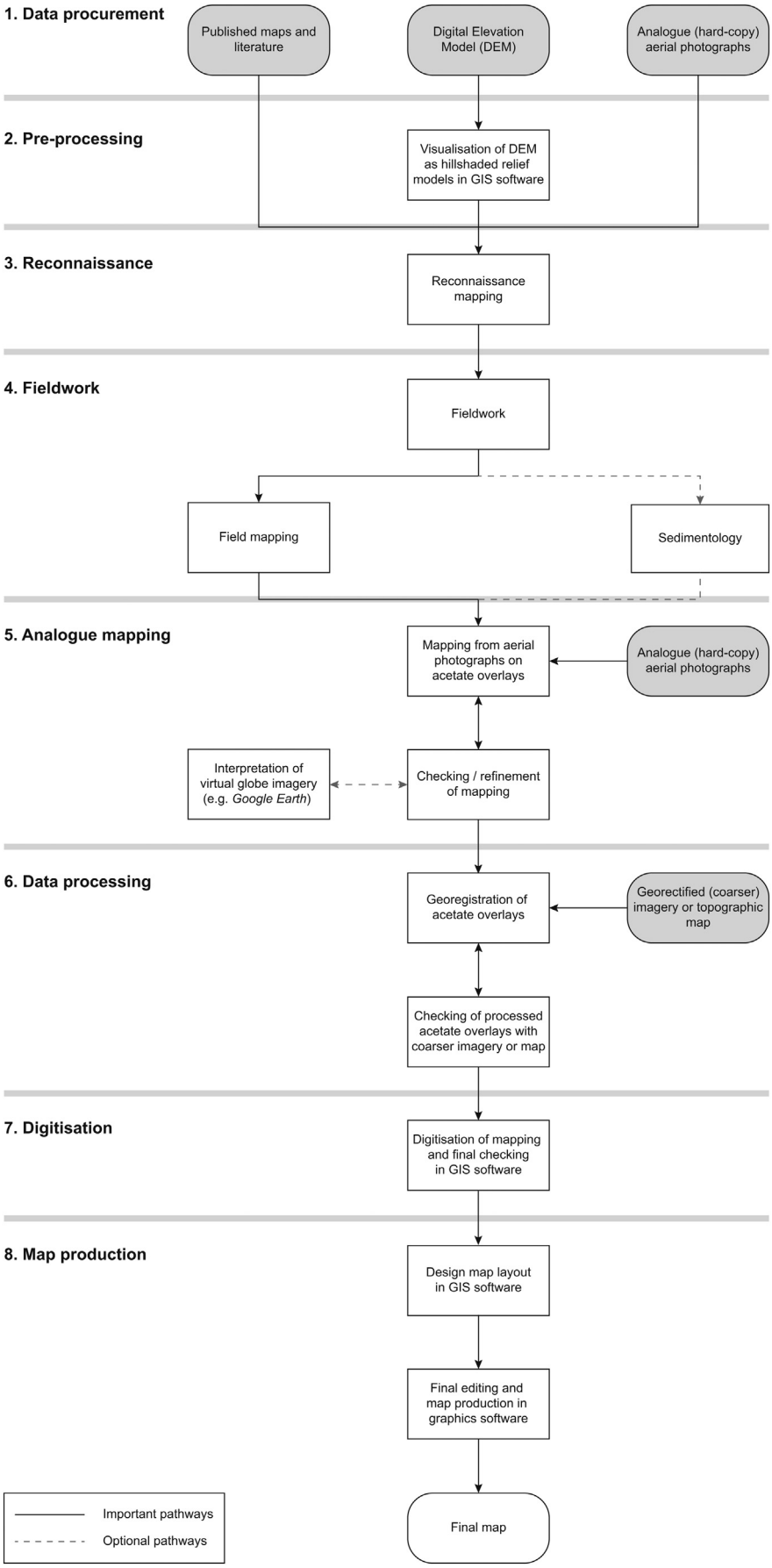

Fig. 20. Idealised workflow for mapping alpine- and plateau-style ice mass geomorphological imprints. In this scenario, analogue (hard-copy) aerial photographs are used and this necessitates image processing after mapping is undertaken. Some pathways are optional (grey dashed lines) depending on data availability and the feasibility and applicability of particular methods. Although sedimentology is shown as 'optional', it is highly desirable to undertake sedimentological investigations, wherever possible. Alternative image processing solutions are available and readers should consult with the detailed processing workflow which is available as Supplementary material.

annotation of aerial photograph extracts may be sufficient. There remain potential temporal limitations with these approaches, namely (i) limitations imposed by the date/year of image capture when mapping on print-outs and (ii) difficulties with correlating survey data with imagery, depending on the time difference and rapidity of landscape changes. In localities where (parts of) the ice-marginal/proglacial landscape cannot be satisfactorily or safely traversed, imagery and elevation control from remotely-sensed sources will be necessary (e.g. Evans et al., 2016e).

6. Frameworks for best practice

Based on our review of the various mapping approaches, we here synthesise *idealised* frameworks for mapping palaeo-ice sheet geomorphological imprints (Section 6.1) and alpine and plateau-style ice mass (cirque glaciers, valley glaciers, ice-fields and ice-caps) geomorphological imprints (Section 6.2). The aim is to provide frameworks for best practice in glacial geomorphological mapping, ensuring robust and systematic geomorphological mapping programmes. The templates outlined can be modified as necessary, depending on the study area size and project scope, along with the datasets, software and time available.

Before outlining the idealised frameworks, we offer four general recommendations for undertaking and reporting glacial geomorphological mapping that are applicable at all scales of investigation:

(1) The methods, datasets and equipment employed in mapping should be clearly stated, including the resolution and format of remotely-sensed data.
(2) Any processing methods and imagery rectification errors (RMSEs) should be reported, as well as mapping uncertainties (both in terms of the location of the landforms and their identification/classification). Where remotely-sensed datasets are obtained as pre-processed, georeferenced products, this should also be stated.
(3) Establishing and reporting criteria for identifying and mapping different landforms is desirable. As a minimum, this could take the form of a brief definition of the mapped landform.
(4) GIS software (e.g. *ArcGIS*, *QGIS*) should be used for geomorphological mapping and vectorisation to provide georeferenced geomorphological data that is also readily transferable for data sharing or community use.

Following the above general recommendations will provide transparency about how the mapping was compiled and what considerations were made during the process, aiding accuracy assessment, comparison and integration of geomorphological data. This is particularly valuable for the incorporation of the geomorphological mapping in large compilations (Bickerdike et al., 2016; Stroeven et al., 2016; Clark et al., 2018a) and any subsequent use of the data for palaeoglaciological reconstructions and/or testing numerical ice sheet models (Stokes et al., 2015; Margold et al., 2018).

In relation to software (recommendation 4), some practitioners may prefer to use graphics software packages (e.g. *Adobe Illustrator*, *Canvas X*, *CorelDRAW*) for the production of final glacial geomorphological maps (e.g. Brynjólfsson et al., 2014; Darvill et al., 2014; Blomdin et al., 2016a; Chandler et al., 2016a; Bendle et al., 2017a; Norris et al., 2017). Such graphics software can provide greater functionality than current GIS packages for fine adjustments of the final cartographic design. However, any modification in graphics software should be kept to a minimum in order to avoid compromising the transferability of the data for other users (e.g. as shapefiles), with the focus instead on adjustments to the map symbology and ensuring optimal map presentation.

6.1. Palaeo-ice sheet geomorphological imprints

For mapping of palaeo-ice sheet geomorphological imprints we recommend the use of multiple remotely-sensed datasets in a synergistic and systematic process, subject to data availability and coverage (Fig. 18). As a minimum, remote sensing investigations should involve reconnaissance-level mapping using multiple remotely-sensed datasets to establish the most suitable dataset (e.g. Stokes et al., 2016a). However, mapping often benefits from utilising a range of imagery types and resolutions, enabling the advantages of each respective method/dataset to be integrated to produce an accurate geomorphological map (see below). At the outset of the mapping, a decision should be made on the level of mapping detail required for particular landforms (i.e. polyline or polygon mapping), in line with the aims and requirements of the study (see Section 5.1.1).

Initially, mapping should involve an assessment of the study area using remotely-sensed data in conjunction with existing maps and literature to identify gaps in the mapping record and localities for focused mapping. Following this reconnaissance stage, the mapper may proceed with mapping from both DEMs and satellite imagery, adding increasing levels of detail with increasingly higher resolution datasets. Recommended techniques for processing the satellite images and DEMs are outlined in Sections 3.3.2 and 3.3.3, including the generation of false-colour composites with different spectral band combinations to aid landform identification (e.g. Jansson and Glasser, 2005; Lovell et al., 2011; Storrar and Livingstone, 2017).

DEMs may provide a superior source of imagery as they directly record the shape of landforms, rather than the interaction of reflected radiation and topography, and therefore allow for more accurate and intuitive mapping. For example, DEMs are often particularly useful for identifying and mapping meltwater channels (e.g. Greenwood et al., 2007; Storrar and Livingstone, 2017). Specific features may also only be identifiable on satellite imagery, such as low-relief corridors of glaciofluvial deposits, due to their distinctive spectral signatures (e.g. Storrar and Livingstone, 2017). Moreover, the typically superior resolution of satellite imagery may enhance landform detectability and allow for more detailed mapping. Many glacial landforms are also clearly distinguishable in one or more sets of remotely-sensed data (or through using a combination of datasets).

To ensure that all landforms are mapped from remotely-sensed data, the datasets should be viewed at a variety of scales and mapping conducted through multiple passes of the area, enabling the addition of increasing levels of detail to and/or refinement of initial mapping with each pass (Norris et al., 2017). It may be advantageous to perform a final check at a small cartographic scale (e.g. 1: 500,000) to ensure there are no errors in the mapping, such as duplication of landforms at image overlaps (e.g. De Angelis, 2007). The mapping should be iterative, with repeated consultations of various remotely-sensed datasets throughout the process recommended.

In this contribution, we have focused on the use of satellite imagery and DEMs for mapping palaeo-ice sheet geomorphological imprints, since these are the most widely used for practical reasons. However, aerial photograph interpretation and fieldwork should not be abandoned altogether in palaeo-ice sheet settings. Aerial photographs, where available, can be used to add further detail and refine the mapping, whilst fieldwork enables ground-truthing of remote mapping (e.g. Hättestrand and Clark, 2006; Kleman et al., 2010; Darvill et al., 2014; Evans et al., 2014). Furthermore, mapping from satellite imagery and DEMs can direct fieldwork, highlighting areas for sedimentological and stratigraphic investigations. Such studies can provide invaluable data on landform genesis, subglacial processes, and ice dynamics (e.g. Livingstone et al., 2010; Evans et al., 2015; Spagnolo et al., 2016; Phillips et al., 2017; Norris et al., 2018). Remote mapping of palaeo-ice sheet geomorphology also guides targeted dating for chronological investigations and should be an essential first phase in such studies (e.g. Stroeven et al., 2011; Darvill et al., 2014, 2015).

6.2. Alpine and plateau-style ice mass geomorphological imprints

Our idealised framework for mapping alpine and plateau-style ice

mass geomorphological imprints is an iterative process involving several consultations of remotely-sensed data and field mapping (Figs. 19 and 20). This methodology provides a robust approach to mapping that has been broadly used in previous studies (e.g. Benn and Ballantyne, 2005; Lukas and Lukas, 2006; Kjær et al., 2008; Boston, 2012a, b; Brynjólfsson et al., 2014; Jónsson et al., 2014; Pearce et al., 2014; Schomacker et al., 2014; Chandler et al., 2016a; Chandler and Lukas, 2017). This framework is also applicable to modern glacial settings as the overarching methods do not differ fundamentally, but practitioners should be aware of issues relating to the temporal resolution of remotely-sensed data (see Section 5.3).

In the initial preparatory stage, the mapper should consult topographic, geological and extant geomorphological maps (where available), and ideally undertake mapping of the study area using remotely-sensed data, at least at a reconnaissance level. This essential phase familiarises the mapper with the study area prior to fieldwork and enables the identification of significant areas for targeted, detailed field mapping (or ground verification) and sedimentological investigations of specific landforms. Conversely, the reconnaissance investigations may also clarify which areas are less important for a field visit and aid route planning. Importantly, this enables a systematic approach to mapping, and is particularly important in previously-unmapped areas (e.g. Boston, 2012a, b). During the initial stage, it may also be desirable to establish a legend/mapping system in readiness for subsequent field mapping (Otto and Smith, 2013).

Following the preparatory/reconnaissance stage, detailed field mapping, or at a minimum some ground verification, should ideally be conducted to avoid overlooking (subtle) landforms and misinterpreting others. Depending on the nature of the project and accessibility limitations, ground verification may be done during a single (and relatively short) field visit (e.g. Lukas, 2012; Chandler et al., 2016a), whilst detailed field mapping would usually require longer field visits or even repeated, long-term field campaigns (e.g. Kjær et al. 2008; Boston, 2012a, b; Schomacker et al., 2014; Evans et al., 2016a). During field surveys, consultation of initial remote mapping helps to ensure accurate representation of landforms on field maps and allows verification of all features identified remotely (e.g. Boston, 2012a, b; Pearce et al., 2014).

Following field mapping, which may be an intermittent and ongoing process in the case of large study areas and long-term research projects, it is ideal to finalise the geomorphological mapping using high-resolution imagery (i.e. aerial photographs, satellite imagery, LiDAR DEMs, UAV-derived imagery). This allows complex patterns of landforms, such as British 'hummocky moraine' (e.g. Lukas and Lukas, 2006; Boston, 2012b), crevasse-squeeze ridges (e.g. Kjær et al., 2008), drumlin fields (e.g. Benediktsson et al., 2016), and sawtooth 'annual' moraines (e.g. Chandler et al., 2016a; Evans et al., 2016a), to be mapped with high spatial accuracy, following landform identification and interpretation in the field. Again, during this stage, previous mapping from DEMs and field maps should be consulted. As highlighted in the scale-appropriate examples, the procurement of remotely-sensed data with appropriate spatial and temporal resolution is important (see Sections 5.2 and 5.3).

Depending on the type of imagery used (hard-copy or digital), the rectification of imagery/overlays may precede or follow aerial photograph mapping: where digital format aerial photographs are used, rectification will be undertaken before mapping (Fig. 19), whilst acetate overlays will be corrected after mapping from hard-copy aerial photographs (Fig. 20) (see also Supplementary Material). Subsequently, acetate overlays can be checked against digital imagery (if available) before being vectorised (digitally traced) in a GIS software package (e.g. *ArcMap, QGIS*).

In our view, geomorphological mapping in cirque glacier, valley glacier, icefield and ice-cap settings should not be reliant solely on the morphological characteristics of features and should ideally be combined with detailed sedimentological investigations of available exposures as part of an inductive-deductive process, using standard procedures (cf. Evans and Benn, 2004; Lukas et al., 2013, and references therein). This reflects the fact that these glacier systems occupy more manageable study areas and, as such, sedimentological analyses can be more readily applied. By combining geomorphological mapping and sedimentology, issues relating to equifinality (Chorley, 1962; Möller and Dowling, 2018) will be avoided, which is important when attempting to establish the wider palaeoglaciological and palaeoclimatic significance of the geomorphological evidence (cf. Benn and Lukas, 2006). This multi-proxy, process-form approach ensures accurate genetic interpretations on geomorphological maps.

7. Conclusions

Geomorphological mapping forms the basis of a wide range of process-oriented, glacial chronological and palaeoglaciological studies. Thus, it is imperative that effective approaches are used to ensure robust assimilation of data and that errors and uncertainties are explicitly reported. This is particularly the case where field mapping and analogue data are transferred to digital format and combined with digital remotely-sensed data.

In general, specific methods and datasets are often applied to particular glacial settings: (i) a mixture of satellite imagery (e.g. Landsat) and DEMs (e.g. ASTER GDEM, SRTM) are typically used for mapping in palaeo-ice sheet settings; and (ii) a combination of aerial photographs and field mapping are widely employed for mapping alpine and plateau-style ice mass geomorphological imprints. Increasingly, UAV-captured aerial imagery and high resolution DEMs (derived from UAV-captured imagery and LiDAR) are being utilised for mapping of modern glacial environments and are likely to be a growth area in future geomorphological mapping studies, enabling high resolution, multi-temporal remotely-sensed datasets to be obtained at relatively low cost. The use of particular methods reflects the spatial and temporal resolution of remotely-sensed datasets, along with the practicality of their application (both in terms of time and finance).

In this contribution, we have highlighted that compromises and pragmatic solutions are often necessary in glacial geomorphological mapping, particularly with respect to processing techniques and the level of mapping detail. For example, detailed GNSS surveys using geodetic-grade equipment are desirable for photogrammetric processing of aerial photographs, but this is impractical for the large areas covered by icefields, ice-caps and ice sheets. Thus, pragmatic approaches may be used, such as georeferencing analogue-derived mapping to existing (coarser) georeferenced datasets (e.g. satellite imagery, DEMs or orthophotographs). In relation to the level of mapping detail, it is often necessary to map particular landforms as linear features (e.g. subglacial bedforms, moraines) or define a maximum scale during mapping, due to image resolution and/or study requirements.

We have outlined idealised frameworks and general recommendations to ensure best practice in future studies. In particular, we emphasise the importance of utilising multiple datasets or mapping approaches in synergy, akin to multi-proxy/-method approaches used in many Earth Science disciplines; multiple remotely-sensed datasets in the case of ice-sheet-scale geomorphology and a combination of remote sensing and field mapping for cirque glaciers to ice-caps. Further key recommendations are the clear reporting of (i) the methods, datasets and equipment employed in mapping, (ii) any processing methods employed and imagery rectification errors (RMSEs) associated with imagery, along with mapping uncertainties, and (iii) the criteria for identifying and mapping different landforms. We also recommend that mapping is conducted in GIS software to provide georeferenced geomorphological data that is easily transferable between users. Finally, we advocate sedimentological investigations of available exposures as part of an inductive-deductive process during fieldwork to ensure accurate genetic interpretations of the geomorphological record as part of a holistic approach. Following these recommendations will aid in comparison, integration, and accuracy assessment of geomorphological data, particularly where geomorphological data are incorporated in

large compilations and subsequently used for palaeoglaciological reconstruction.

Acknowledgements

We are grateful to numerous colleagues for informal discussions that have directly or indirectly helped shape this paper. Alex Clayton is thanked for kindly supplying the UAV imagery and DEM for the Skálafellsjökull foreland, whilst Jon Merritt is thanked for providing CMB and SL with access to aerial photographs at the British Geological Survey in Edinburgh. We are also grateful to Jacob Bendle, Natacha Gribenski and Sophie Norris for kindly providing figures for inclusion in this contribution. The NEXTMap Great Britain™ data for Ben More Coigach was licensed to BMPC by the NERC Earth Observation Data Centre under a Demonstration Use License Agreement. CMB and HL obtained access to aerial photographs and NEXTMap Great Britain™ data through NERC Earth Observation Data Centre whilst in receipt of NERC Algorithm studentships NE/G52368X/1 (CMB) and NE/I528050/1 (HL). This contribution was written whilst BMPC was in receipt of a Queen Mary Natural and Environmental Science Studentship, which is gratefully acknowledged. We thank Richard Waller and an anonymous reviewer for constructive comments that helped improve the clarity of this contribution, along with Ian Candy for editorial handling.

Appendix A. Supplementary data

Supplementary data to this article can be found online at https://doi.org/10.1016/j.earscirev.2018.07.015.

References

Akçar, N., Yavuz, V., Ivy-Ochs, S., Reber, R., Kubik, P.W., Zahno, C., Schlüchter, C., 2014. Glacier response to the change in atmospheric circulation in the eastern Mediterranean during the Last Glacial Maximum. Quat. Geochronol. 19, 27–41.

Alexanderson, H., Adrielsson, L., Hjort, C., Möller, P., Antonov, O., Eriksson, S., Pavlov, M., 2002. Depositional history of the North Taymyr ice-marginal zone, Siberia—a landsystem approach. J. Quat. Sci. 17 (4), 361–382.

Allaart, L., Friis, N., Ingólfsson, Ó., Håkansson, L., Noormets, R., Farnsworth, W.R., Mertes, J., Schomacker, A., 2018. Drumlins in the Nordenskiöldbreen forefield, Svalbard. GFF 140, 170–188.

Andrews, J.T., Miller, G.H., 1979. Glacial erosion and ice sheet divides, northeastern Laurentide Ice Sheet, on the basis of the distribution of limestone erratics. Geology 7 (12), 592–596.

Astakhov, V., Shkatova, V., Zastrozhnov, A., Chuyko, M., 2016. Glaciomorphological Map of the Russian Federation. Quat. Int. 420, 4–14.

Atkinson, N., Pawley, S., Utting, D.J., 2016. Flow-pattern evolution of the Laurentide and Cordilleran ice sheets across west-central Alberta, Canada: implications for ice sheet growth, retreat and dynamics during the last glacial cycle. J. Quat. Sci. 31 (7), 753–768.

Aylsworth, J.M., Shilts, W.W., 1989. Glacial features around the Keewatin Ice Divide: Districts of Mackenzie and Keewatin. In: Geological Survey of Canada paper, pp. 88–124.

Bakke, J., Dahl, S.O., Paasche, Ø., Løvlie, R., Nesje, A., 2005. Glacier fluctuations, equilibrium-line altitudes and palaeoclimate in Lyngen, northern Norway, during the Lateglacial and Holocene. The Holocene 15, 518–540.

Ballantyne, C.K., 1989. The Loch Lomond Readvance on the Isle of Skye, Scotland: glacier reconstruction and palaeoclimatic implications. J. Quat. Sci. 4, 95–108.

Ballantyne, C.K., 2002. The Loch Lomond Readvance on the Isle of Mull, Scotland: glacier reconstruction and palaeoclimatic implications. J. Quat. Sci. 17, 759–771.

Ballantyne, C.K., 2007a. The Loch Lomond Readvance on north Arran, Scotland: glacier reconstruction and palaeoclimatic implications. J. Quat. Sci. 22, 343–359.

Ballantyne, C.K., 2007b. Loch Lomond Stadial glacier on North Harris, Outer Hebrides, North-West Scotland: glacier reconstruction and palaeoclimatic implications. Quat. Sci. Rev. 26, 3134–3149.

Barchyn, T.E., Dowling, T.P.F., Stokes, C.R., Hugenholtz, C.H., 2016. Subglacial bed form morphology controlled by ice speed and sediment thickness. Geophys. Res. Lett. 43, 7572–7580.

Barr, I.D., Clark, C.D., 2009. Distribution and pattern of moraines in Far NE Russia reveal former glacial extent. J. Maps 5, 186–193.

Barr, I.D., Clark, C.D., 2012. An updated moraine map of Far NE Russia. J. Maps 8, 431–436.

Barrell, D.J.A., Andersen, B.G., Denton, G.H., Lyttle, B.S., 2011. Glacial geomorphology of the central South Island, New Zealand. GNS Science Monograph 27 GNS Science, Lower Hutt, 81 pp + map (5 sheets).

Barrell, D.J.A., Andersen, B.G., Denton, G.H., Lyttle, B.S., 2013. Glacial geomorphology of the central South Island, New Zealand – digital data. GNS Science Monograph 27a GNS Science, 17 pp (GIS digital data files + explanatory notes.

Barrow, G., Hinxman, L.W., Cunningham Craig, E.H., 1913. The Geology of Upper Strathspey, Gaick, and the Forest of Atholl (Explanation of Sheet 64). In: Memoirs of the Geological Survey. HMSO, Edinburgh, Scotland.

Batchelor, C., Dowdeswell, J.A., Ottesen, D., 2017. Submarine Glacial Landforms. In: Micallef, A., Krastel, S., Savini, A. (Eds.), Submarine Geomorphology. Springer, Cham, Switzerland, pp. 207–234.

Beedle, M.J., Menounos, B., Luckman, B.H., Wheate, R., 2009. Annual push moraines as climate proxy. Geophys. Res. Lett. 36, L20501.

Bendle, J.M., Glasser, N.F., 2012. Palaeoclimatic reconstruction from Lateglacial (Younger Dryas Chronozone) cirque glaciers in Snowdonia, North Wales. Proceedings of the Geologists' Association 123, 130–145.

Bendle, J.M., Thorndycraft, V.R., Palmer, A.P., 2017a. The glacial geomorphology of the Lago Buenos Aires and Lago Pueyrredón ice lobes of central Patagonia. J. Maps 13, 654–673.

Bendle, J.M., Palmer, A.P., Thorndycraft, V.R., Matthews, I.P., 2017b. High-resolution chronology for deglaciation of the Patagonian Ice Sheet at Lago Buenos Aires (46.5° S) revealed through varve chronology and Bayesian age modelling. Quat. Sci. Rev. 177, 314–339.

Benediktsson, Í.Ö., Möller, P., Ingólfsson, Ó., van der Meer, J.J.M., Kjær, K.H., Krüger, J., 2008. Instantaneous end moraine and sediment wedge formation during the 1890 glacier surge of Brúarjökull. Iceland. Quat. Sci. Rev. 27, 209–234.

Benediktsson, Í.Ö., Ingólfsson, Ó., Schomacker, A., Kjaer, K.H., 2009. Formation of submarginal and proglacial end moraines: implications of ice-flow mechanism during the 1963-64 surge of Brúarjökull, Iceland. Boreas 38, 440–457.

Benediktsson, Í.Ö., Schomacker, A., Lokrantz, H., Ingólfsson, Ó., 2010. The 1890 surge end moraine at Eyjabakkajökull, Iceland: a re-assessment of a classic glaciotectonic locality. Quat. Sci. Rev. 29, 484–506.

Benediktsson, Í.Ö., Schomacker, A., Johnson, M.D., Geiger, A.J., Ingólfsson, Ó., Guðmundsdóttir, E.R., 2015. Architecture and structural evolution of an early Little Ice Age terminal moraine at the surge-type glacier Múlajökull. Iceland. J. Geophys. Res.: Earth Surf. 120, 1895–1910.

Benediktsson, Í.Ö., Jónsson, S.A., Schomacker, A., Johnson, M.D., Ingólfsson, Ó., Zoet, L., Iverson, N.R., Stötter, J., 2016. Progressive formation of modern drumlins at Múlajökull, Iceland: stratigraphical and morphological evidence. Boreas 45, 567–583.

Benn, D.I., 1990. Scottish Lateglacial moraines: debris supply, genesis and significance. Unpublished PhD thesis. University of St Andrews.

Benn, D.I., 1994. Fluted moraine formation and till genesis below a temperate valley glacier: Slettmarkbreen, Jotunheimen, southern Norway. Sedimentology 41, 279–292.

Benn, D.I., 2006. Interpreting glacial sediments. In: Knight, P. (Ed.), Glacier Science and Environmental Change. Blackwell, Oxford, pp. 434–439.

Benn, D.I., Ballantyne, C.K., 2005. Palaeoclimatic reconstruction from Loch Lomond Readvance glaciers in the West Drumochter Hills. Scotland. J. Quat. Sci. 20, 577–592.

Benn, D.I., Evans, D.J.A., 2010. Glaciers and Glaciation, 2nd Edition. Hodder Education, London 802 pp.

Benn, D.I., Lukas, S., 2006. Younger Dryas glacial landsystems in North West Scotland: an assessment of modern analogues and palaeoclimatic implications. Quat. Sci. Rev. 25, 2390–2408.

Benn, D.I., Lowe, J.J., Walker, M.J.C., 1992. Glacier response to climatic change during the Loch Lomond Stadial and early Flandrian: geomorphological and palynological evidence from the Isle of Skye. Scotland. J. Quat. Sci. 7, 125–144.

Bennett, M.R., 1991. Scottish "hummocky moraine": its implications for the deglaciation of the North West Highlands during the Younger Dryas or Loch Lomond Stadial. University of Edinburgh Unpublished PhD thesis, 362 pp.

Bennett, G.L., Evans, D.J.A., 2012. Glacier retreat and landform production on an overdeepened glacier foreland: the debris-charged glacial landsystem at Kviárjökull. Iceland. Earth Surf. Process. Land. 37, 1584–1602.

Bennett, M.R., Huddart, D., Waller, R.I., Cassidy, N., Tomio, A., Zukowskyj, P., Midgley, N.G., Cook, S.J., Gonzalez, S., Glasser, N.F., 2004. Sedimentary and tectonic architecture of a large push moraine: a case study from Hagafellsjökull-Eystri. Iceland. Sedi. Geol. 172, 269–292.

Bennett, G.L., Evans, D.J.A., Carbonneau, P., Twigg, D.R., 2010. Evolution of a debris-charged glacier landsystem, Kviárjökull. Iceland. J. Maps 6, 40–67.

Bickerdike, H.L., Evans, D.J.A., Ó Cofaigh, C., Stokes, C.R., 2016. The glacial geomorphology of the Loch Lomond Stadial in Britain: a map and geographic information system resource of published evidence. J. Maps 12 (5), 1178–1186.

Bickerdike, H.L., Ó Cofaigh, C., Evans, D.J.A., Stokes, C.R., 2018. Glacial landsystems, retreat dynamics and controls on Loch Lomond Stadial (Younger Dryas) glaciation in Britain. Boreas 47, 202–224.

Bickerton, R.W., Matthews, J.A., 1992. On the accuracy of lichenometric dates: an assessment based on the 'Little Ice Age' moraine sequence of Nigardsbreen, southern Norway. The Holocene 2, 227–237.

Bickerton, R.W., Matthews, J.A., 1993. 'Little ice age' variations of outlet glaciers from the jostedalsbreen ice-cap, Southern Norway: A regional lichenometric-dating study of ice-marginal moraine sequences and their climatic significance. J. Quat. Sci. 8, 45–66.

Blomdin, R., Heyman, J., Stroeven, A.P., Hättestrand, C., Harbor, J.M., Gribenski, N., Jansson, K.N., Petrakov, D.A., Ivanov, M.N., Alexander, O., Rudoy, A.N., Walther, M., 2016a. Glacial geomorphology of the Altai and Western Sayan Mountains. Central Asia. J. Maps 12 (1), 123–136.

Blomdin, R., Stroeven, A.P., Harbor, J.M., Lifton, N.A., Heyman, J., Gribenski, N., Petrakov, D.A., Caffee, M.W., Ivanov, M.N., Hättestrand, C., Rogozhina, I., Usubaliev, R., 2016b. Evaluating the timing of former glacier expansions in the Tian Shan: A key step towards robust spatial correlations. Quat. Sci. Rev. 153, 78–96.

Blomdin, R., Stroeven, A.P., Harbor, J.M., Gribenski, N., Caffee, M.W., Heyman, J., Rogozhina, I., Ivanov, M.N., Petrakov, D.A., Walther, M., Rudoy, A.N., Zhang, W., Orkhonselenge, A., Hättestrand, C., Lifton, N.A., Jansson, K.N., 2018. Timing and dynamics of glaciation in the Ikh Turgen Mountains, Altai region, High Asia. Quat. Geochron. 47, 54–71.
Bolch, T., Loibl, D., 2017. GIS for Glaciers and Glacial Landforms. In: Reference Module in Earth Systems and Environmental Sciences.
Borsellino, R., Shulmeister, J., Winkler, S., 2017. Glacial geomorphology of the Barbizon & Butler Downs, Rangitata Valley, South Island. New Zealand. J. Maps 13, 502–510.
Boston, C.M., 2012a. A Lateglacial plateau icefield in the Monadhliath Mountains, Scotland: reconstruction, dynamics and palaeoclimatic implications. Unpublished PhD thesis. Queen Mary University of London 295 pp.
Boston, C.M., 2012b. A glacial geomorphological map of the Monadhliath Mountains, Central Scottish Highlands. J. Maps 8 (4), 437–444.
Boston, C.M., Lukas, S., Carr, S.J., 2015. A Younger Dryas plateau icefield in the Monadhliath, Scotland, and implications for regional palaeoclimate. Quat. Sci. Rev. 108, 139–162.
Boulton, G.S., Clark, C.D., 1990a. A highly mobile Laurentide ice sheet revealed by satellite images of glacial lineations. Nature 346 (6287), 813–817.
Boulton, G.S., Clark, C.D., 1990b. The Laurentide ice sheet through the last glacial cycle: the topology of drift lineations as a key to the dynamic behaviour of former ice sheets. Earth Environ. Sci. Trans. R. Soc. Edinb. 81 (4), 327–347.
Boulton, G.S., Dongelmans, P., Punkari, M., Broadgate, M., 2001. Palaeoglaciology of an ice sheet through a glacial cycle: the European ice sheet through the Weichselian. Quat. Sci. Rev. 20 (4), 591–625.
Bradwell, T., Stoker, M.S., Golledge, N.R., Wilson, C.K., Merritt, J.W., Long, D., Everest, J.D., Hestvik, O.B., Stevenson, A.G., Hubbard, A.L., Finlayson, A.G., Mathers, H.E., 2008. The northern sector of the last British Ice Sheet: maximum extent and demise. Earth-Sci. Rev. 88, 207–226.
Bradwell, T., Sigurðsson, O., Everest, J., 2013. Recent, very rapid retreat of a temperate glacier in SE Iceland. Boreas 42, 959–973.
Brodzikowski, K., van Loon, A.J., 1991. Glacigenic Sediments. Elsevier, Amsterdam 674 pp.
Brook, M.S., Kirkbride, M.P., 2018. Reconstruction and paleoclimatic significance of late Quaternary glaciers in the Tararua Range, North Island, New Zealand. Quat. Int. 470 (A), 53–66.
Brown, V.H., Evans, D.J.A., Evans, I.S., 2011a. The Glacial Geomorphology and Surficial Geology of the South-West English Lake District. J. Maps 7 (1), 221–243.
Brown, V.H., Stokes, C.R., Ó Cofaigh, C., 2011b. The Glacial Geomorphology of the North-West sector of the Laurentide Ice Sheet. J. Maps 7, 409–428.
Brynjólfsson, S., Schomacker, A., Ingólfsson, Ó., 2014. Geomorphology and the Little Ice Age extent of the Drangajökull ice cap, NW Iceland, with focus on its three surge-type outlets. Geomorphology 213, 292–304.
Brynjólfsson, S., Schomacker, A., Korsgaard, N.J., Ingólfsson, Ó., 2016. Surges of outlet glacier from the Drangajökull ice cap, northwest Iceland. Earth Planet. Sci. Lett. 450, 140–151.
Butler, J., Lane, S., Chandler, J., 1998. Assessment of DEM quality for characterizing surface roughness using close range digital photogrammetry. The Photogramm. Rec. 16 (92), 271–291.
Caldenius, C.C., 1932. Las glaciaciones cuaternarias en la Patagonia y Tierra del Fuego. Geogr. Ann. 14, 1–164.
Campbell, R.B., 1967a. Geology of Glenlyon map-area, Yukon Territory. Geological Survey of Canada, Memoir 352 92 pp.
Campbell, R.B., 1967b. Surficial Geology, Glenlyon, Yukon Territory. In: Geological Survey of Canada, "A" Series Map 1222A. 1. pp. 440.
Campbell, J.B., Wynne, R.H., 2011. Introduction to remote sensing, 5th Edition. Taylor and Francis, London 667 pp.
Carbonneau, P.E., Dietrich, J.T., 2017. Cost-effective non-metric photogrammetry from consumer-grade sUAS: implications for direct georeferencing of structure from motion photogrammetry. Earth Surf. Proc. Land. 42, 473–486.
Carrivick, J.L., Smith, M.W., Quincey, D.J., 2016. Structure from Motion in the Geosciences. New Analytical Methods in Earth and Environmental Science Series. John Wiley & Sons, Chichester, UK 208 pp.
Carrivick, J.L., Yde, J., Russell, A.J., Quincey, D.J., Ingeman-Nielsen, T., Mallalieu, J., 2017. Ice-margin and meltwater dynamics during the mid-Holocene in the Kangerlussuaq area of west Greenland. Boreas 46, 369–387.
Chamberlin, T.C., 1897/1965. The method of multiple working hypotheses. Science 148, 745–759.
Chandler, B.M.P., Lukas, S., 2017. Reconstruction of Loch Lomond Stadial (Younger Dryas) glaciers on Ben More Coigach, NW Scotland, and implications for reconstructing palaeoclimate using small ice masses. J. Quat. Sci. 32 (4), 475–492.
Chandler, B.M.P., Evans, D.J.A., Roberts, D.H., Ewertowski, M.W., Clayton, A.I., 2016a. Glacial geomorphology of the Skálafellsjökull foreland, Iceland: A case study of 'annual' moraines. J. Maps 12 (5), 904–916.
Chandler, B.M.P., Evans, D.J.A., Roberts, D.H., 2016b. Characteristics of recessional moraines at a temperate glacier in SE Iceland: Insights into patterns, rates and drivers of glacier retreat. Quat. Sci. Rev. 135, 171–205.
Chorley, R.J., 1962. Geomorphology and General Systems Theory. In: United States Geological Survey, Professional Paper 500B.
Clark, C.D., 1993. Mega-scale glacial lineations and cross-cutting ice-flow landforms. Earth Surf. Proc. Land. 18 (1), 1–29.
Clark, C.D., 1997. Reconstructing the evolutionary dynamics of former ice sheets using multi-temporal evidence, remote sensing and GIS. Quat. Sci. Rev. 16, 1067–1092.
Clark, C.D., Stokes, C.R., 2001. Extent and basal characteristics of the M'Clintock Channel Ice Stream. Quat. Int. 86, 81–101.
Clark, C.D., Knight, J.K., Gray, J.T., 2000. Geomorphological reconstruction of the Labrador sector of the Laurentide Ice Sheet. Quat. Sci. Rev. 19 (13), 1343–1366.
Clark, C.D., Evans, D.J.A., Khatwa, A., Bradwell, T., Jordan, C.J., Marsh, S.H., Mitchell, W.A., Bateman, M.D., 2004. Map and GIS database of glacial landforms and features related to the last British Ice Sheet. Boreas 33, 359–375.
Clark, C.D., Hughes, A.L.C., Greenwood, S.L., Spagnolo, M., Ng, F.S.L., 2009. Size and shape characteristics of drumlins, derived from a large sample, and associated scaling laws. Quat. Sci. Rev. 28, 677–692.
Clark, C.D., Hughes, A.L.C., Greenwood, S.L., Jordan, C., Sejrup, H.P., 2012. Pattern and timing of retreat of the last British-Irish Ice Sheet. Quat. Sci. Rev. 44, 112–146.
Clark, C.D., Ely, J.C., Greenwood, S.L., Hughes, A.L.C., Meehan, R., Barr, I.D., Bateman, M.D., Bradwell, T., Doole, J., Evans, D.J.A., Jordan, C.J., Monteys, X., Pellicer, X.M., Sheehy, M., 2018a. BRITICE Glacial Map, version 2: a map and GIS database of glacial landforms of the last British–Irish Ice Sheet. Boreas 47, 11–27.
Clark, C.D., Ely, J.C., Spagnolo, M., Hahn, U., Hughes, A.L.C., Stokes, C.R., 2018b. Spatial organization of drumlins. Earth Surf. Proc. Land. 43, 499–513.
Clayton, L., Teller, J.T., Attig, J.W., 1985. Surging of the southwestern part of the Laurentide Ice Sheet. Boreas 14 (3), 235–241.
Close, M.H., 1867. Notes on the general glaciation of Ireland. J. R. Geogr. Soc. Lond. Dublin 1, 207–242.
Coray, S., 2007. Glazialsedimentologische Untersuchungen an Flutes im Vorfeld des Findelengletschers. Unpublished MSc Thesis. Universität Bern 109 pp.
Coronato, A., Seppälä, M., Ponce, J.F., Rabassa, J., 2009. Glacial geomorphology of the Pleistocene lake Fagnano ice lobe, Tierra del Fuego, southern South America. Geomorphology 112 (1), 67–81.
Craig, B.G., 1961. Surficial geology of northern District of Keewatin, Northwest Territories. In: Geological Survey of Canada, Map 7-1961, Scale 1, pp. 1013760.
Craig, B.G., 1964. Surficial geology of east-central District of Mackenzie. Geological Survey of Canada, Bulletin 99.
Cumming, I.G., Wong, F.H., 2005. Digital Processing of Synthetic Aperture Radar Data: Algorithms and Implementation. Artech House, Boston.
da Rosa, K.K., Vieira, R., Fernandez, G.B., Simoes, F.L., Simoes, J.C., 2011. Formas glaciales y procesos glaciológicos del glaciar templado Wanda, Shetland del Sur. Investig. Geogr. 43, 3–16.
da Rosa, K.K., Vieira, R., Júnior, C.W.M., de Souza Júnior, E., Simões, J.C., 2013. Compilation of geomorphological map for reconstructing the deglaciation of ice-free areas in the Martel Inlet, King George Island. Antarctica. Rev. Bras. Geomorfol. 14 (2), 181–187.
Darvill, C.M., Stokes, C.R., Bentley, M.R., Lovell, H., 2014. A glacial geomorphological map of the southernmost ice lobes of Patagonia: the Bahía Inútil – San Sebastián, Magellan, Otway. Skyring and Río Gallegos lobes. J. Maps 10 (3), 500–520.
Darvill, C.M., Bentley, M.J., Stokes, C.R., Hein, A.S., Rodés, Á., 2015. Extensive MIS 3 glaciation in southernmost Patagonia revealed by cosmogenic nuclide dating of outwash sediments. Earth Planet. Sci. Lett. 429, 157–169.
Darvill, C.M., Stokes, C.R., Bentley, M.J., Evans, D.J.A., Lovell, H., 2017. Dynamics of former ice lobes of the southernmost Patagonian Ice Sheet based on a glacial landsystems approach. J. Quat. Sci. 32, 857–876.
De Angelis, H., 2007. Glacial geomorphology of the east-central Canadian Arctic. J. Maps 3, 323–341.
De Angelis, H., Kleman, J., 2007. Palaeo-ice streams in the Foxe/Baffin sector of the Laurentide Ice Sheet. Quat. Sci. Rev. 26 (9), 1313–1331.
De Geer, G., 1910. Den svenska Setsbergsexkursionen 1910 för deltagare i den 11:te internationella geologkonferensen i Stockholm. Ymer 30, 305–310.
Demek, J., 1972. Manual of detailed geomorphological mapping. IUG, Prague 344 pp.
Dowdeswell, J.A., Vásquez, M., 2013. Submarine landforms in the fjords of southern Chile: implications for glacimarine processes and sedimentation in a mild glacier-influenced environment. Quat. Sci. Rev. 64, 1–19.
Dowdeswell, J.A., Canals, M., Jakobsson, M., Todd, B.J., Dowdeswell, E.K., Hogan, K.A., 2016. Atlas of Submarine Glacial landforms: Modern. In: Quaternary and Ancient. Geological Society, London Memoirs, No. 46.
Dowling, T.P.F., Alexanderson, H., Möller, P., 2013. The new high-resolution LiDAR digital height model ('Ny Nationell Höjdmodell') and its application to Swedish Quaternary geomorphology. GFF 135 (2), 145–151.
Dowling, T.P.F., Spagnolo, M., Möller, P., 2015. Morphometry and core type of streamlined bedforms in southern Sweden from high resolution LiDAR. Geomorphology 236, 54–63.
Dowling, T.P.F., Möller, P., Spagnolo, M., 2016. Rapid subglacial streamlined bedform formation at a calving bay margin. J. Quat. Sci. 31, 879–892.
Dunstone, R.B., 2014. Testing the groove-ploughing theory for mega-scale glacial lineaton (MSGL) formation, using a large dataset of their morphology. Unpublished MSc thesis. University of Durham 127 pp. [Available at Durham e-theses]. http://etheses.dur.ac.uk/9457/.
Duveiller, G., Defourny, P., 2010. A conceptual framework to define the spatial resolution requirements for agricultural monitoring using remote sensing. Remote Sens. Environ. 114 (11), 2637–2650.
Dyke, A.S., 1990. Quaternary geology of the Frances Lake map area, Yukon and Northwest Territories. Geological Survey of Canada, Memoir 426.
Dyke, A.S., Hooper, J.M.G., 2001. Deglaciation of northwest Baffin Island, Nunavut. In: Geological Survey of Canada Map 1999A, Scale 1, pp. 500000.
Dyke, A.S., Prest, V.K., 1987a. Late Wisconsinan and Holocene History of the Laurentide Ice Sheet. Géogr. Phys. Quat. 41, 237–263.
Dyke, A.S., Prest, V.K., 1987b. Late Wisconsinan and Holocene retreat of the Laurentide Ice Sheet, Map 1702A. Geological Survey of Canada, Ottawa.
Dyke, A.S., Prest, V.K., 1987c. Paleogeography of northern North America, 18 000 - 5 000 years ago, Map 1703A. Geological Survey of Canada, Ottawa.
Dyke, A.S., Morris, T.F., Green, D.E.C., England, J., 1992. Quaternary geology of Prince of Wales Island, arctic Canada. Geological Survey of Canada Memoir 433.

Eisank, C., Smith, M., Hillier, J., 2014. Assessment of multiresolution segmentation for delimiting drumlins in digital elevation models. Geomorphology 214, 452–464.
Ely, J.C., Clark, C.D., Spagnolo, M., Stokes, C.R., Greenwood, S.L., Hughes, A.L.C., Dunlop, P., Hess, D., 2016a. Do subglacial bedforms comprise a size and shape continuum? Geomorphology 257, 108–119.
Ely, J.C., Gribble, E.A., Clark, C.D., 2016b. The glacial geomorphology of the western cordilleran ice sheet and Ahklun ice cap, Southern Alaska. J. Maps 12 (Sup. 1), 415–424.
Ely, J.C., Graham, C., Barr, I.D., Rea, B.R., Spagnolo, M., Evans, J., 2017. Using UAV acquired photography and structure from motion techniques for studying glacier landforms: application to the glacial flutes at Isfallsglaciären. Earth Surf. Proc. Land. 42 (6), 877–888.
Ely, J.C., Clark, C.D., Spagnolo, M., Hughes, A.L., Stokes, C.R., 2018. Using the size and position of drumlins to understand how they grow, interact and evolve. Earth Surf. Proc. Land. 43 (5), 1073–1087.
Ercolano, B., Coronato, A., Tiberi, P., Corbella, H., Marderwald, G., 2016. Glacial geomorphology of the tableland east of the Andes between the Coyle and Gallegos river valleys, Patagonia, Argentina. J. Maps 12 (1), 304–313.
Espinoza, J.M., 2016. Glacial geomorphology and paleoglacial behaviour estimation in the Sierra Baguales (50°S): Paleoclimatic factors that controlled glacier variations within the Pleistocene – Holocene regional context. Unpublished PhD thesis. Universidad de Chile.
Etzelmüller, B., Hagen, J.O., Vatne, G., Ødegård, R.S., Sollid, J.L., 1996. Glacier debris accumulation and sediment deformation influenced by permafrost: examples from Svalbard. Ann. Glaciol. 22, 53–62.
Evans, I.S., 1990. Cartographic techniques in geomorphology. In: Goudie, A.S. (Ed.), Geomorphological techniques, 2nd Edition. Routledge, London, pp. 97–108.
Evans, D.J.A. (Ed.), 2003. Glacial Landsystems. Arnold, London 532 pp.
Evans, D.J.A., 2003b. Ice-Marginal Terrestrial Landsystems: Active Temperate Glacier Margins. In: Evans, D.J.A. (Ed.), Glacial Landsystems. Arnold, London, pp. 12–43.
Evans, D.J.A., 2009. Glacial Geomorphology at Glasgow. Scottish Geographical Journal 125, 285–320.
Evans, D.J.A., 2010. Controlled moraine development and debris transport pathways in polythermal plateau icefields: examples from Tungnafellsjökull. Iceland. Earth Surf. Proc. Land. 35, 1430–1444.
Evans, D.J.A., 2011. Glacial landsystems of Satujökull, Iceland: A modern analogue for glacial landsystem overprinting by mountain icecaps. Geomorphology 129, 225–237.
Evans, I.S., 2012. Geomorphometry and landform mapping: What is a landform? Geomorphology 137, 94–106.
Evans, D.J.A., 2017. Chapter 4 – Conceptual glacial ground models: British and Irish case studies. In: Griffiths, J.S., Martin, C.J. (Eds.), Engineering Geology and Geomorphology of Glaciated and Periglaciated Terrains: Engineering Group Working Party Report. Engineering Geology Special Publication 28. The Geological Society, London, pp. 369–500.
Evans, D.J.A., Benn, D.I. (Eds.), 2004. A Practical Guide to the Study of Glacial Sediments. Arnold, London 266 pp.
Evans, D.J.A., Orton, C., 2015. Heinabergsjökull and Skalafellsjökull, Iceland: Active Temperate Piedmont Lobe and Outwash Head Glacial Landsystem. J. Maps 11 (3), 415–431.
Evans, D.J.A., Rea, B.R., 2003. Surging Glacier Landsystem. In: Evans, D.J.A. (Ed.), Glacial Landsystems. Arnold, London, pp. 259–288.
Evans, D.J.A., Twigg, D.R., 2002. The active temperate glacial landsystem: a model based on Breiðamerkurjökull and Fjallsjökull. Iceland. Quat. Sci. Rev. 21, 2143–2177.
Evans, D.J.A., Lemmen, D.S., Rea, B.R., 1999. Glacial landsystems of the southwest Laurentide Ice Sheet: modern Icelandic analogues. J. Quat. Sci. 14, 673–691.
Evans, D.J.A., Twigg, D.R., Shand, M., 2006. Surficial geology and geomorphology of the þórisjökull plateau icefield, west-central Iceland. J. Maps 2, 17–29.
Evans, D.J.A., Clark, C.D., Rea, B.R., 2008. Landform and sediment imprints of fast glacier flow in the southwest Laurentide Ice Sheet. J. Quat. Sci. 23 (3), 249–272.
Evans, D.J.A., Twigg, D.R., Rea, B.R., Orton, C., 2009a. Surging glacier landsystem of Tungnaárjökull. Iceland. J. Maps 5, 134–151.
Evans, D.J.A., Livingstone, S.J., Vieli, A., Ó Cofaigh, C., 2009b. The palaeoglaciology of the central sector of the British and Irish Ice Sheet: reconciling glacial geomorphology and preliminary ice sheet modelling. Quat. Sci. Rev. 28, 739–757.
Evans, D.J.A., Strzelecki, M., Milledge, D.G., Orton, C., 2012. Hørbyebreen polythermal glacial landsystem. Svalbard. J. Maps 8, 146–156.
Evans, D.J.A., Young, N.J.P., Ó Cofaigh, C., 2014. Glacial geomorphology of terrestrial-terminating fast flow lobes/ice stream margins in the southwest Laurentide Ice Sheet. Geomorphology 204, 86–113.
Evans, D.J.A., Roberts, D.H., Ó Cofaigh, C.Ó., 2015. Drumlin sedimentology in a hard-bed, lowland setting, Connemara, western Ireland: implications for subglacial bedform generation in areas of sparse till cover. J. Quat. Sci. 30, 537–557.
Evans, D.J.A., Ewertowski, M., Orton, C., 2016a. Fláajökull (north lobe), Iceland: active temperate piedmont lobe glacial landsystem. J. Maps 12 (5), 777–789.
Evans, D.J.A., Ewertowski, M., Jamieson, S.S.R., Orton, C., 2016b. Surficial geology and geomorphology of the Kumtor Gold Mine, Kyrgyzstan: human impacts on mountain glacier landsystems. J. Maps 12 (5), 757–769.
Evans, D.J.A., Ewertowski, M., Orton, C., 2016c. Eiríksjökull plateau icefield landsystem. Iceland. J. Maps 12 (5), 747–756.
Evans, D.J.A., Storrar, R.D., Rea, B.R., 2016d. Crevasse-squeeze ridge corridors: Diagnostic features of late-stage palaeo-ice stream activity. Geomorphology 258, 40–50.
Evans, D.J.A., Ewertowski, M., Orton, C., Harris, C., Guðmundsson, S., 2016e. Snæfellsjökull volcano-centred ice cap landsystem. West Iceland. J. Maps 12 (5), 1128–1137.
Evans, D.J.A., Ewertowski, M., Orton, C., 2017. Skaftafellsjökull, Iceland: glacial geomorphology recording glacier recession since the Little Ice Age. J. Maps 13, 358–368.
Everest, J.D., Bradwell, T., 2003. Buried glacier ice in southern Iceland and its wider significance. Geomorphology 52, 347–358.
Everest, J., Bradwell, T., Jones, L., Hughes, L., 2017. The geomorphology of Svínafellsjökull and Virkisjökull-Falljökull glacier forelands, southeast Iceland. J. Maps 13, 936–945.
Ewertowski, M.W., 2014. Recent transformations in the high-Arctic glacier landsystem, Ragnarbreen, Svalbard. Geogr. Ann. 96A (3), 265–285.
Ewertowski, M.W., Tomczyk, A.M., 2015. Quantification of the ice-cored moraines' short-term dynamics in the high-Arctic glaciers Ebbabreen and Ragnarbreen, Petuniabukta, Svalbard. Geomorphology 234, 211–227.
Ewertowski, M.W., Evans, D.J.A., Roberts, D.H., Tomczyk, A.M., 2016. Glacial geomorphology of the terrestrial margins of the tidewater glacier, Nordenskiöldbreen, Svalbard. J. Maps 12 (Sup. 1), 476–487.
Ewertowski, M.W., Kijowski, A., Szuman, I., Tomczyk, A.M., Kasprzak, L., 2017. Low-altitude remote sensing and GIS-based analysis of cropmarks: classification of past thermal-contraction-crack polygons in central western Poland. Geomorphology 293B, 418–432.
Eyles, N. (Ed.), 1983. Glacial Geology: An Introduction for Engineers and Earth Scientists. Permagon, Oxford 409 pp.
Fabel, D., Stroeven, A.P., Harbor, J., Kleman, J., Elmore, D., Fink, D., 2002. Landscape preservation under Fennoscandian ice sheets determined from in situ produced 10Be and 26Al. Earth Planet. Sci. Lett. 201, 397–406.
Fabel, D., Fink, D., Fredin, O., Harbor, J., Land, M., Stroeven, A.P., 2006. Exposure ages from relict lateral moraines overridden by the Fennoscandian ice sheet. Quat. Res. 65, 136–146.
Federici, P.R., Pappalardo, M., Ribolini, A., 2003. Geomorphological Map of the Maritime Alps Natural Park and surroundings (Argentera Massif, Italy), 1: 25000 scale. Selca, Florence.
Federici, P.R., Ribolini, A., Spagnolo, M., 2017. Glacial history of the Maritime Alps from the Last Glacial Maximum to the Little Ice Age. Geological Society, London, Special Publications 433 (1), 137–159.
Finke, L., 1980. Anforderungen aus der Planungspraxis an ein geomorphologisches Kartenwerk. In: Barsch, D., Liedtke, H. (Eds.), Methoden und Anwendbarkeit geomorphologischer Detailkarten. Freie Universität Berlin, Berlin, pp. 75–81.
Finlayson, A., Merritt, J., Browne, M., Merritt, J., McMillan, A., Whitbread, K., 2010. Ice sheet advance, dynamics, and decay configurations: evidence from west central Scotland. Quat. Sci. Rev. 29, 969–988.
Finlayson, A.G., Golledge, N., Bradwell, T., Fabel, D., 2011. Evolution of a Lateglacial mountain icecap in northern Scotland. Boreas 40, 536–554.
Flink, A.E., Noormets, R., Kirchner, N., Benn, D.I., Luckman, A., Lovell, H., 2015. The evolution of a submarine landform record following recent and multiple surges of Tunabreen glacier. Svalbard. Quat. Sci. Rev. 108, 37–50.
Flint, R.F., Colton, R.B., Goldthwait, R.P., Willman, H.B., 1959. Glacial map of the United States east of the Rocky Mountains. Geological Society of America.
Follestad, B., Bergstrøm, B., 2004. Otta 1718-IV. In: Quaternary geology map with description. 1. Norwegian Geological Survey, pp. 50000.
Fourrière, A., Claudin, P., Andreotti, B., 2010. Bedforms in a turbulent stream: Formation of ripples by primary linear instability and of dunes by nonlinear pattern coarsening. J. Fluid Mech. 649, 287–328.
Fu, P., Heyman, J., Hättestrand, C., Stroeven, A.P., Harbor, J.M., 2012. Glacial geomorphology of the Shaluli Shan area, southeastern Tibetan Plateau. J. Maps 8, 48–55.
Garcia, J.L., Kaplan, M.R., Hall, B.L., Schaefer, J.M., Vega, R.M., Schwartz, R., Finkel, R., 2012. Glacier expansion in southern Patagonia throughout the Antarctic cold reversal. Geology 40, 859–862.
Glasser, N.F., Jansson, K.N., 2005. Fast-flowing outlet glaciers of the last glacial maximum Patagonian Icefield. Quat. Res. 63 (2), 206–211.
Glasser, N., Jansson, K., 2008. The Glacial Map of southern South America. J. Maps 4, 175–196.
Glasser, N.F., Jansson, K.N., Harrison, S., Rivera, A., 2005. Geomorphological evidence for variations of the North Patagonian Icefield during the Holocene. Geomorphology 71 (3-4), 263–277.
Glasser, N.F., Jansson, K.N., Harrison, S., Kleman, J., 2008. The glacial geomorphology and Pleistocene history of South America between 38 S and 56 S. Quat. Sci. Rev. 27 (3), 365–390.
Golledge, N.R., Stoker, M.S., 2006. A palaeo-ice-stream of the British Ice Sheet in eastern Scotland. Boreas 35, 231–243.
Golledge, N.R., Hubbard, A., Sugden, D.E., 2008. High-resolution numerical simulation of Younger Dryas glaciation in Scotland. Quat. Sci. Rev. 27, 888–904.
Goodchild, J.G., 1875. The glacial phenomena of the Eden Valley and the western part of the Yorkshire-dale District. Quart. J. Geol. Soc. Lond. 31, 55–99.
Graf, A., 2007. Genese alpiner Seitenmoränen am Beispiel des Findelengletschers bei Zermatt (VS). Unpublished MSc Thesis. Universität Bern 126 pp.
Greenwood, S.L., Clark, C.D., 2008. Subglacial bedforms of the Irish Ice Sheet. J. Maps 4, 332–357.
Greenwood, S.L., Clark, C.D., 2009a. Reconstructing the last Irish Ice Sheet 1: changing flow geometries and ice flow dynamics deciphered from the glacial landform record. Quat. Sci. Rev. 28, 3085–3100.
Greenwood, S.L., Clark, C.D., 2009b. Reconstructing the last Irish Ice Sheet 2: a geomorphologically-driven model of ice sheet growth, retreat and dynamics. Quat. Sci. Rev. 28 (27), 3101–3123.
Greenwood, S.L., Kleman, J., 2010. Glacial landforms of extreme size in the Keewatin sector of the Laurentide Ice Sheet. Quat. Sci. Rev. 29 (15), 1894–1910.
Greenwood, S.L., Clark, C.D., Hughes, A.L.C., 2007. Formalising an inversion methodology for reconstructing ice-sheet retreat patterns from meltwater channels:

application to the British Ice Sheet. J. Quat. Sci. 22, 637–645.
Greenwood, S.L., Clason, C.C., Mikko, H., Nyberg, J., Peterson, G., Smith, C.A., 2015. Integrated use of lidar and multibeam bathymetry reveals onset of ice streaming in the northern Bothnian Sea. GFF 137, 284–292.
Greenwood, S.L., Clason, C.C., Nyberg, J., Jakobsson, M., Holmlund, P., 2017. The Bothnian Sea ice stream: early Holocene retreat dynamics of the south-central Fennoscandian Ice Sheet. Boreas 46, 346–362.
Gribenski, N., Jansson, K.N., Lukas, S., Stroeven, A.P., Harbor, J.M., Blomdin, R., Ivanov, M.N., Heyman, J., Petrakov, D.A., Rudoy, A., Clifton, T., Lifton, N.A., Caffee, M.W., 2016. Complex patterns of glacier advances during the late glacial in the Chagan Uzun Valley, Russian Altai. Quat. Sci. Rev. 149, 288–305.
Gribenski, N., Jansson, K.N., Preusser, F., Harbor, J.M., Stroeven, A.P., Trauerstein, M., Blomdin, R., Heyman, J., Caffee, M.W., Lifton, N.A., Zhang, W., 2018. Re-evaluation of MIS 3 glaciation using cosmogenic radionuclide and single grain luminescence ages, Kanas Valley, Chinese Altai. J. Quat. Sci. 33, 55–67.
Griffiths, J.S., Martin, C.J. (Eds.), 2017. Engineering Geology and Geomorphology of Glaciated and Periglaciated Terrains: Engineering Group Working Party Report. Engineering Geology Special Publication 28 The Geological Society, London 953 pp.
Grodecki, J., Dial, G., 2003. Block Adjustment of High-Resolution Satellite Images Described by Rational Polynomials. Photogramm. Eng. Remote Sens. 69 (1), 59–68.
Gustavsson, M., Kolstrup, E., Seijmonsbergen, A.C., 2006. A new symbol-and-GIS based detailed geomorphological mapping system: Renewal of a scientific discipline for understanding landscape development. Geomorphology 77 (1–2), 90–111.
Gustavsson, M., Seijmonsbergen, A.C., Kolstrup, E., 2008. Structure and contents of a new geomorphological GIS database linked to a geomorphological map – With an example from Liden, central Sweden. Geomorphology 95, 335–349.
Harbor, J., Stroeven, A.P., Fabel, D., Clarhäll, A., Kleman, J., Li, Y.K., Elmore, D., Fink, D., 2006. Cosmogenic nuclide evidence for minimal erosion across two subglacial sliding boundaries of the late glacial Fennoscandian ice sheet. Geomorphology 75, 90–99.
Hardt, J., Hebenstreit, R., Lüthgens, C., Böse, M., 2015. High-resolution mapping of ice-marginal landforms in the Barnim region, northeast Germany. Geomorphology 250, 41–52.
Hättestrand, C., 1998. The glacial geomorphology of central and northern Sweden. Sver. Geol. Unders. Ca 85, 1–47.
Hättestrand, C., Clark, C.D., 2006. The glacial geomorphology of Kola Peninsula and adjacent areas in the Murmansk Region. Russia. J. Maps 2, 30–42.
Hättestrand, C., Stroeven, A.P., 1996. Field evidence for wet-based ice sheet erosion from the south-central Queen Elizabeth Islands, Northwest Territories. Canada. Arct. Alp. Res. 28, 466–474.
Hättestrand, C., Stroeven, A.P., 2002. A relict landscape in the centre of Fennoscandian glaciation: Geomorphological evidence of minimal Quaternary glacial erosion. Geomorphology 44 (1), 127–143.
Hättestrand, C., Goodwillie, D., Kleman, J., 1999. Size distribution of two cross-cutting drumlin systems in northern Sweden: a measure of selective erosion and formation time length. Ann. Glaciol. 28, 146–152.
Hättestrand, C., Kosche, S., Näslund, J.-O., Fabel, D., Stroeven, A.P., 2004. Drumlin formation time - evidence from northern and central Sweden. Geogr. Ann. 86A, 155–167.
Hättestrand, C., Kolka, V., Stroeven, A.P., 2007. The Keiva ice marginal zone on the Kola Peninsula, northwest Russia: a key component for reconstructing the palaeoglaciology of the northeastern Fennoscandian Ice Sheet. Boreas 36, 352–370.
Heiser, P.A., Roush, J.J., 2001. Pleistocene glaciations in Chukotka, Russia: moraine mapping using satellite synthetic aperture radar (SAR) imagery. Quat. Sci. Rev. 20 (1), 393–404.
Hess, D.P., Briner, J.P., 2009. Geospatial analysis of controls on subglacial bedform morphometry in the New York Drumlin Field – implications for Laurentide Ice Sheet dynamics. Earth Surf. Proc. Land. 34, 1126–1135.
Heyman, J., Hättestrand, C., Stroeven, A.P., 2008. Glacial geomorphology of the Bayan Har sector of the NE Tibetan Plateau. J. Maps 4 (1), 42–62.
Hillier, J.K., Smith, M.J., Clark, C.D., Stokes, C.R., Spagnolo, M., 2013. Subglacial bedforms reveal an exponential size–frequency distribution. Geomorphology 190, 82–91.
Hillier, J.K., Smith, M.J., Armugam, R., Barr, I., Boston, C.M., Clark, C.D., Ely, J., Frankl, A., Greenwood, S.L., Gosselin, L., Hättestrand, C., Hogan, K., Hughes, A.L.C., Livingstone, S.J., Lovell, H., McHenry, M., Munoz, Y., Pellicer, X.M., Pellitero, R., Robb, C., Roberson, S., Ruther, D., Spagnolo, M., Standell, M., Stokes, C.R., Storrar, R., Tate, N.J., Wooldridge, K., 2015. Manual mapping of drumlins in synthetic landscapes to assess operator effectiveness. J. Maps 11, 719–729.
Hillier, J.K., Kougioumtzoglou, I.A., Stokes, C.R., Smith, M.J., Clark, C.D., Spagnolo, M.S., 2016. Exploring Explanations of Subglacial Bedform Sizes Using Statistical Models. PLoS One 11, e0159489.
Hillier, J.K., Benediktsson, Í.Ö., Dowling, T.P.F., Schomacker, A., 2018. Production and preservation of the smallest drumlins. GFF 140 (2), 136–152.
Hochreuther, P., Loibl, D., Wernicke, J., Zhu, H., Grießinger, J., Bräuning, A., 2015. Ages of major Little Ice Age glacier fluctuations on the southeast Tibetan Plateau derived from tree-ring-based moraine dating. Palaeogeogr., Palaeoclimatol. Palaeoecol. 422, 1–10.
Hodgson, D.A., Vincent, J.S., Fyles, J.G., 1984. Quaternary geology of central Melville Island, Northwest Territories. In: Geological Survey of Canada paper 83-16.
Hodgson, D.A., Graham, A.G.C., Griffiths, H.J., Roberts, S.J., Ó Cofaigh, C., Bentley, M.J., Evans, D.J.A., 2014. Glacial history of sub-Antarctic South Georgia based on the submarine geomorphology of its fjords. Quat. Sci. Rev. 89, 129–147.
Hollingworth, S.E., 1931. The glaciation of western Edenside and adjoining areas and the drumlins of Edenside and the Solway Basin. Quart. J. Geol. Soc. Lond. 87, 281–359.
Horsfield, B.R., 1983. The deglaciation pattern of the western Grampians of Scotland. Unpublished PhD thesis. University of East Anglia.
Houmark-Nielsen, M., Kjær, K.H., 2003. Southwest Scandinavia, 40-15 kyr BP: Palaeogeography and environmental change. J. Quat. Sci. 18, 769–786.
Howarth, P.J., 1968. Geomorphological and Glaciological Studies, Eastern Breiðamerkurjökull, Iceland. Unpublished PhD thesis. University of Glasgow.
Howarth, P.J., Welch, R., 1969a. Breiðamerkurjökull, South-east Iceland, August 1945, 1:30,000 scale map. University of Glasgow.
Howarth, P.J., Welch, R., 1969b. Breiðamerkurjökull, South-east Iceland, August 1965, 1:30,000 scale map. University of Glasgow.
Hubbard, B., Glasser, N.F., 2005. Field techniques in glaciology and glacial geomorphology. John Wiley and Sons, Chichester 400 pp.
Hubbard, A., Bradwell, T., Golledge, N., Hall, A., Patton, H., Sugden, D., Cooper, R., Stoker, M., 2009. Dynamic cycles, ice streams and their impact on the extent, chronology and deglaciation of the British–Irish ice sheet. Quat. Sci. Rev. 28, 758–776.
Hughes, A.L.C., Clark, C.D., Jordan, C.J., 2010. Subglacial bedforms of the last British Ice Sheet. J. Maps 6, 543–563.
Hughes, A.L.C., Clark, C.D., Jordan, C.J., 2014. Flow-pattern evolution of the last British Ice Sheet. Quat. Sci. Rev. 89, 148–168.
Hughes, A.L.C., Gyllencreutz, R., Lohne, Ø.S., Mangerud, J., Svendsen, J.I., 2016. The last Eurasian ice sheets - a chronological database and time-slice reconstruction, DATED-1. Boreas 45, 1–45.
Hyatt, O.M., 2010. Insights into New Zealand Glacial Processes from studies of glacial geomorphology and sedimentology in Rakaia and other South Island Valleys. Unpublished PhD thesis. University of Canterbury 251 pp.
Immerzeel, W.W., Kraaijenbrink, P.D.A., Shea, J.M., Shrestha, A.B., Pellicciotti, F., Bierkens, M.F.P., de Jong, S.M., 2014. High-resolution monitoring of Himalayan glacier dynamics using unmanned aerial vehicles. Remote Sens. Environ. 150, 93–103.
Izagirre, E., Darvill, C.M., Rada, C., Aravena, J.C., 2018. Glacial geomorphology of the Marinelli and Pigafetta glaciers, Cordillera Darwin Icefield, southernmost Chile. J. Maps 14, 269–281.
Jakobsson, M., Mayer, L., Coakley, B., Dowdeswell, J.A., Forbes, S., Fridman, B., Hodnesdal, H., Noormets, R., Pedersen, R., Rebesco, M., Schenke, H.W., Zarayskaya, Y., Accettella, D., Armstrong, A., Anderson, R.M., Bienhoff, P., Camerlenghi, A., Church, I., Edwards, M., Gardner, J.V., Hall, J.K., Hell, B., Hestvik, O., Kristoffersen, Y., Marcussen, C., Mohammad, R., Mosher, D., Nghiem, S.V., Pedrosa, M.T., Travaglini, P.G., Weatherall, P., 2012. The International Bathymetric Chart of the Arctic Ocean (IBCAO) Version 3.0. Geophys. Res. Lett. 39, L12609.
James, M.R., Robson, S., Smith, M.W., 2017. 3-D uncertainty-based topographic change detection with structure-from-motion photogrammetry: precision maps for ground control and directly georeferenced surveys. Earth Surf. Process. Land. 42, 1769–1788.
Jamieson, S.S.R., Ewertowski, M.W., Evans, D.J.A., 2015. Rapid advance of two mountain glaciers in response to mine-related debris loading. J. Geophys. Res.: Earth Surf. 120, 1418–1435.
Jansson, K.N., 2003. Early Holocene glacial lakes and ice marginal retreat pattern in Labrador/Ungava, Canada. Palaeogeogr., Palaeoclim. Palaeoecol. 193, 473–501.
Jansson, K.N., Glasser, N.F., 2005. Using Landsat 7 ETM+ imagery and Digital Terrain Models for mapping glacial lineaments on former ice sheet beds. Int. J. Remote Sens. 26 (18), 3931–3941.
Jansson, K.N., Kleman, J., Marchant, D.R., 2002. The succession of ice-flow patterns in north-central Québec-Labrador. Canada. Quat. Sci. Rev. 21 (4), 503–523.
Jansson, K.N., Stroeven, A.P., Kleman, J., 2003. Configuration and timing of Ungava Bay ice streams, Labrador–Ungava, Canada. Boreas 32 (1), 256–262.
Johnson, M.D., Fredin, O., Ojala, A.E.K., Peterson, G., 2015. Unravelling Scandinavian geomorphology: the LiDAR revolution. GFF 137, 245–251.
Jónsson, S.A., Schomacker, A., Benediktsson, Í.Ö., Ingólfsson, Ó., Johnson, M.D., 2014. The drumlin field and the geomorphology of the Múlajökull surge-type glacier, central Iceland. Geomorphology 207, 213–220.
Jónsson, S.A., Benediktsson, Í.Ö., Ingólfsson, Ó., Schomacker, A., Bergsdóttir, H.L., Jacobsson, W.R., Linderson, H., 2016. Submarginal drumlin formation and late Holocene history of Fláajökull, southeast Iceland. Ann. Glaciol. 57, 128–141.
Jorge, M.G., Brennand, T.A., 2017a. Measuring (subglacial) bedform orientation, length, and longitudinal asymmetry–Method assessment. PloS one 12 (3), e0174312.
Jorge, M.G., Brennand, T.A., 2017b. Semi-automated extraction of longitudinal subglacial bedforms from digital terrain models–Two new methods. Geomorphology 288, 148–163.
Juyal, N., Thakkar, P.S., Sundriyal, Y.P., 2011. Geomorphic evidence of glaciations around Mount Kailash (Inner Kora): implication to past climate. Current Science 100 (4), 535–541.
Karlén, W., 1973. Holocene glacier and climatic variations, Kebnekaise Mountains, Swedish Lapland. Geogr. Ann. 55A, 29–63.
Kassab, C., Wang, J., Harbor, J., 2013. Glacial geomorphology of the Dalijia Shan region, northeastern Tibetan Plateau. J. Maps 9 (1), 98–105.
Kelley, S.E., Kaplan, M.R., Schaefer, J.M., Andersen, B.G., Barrell, D.J.A., Putnam, A.E., Denton, G.H., Schwartz, R., Finkel, R.C., Doughty, A.M., 2014. High-precision 10Be chronology of moraines in the Southern Alps indicates synchronous cooling in Antarctica and New Zealand 42,000 years ago. Earth Planet. Sci. Lett. 405, 194–206.
Kendall, P.F., 1902. A system of glacier lakes in the Cleveland Hills. Quart. J. Geol. Soc. Lond. 58, 471–571.
Kerschner, H., Kaser, G., Sailer, R., 2000. Alpine Younger Dryas glaciers as palaeo-precipitation gauges. Ann. Glaciol. 31, 80–84.
Kienholz, H., 1977. Kombinierte geomorphologische Gefahrenkarte 1:10,000 von Grindelwald. Geographica Bernensia G4, 1–204.
King, E.C., Woodward, J., Smith, A.M., 2007. Seismic and radar observations of subglacial bed forms beneath the onset zone of Rutford Ice Stream. Antarctica. J. Glaciol. 53 (183), 665–672.
King, E.C., Hindmarsh, R.C., Stokes, C.R., 2009. Formation of mega-scale glacial

lineations observed beneath a West Antarctic ice stream. Nat. Geosci. 2 (8), 585–588.
King, E.C., Pritchard, H.D., Smith, A.M., 2016a. Subglacial landforms beneath Rutford Ice Stream, Antarctica: detailed bed topography from ice-penetrating radar. Earth Syst. Sci. Data 8 (1), 151–158.
King, O., Hambrey, M.J., Irvine-Fynn, T.D.L., Holt, T.O., 2016b. The structural, geometric and volumetric changes of a polythermal Arctic glacier during a surge cycle: Comfortlessbreen. Svalbard. Earth Surf. Process. Land. 41, 162–177.
King, O., Quincey, D.J., Carrivick, J.L., Rowan, A.V., 2017. Spatial variability in mass loss of glaciers in the Everest region, central Himalayas, between 2000 and 2015. The Cryosphere 11, 407–426.
Kirchner, N., Greve, R., Stroeven, A.P., Heyman, J., 2011. Paleoglaciological reconstructions for the Tibetan Plateau during the last glacial cycle: evaluating numerical ice sheet simulations driven by GCM-ensembles. Quat. Sci. Rev. 30, 248–267.
Kirkbride, M.P., Winkler, S., 2012. Correlation of Late Quaternary moraines: impact of climate variability, glacier response, and chronological resolution. Quat. Sci. Rev. 46, 1–29.
Kjær, K.H., Krüger, J., 2001. The final phase of dead-ice moraine development: processes and sediment architecture, Kotlujokull, Iceland. Sedimentology 48, 935–952.
Kjær, K.H., Houmark-Nielsen, M., Richardt, N., 2003. Ice-flow patterns and dispersal of erratics at the southwestern margin of the last Scandinavian Ice Sheet: signature of paleo-ice streams. Boreas 32, 130–148.
Kjær, K.H., Korsgaard, N.J., Schomacker, A., 2008. Impact of multiple glacier surges – a geomorphological map from Brúarjökull. East Iceland. J. Maps 4, 5–20.
Kłapyta, P., 2013. Application of Schmidt hammer relative age dating to Late Pleistocene moraines and rock glaciers in the Western Tatra Mountains, Slovakia. Catena 111, 104–121.
Klassen, R.A., 1993. Quaternary geology and glacial history of Bylot Island. Northwest Territories. Geological Survey of Canada Memoir 429.
Kleman, J., 1990. On the use of glacial striae for reconstruction of palaeo-ice sheet flow patterns. Geogr. Ann. 72A, 217–236.
Kleman, J., 1992. The Palimpsest Glacial Landscape in Northwestern Sweden. Late Weichselian Deglaciation Landforms and Traces of Older West-Centered Ice Sheets. Geogr. Ann. 74A (4), 305–325.
Kleman, J., Borgström, I., 1996. Reconstruction of Palaeo-Ice Sheets: The Use of Geomorphological Data. Earth Surf. Process. Land. 21, 893–909.
Kleman, J., Stroeven, A.P., 1997. Preglacial surface remnants and Quaternary glacial regimes in northwestern Sweden. Geomorphology 19 (1–2), 35–54.
Kleman, J., Hättestrand, C., Borgström, I., Stroeven, A., 1997. Fennoscandian palaeoglaciology reconstructed using a glacial geological inversion model. J. Glaciol. 43 (144), 283–299.
Kleman, J., Fastook, J., Stroeven, A.P., 2002. Geologically and geomorphologically constrained numerical model of Laurentide Ice Sheet inception and build-up. Quat. Int. 95-96, 87–98.
Kleman, J., Hättestrand, C., Stroeven, A.P., Jansson, K.N., De Angelis, H., Borgström, I., 2006. Reconstruction of palaeo-ice sheets; inversion of their glacial geomorphological record. In: Knight, P.G. (Ed.), Glacier Science and Environmental Change. Blackwell, Oxford, pp. 192–199.
Kleman, J., Stroeven, A.P., Lundqvist, J., 2008. Patterns of Quaternary ice sheet erosion and deposition in Fennoscandia. Geomorphology 97, 73–90.
Kleman, J., Jansson, K., De Angelis, H., Stroeven, A.P., Hättestrand, C., Alm, G., Glasser, N., 2010. North American Ice Sheet build-up during the last glacial cycle, 115–21kyr. Quat. Sci. Rev. 29, 2036–2051.
Klimaszewski, M., 1990. Thirty years of detailed geomorphological mapping. Geogr. Pol. 58, 11–18.
Kneisel, C., Lehmkuhl, F., Winkler, S., Tressel, E., Schröder, H., 1998. Legende für geomorphologische Kartierungen in Hochgebirgen (GMK Hochgebirge). Trier. Geogr. Stud. 18, 1–24.
Knight, J., Mitchell, W., Rose, J., 2011. Geomorphological Field Mapping. In: Smith, M.J., Paron, P., Griffiths, J. (Eds.), Geomorphological Mapping: Methods and Applications. Developments in Earth Surface Processes 15. Elsevier, London, pp. 151–188.
Kocurek, G., Ewing, R.C., Mohrig, D., 2010. How do bedform patterns arise? New views on the role of bedform interactions within a set of boundary conditions. Earth Surf. Process. Land. 35, 51–63.
Korsgaard, N.J., Schomacker, A., Benediktsson, Í.Ö., Larsen, N.K., Ingólfsson, Ó., Kjær, K.H., 2015. Spatial distribution of erosion and deposition during a glacier surge: Brúarjökull, Iceland. Geomorphology 250, 258–270.
Kraak, M.J., Oremling, F.J., 2010. Cartography: visualization of spatial data, 3rd Edition. Routledge, London.
Kronberg, P., 1984. Photogeologie. Eine Einfhrung in die Grundlagen und Methoden der geologischen Auswertung von Luftbildern. Enke, Stuttgart.
Krüger, J., 1994. Glacial processes, sediments, landforms and stratigraphy in the terminus region of Mýrdalsjökull, Iceland. Folia Geographica Danica 21, 1–233.
Krüger, J., 1995. Origin, chronology and climatological significance of annual moraine ridges at Mýrdalsjökull, Iceland. The Holocene 5, 420–427.
Krüger, J., Kjær, K.H., 2000. De-icing progression of ice-cored moraines in a humid, subpolar climate, Kötlujökull, Iceland. The Holocene 10, 737–747.
Krygowski, B., 1963. Mapa Geomorfologiczna Niziny Wielkopolsko-Kujawskiej [Geomorphological Map of Wielkopolska-Kujawy lowland]. In: 1: 300,000 Map. Adam Mickiewicz University.
Kuhle, M., 1990. Quantificational reductionism as a risk in geography instanced by the 1:25,000 Geomorphological Map of the Federal Republic of Germany. Geogr. Pol. 58, 41–54.
Lam, N.S.N., Quattrochi, D.A., 1992. On the issues of scale, resolution, and fractal analysis in the mapping sciences. The Prof. Geogr. 44 (1), 88–98.
Lane, S.N., Reid, S.C., Westaway, R.M., Hicks, D.M., 2005. Remotely sensed topographic data for river channel research: the identification, explanation and management of error. In: Kelly, R.E.J., Drake, N.A., Barr, S.L. (Eds.), Spatial Modelling of the Terrestrial Environment. John Wiley & Sons, Ltd, Chichester, UK, pp. 113–136.
Lardeux, P., Glasser, N., Holt, T., Hubbard, B., 2015. Glaciological and geomorphological map of Glacier Noir and Glacier Blanc. French Alps. J. Maps 12, 582–596.
Leser, H., 1983. Anwendung und Auswertung geomorphologischer Kartierungen und Karten. Mater. Physiogeogr. 5, 5–13.
Leser, H., Stäblein, G., 1975. Geomorphologische Kartierung – Richtlinien zur Herstellung geomorphologischer Karten 1: 25,000. Berliner Geographische Abhandlungen Sonderheft 1–33.
Levy, L.B., Larsen, N.K., Davidson, T.A., Strunk, A., Olsen, J., Jeppesen, E., 2017. Contrasting evidence of Holocene ice margin retreat, south-western Greenland. J. Quat. Sci. 32, 604–616.
Li, Y., Li, Y., Chen, Y., Lu, X., 2016. Presumed Little Ice Age glacial extent in the eastern Tian Shan. China. J. Maps 12 (1), 71–78.
Lidmar-Bergström, K., Elvhage, C., Ringberg, B., 1991. Landforms in Skane, south Sweden. Geografiska Annaler 73A, 61–91.
Lifton, N., Beel, C., Hättestrand, C., Kassab, C., Rogozhina, I., Heermance, R., Oskin, M., Burbank, D., Blomdin, R., Gribenski, N., Caffee, M., 2014. Constraints on the late Quaternary glacial history of the Inylchek and Sary-Dzaz valleys from in situ cosmogenic 10Be and 26Al, eastern Kyrgyz Tian Shan. Quat. Sci. Rev. 101, 77–90.
Lillesand, T.M., Kiefer, R.W., Chipman, J.W., 2015. Remote Sensing and Image Interpretation (7th Edition). John Wiley & Sons, Hoboken, USA 768 pp.
Lindholm, M.S., Heyman, J., 2016. Glacial geomorphology of the Maidika region, Tibetan Plateau. J. Maps 12 (5), 797–803.
Livingstone, S.J., Ó Cofaigh, C., Evans, D.J.A., 2008. The glacial geomorphology of the central sector of the British-Irish Ice Sheet. J. Maps 4, 358–377.
Livingstone, S.J., Evans, D.J.A., Ó Cofaigh, C., 2010. Re-advance of Scottish ice into the Solway Lowlands (Cumbria, UK) during the Main Late Devensian deglaciation. Quat. Sci. Rev. 29, 2544–2570.
Livingstone, S.J., Ó Cofaigh, C., Stokes, C., Hillenbrand, C.-D., Vieli, A., Jamieson, S.S.R., 2012. Antarctic palaeo-ice streams. Earth-Sci. Rev. 111, 90–128.
Livingstone, S.J., Storrar, R.D., Hillier, J.K., Stokes, C.R., Clark, C.D., Tarasov, L., 2015. An ice-sheet scale comparison of eskers with modelled subglacial drainage routes. Geomorphology 246, 104–112.
Loibl, D., Hochreuther, P., Schulte, P., Hülle, D., Zhu, H., Bräuning, A., Lehmkuhl, F., 2015. Toward a late Holocene glacial chronology for the eastern Nyainqêntanglha Range, southeastern Tibet. Quat. Sci. Rev. 107, 243–259.
Lønne, I., 2016. A new concept for glacial geological investigations of surges, based on High-Arctic examples (Svalbard). Quat. Sci. Rev. 132, 74–100.
Lovell, H., 2014. On the ice-sediment-landform associations of surging glaciers on Svalbard. Unpublished PhD thesis. Queen Mary University of London 312 pp.
Lovell, H., Boston, C.M., 2017. Glacitectonic composite ridge systems and surge-type glaciers: an updated correlation based on Svalbard, Norway. arktos 3, 2.
Lovell, H., Stokes, C.R., Bentley, M.J., 2011. A glacial geomorphological map of the Seno Skyring-Seno Otway-Strait of Magellan region, southernmost Patagonia. J. Maps 7, 318–339.
Lovell, H., Stokes, C.R., Bentley, M.J., Benn, D.I., 2012. Evidence for rapid ice flow and proglacial lake evolution around the central Strait of Magellan region, southernmost Patagonia. J. Quat. Sci. 27, 625–638.
Lovell, H., Benn, D.I., Lukas, S., Spagnolo, M., Cook, S.J., Swift, D.A., Clark, C.D., Yde, J.C., Watts, T.P., 2018. Geomorphological investigation of multiphase glacitectonic composite ridge systems in Svalbard. Geomorphology 300, 176–188.
Lueder, D.R., 1959. Aerial Photographic Interpretation – Principles and Applications. McGraw-Hill, New York.
Lukas, S., 2002. Geomorphological evidence for the pattern of deglaciation around the Drumochter Pass, Central Grampian Highlands, Scotland. Unpublished MSc thesis. Ruhr-University of Bochum, Germany 115 pp.
Lukas, S., 2005. A test of the englacial thrusting hypothesis of 'hummocky' moraine formation – case studies from the north-west Highlands, Scotland. Boreas 34, 287–307.
Lukas, S., 2006. Morphostratigraphic principles in glacier reconstruction -a perspective from the British Younger Dryas. Prog. Phys. Geogr. 30, 719–736.
Lukas, S., 2007a. Early-Holocene glacier fluctuations in Krundalen, south central Norway: palaeo-glacier dynamics and palaeoclimate. The Holocene 17, 585–598.
Lukas, S., 2007b. 'A test of the englacial thrusting hypothesis of "hummocky" moraine formation: case studies from the northwest Highlands, Scotland': Reply to comments. Boreas 36, 108–113.
Lukas, S., 2011. Ice-cored moraines. In: Singh, V., Singh, P., Haritashya, U.K. (Eds.), Encyclopedia of Snow. Ice and Glaciers. Springer, Heidelberg, pp. 616–619.
Lukas, S., 2012. Processes of annual moraine formation at a temperate alpine valley glacier: insights into glacier dynamics and climatic controls. Boreas 41 (3), 463–480.
Lukas, S., Benn, D.I., 2006. Retreat dynamics of Younger Dryas glacier in the far NW Scottish Highlands reconstructed from moraine sequences. Scott. Geogr. J. 122, 308–325.
Lukas, S., Lukas, T., 2006. A glacial geological and geomorphological map of the far NW Highlands, Scotland. Parts 1 and 2. J. Maps 2, 43–56 56–58.
Lukas, S., Sass, O., 2011. The formation of Alpine lateral moraines inferred from sedimentology and radar reflection patterns: a case study from Gornergletscher, Switzerland. Geological Society, London, Special Publications 354, 77–92.
Lukas, S., Nicholson, L.I., Ross, F.H., Humlum, O., 2005. Formation, meltout processes and landscape alteration of High-Arctic ice-cored moraines—examples from Nordenskiöld Land. Central Spitsbergen. Polar Geogr. 29, 157–187.
Lukas, S., Nicholson, L.I., Humlum, O., 2007. Comment on Lønne and Lysså (2005): "Deglaciation dynamics following the Little Ice Age on Svalbard: Implications for shaping of landscapes at high latitudes", Geomorphology 72, 300–319. Geomorphology 84, 145–149.
Lukas, S., Benn, D.I., Boston, C.M., Brook, M.S., Coray, S., Evans, D.J.A., Graf, A., Kellerer-

Pirklbauer-Eulenstein, A., Kirkbride, M.P., Krabbendam, M., Lovell, H., Machiedo, M., Mills, S.C., Nye, K., Reinardy, B.T.I., Ross, F.H., Signer, M., 2013. Clast shape analysis and clast transport paths in glacial environments: A critical review of methods and the role of lithology. Earth-Sci. Rev. 121, 96–116.
Lukas, S., Preusser, F., Evans, D.J.A., Boston, C.M., Lovell, H., 2017. Chapter 2 – The Quaternary. In: Griffiths, J.S., Martin, C.J. (Eds.), Engineering Geology and Geomorphology of Glaciated and Periglaciated Terrains: Engineering Group Working Party Report. Engineering Geology Special Publication 28. The Geological Society, London, pp. 31–57.
Maclachlan, J.C., Eyles, C.H., 2013. Quantitative geomorphological analysis of drumlins in the Peterborough drumlin field, Ontario. Canada. Geogr. Ann. 95A, 125–144.
Mäkinen, J., Kajuutti, K., Palmu, J., Ojala, A., Ahokangas, E., 2017. Triangular-shaped landforms reveal subglacial drainage routes in SW Finland. Quat. Sci. Rev. 164, 37–53.
Małecki, J., Lovell, H., Ewertowski, W., Górski, Ł., Kurczba, T., Latos, B., Miara, M., Piniarska, D., Płocieniczak, J., Sowada, T., Spiralski, M., Warczachowska, A., Rabatel, A., 2018. The glacial landsystem of a tropical glacier: Charquini Sur, Bolivian Andes. Earth Surf. Proc. Land. https://doi.org/10.1002/esp.4417. in press.
Marc, O., Hovius, N., 2015. Amalgamation in landslide maps: effects and automatic detection. Nat. Hazards Earth Syst. Sci. 15, 723–733.
Margold, M., Jansson, K.N., 2011. Glacial geomorphology and glacial lakes of central Transbaikalia, Siberia. Russia. J. Maps 7, 18–30.
Margold, M., Jansson, K.N., Kleman, J., Stroeven, A.P., 2011. Glacial meltwater landforms of central British Columbia. J. Maps 7, 486–506.
Margold, M., Stokes, C.R., Clark, C.D., Kleman, J., 2015a. Ice streams in the Laurentide Ice Sheet: a new mapping inventory. J. Maps 11, 380–395.
Margold, M., Stokes, C.R., Clark, C.D., 2015b. Ice streams in the Laurentide Ice Sheet: Identification, characteristics and comparison to modern ice sheets. Earth-Sci. Rev. 143, 117–146.
Margold, M., Stokes, C.R., Clark, C.D., 2018. Reconciling records of ice streaming and ice margin retreat to produce a palaeogeographic reconstruction of the deglaciation of the Laurentide Ice Sheet. Quat. Sci. Rev. 189, 1–30.
Mather, A.E., Mills, S., Stokes, M., Fyfe, R., 2015. Ten years on: what can Google Earth offer the Geoscience community? Geology Today 31 (6), 216–221.
May, J.H., Zech, J., Zech, R., Preusser, F., Argollo, J., Kubik, P.W., Veit, H., 2011. Reconstruction of a complex late Quaternary glacial landscape in the Cordillera de Cochabamba (Bolivia) based on a morphostratigraphic and multiple dating approach. Quat. Res. 76 (1), 106–118.
McDougall, D.A., 2001. The geomorphological impact of Loch Lomond (Younger Dryas) Stadial plateau icefields in the central Lake District, northwest England. J. Quat. Sci. 16, 531–543.
McDougall, D.A., 2013. Glaciation style and the geomorphological record: evidence for Younger Dryas glaciers in the eastern Lake District, northwest England. Quat. Sci. Rev. 73, 48–58.
McHenry, M., Dunlop, P., 2016. The subglacial imprint of the last Newfoundland Ice Sheet. Canada. J. Maps 12 (3), 462–483.
Melander, O., 1975. Geomorfologiska kartbladet 29 I Kebnekaise. Statens naturvårdsverk. 78 pp., map scale 1:250,000.
Mertes, J.R., Gulley, J.D., Benn, D.I., Thompson, S.S., Nicholson, L.I., 2017. Using structure-from-motion to create glacier DEMs and orthoimagery from historical terrestrial and oblique aerial imagery. Earth Surf. Process. Land. 42, 2350–2364.
Midgley, N.G., Tonkin, T.N., 2017. Reconstruction of former glacier surface topography from archive oblique aerial images. Geomorphology 282, 18–26.
Midgley, N.G., Cook, S.J., Graham, D.J., Tonkin, T.N., 2013. Origin, evolution and dynamic context of a Neoglacial lateral–frontal moraine at Austre Lovénbreen, Svalbard. Geomorphology 198, 96–106.
Midgley, N.G., Tonkin, T.N., Graham, D.J., Cook, S.J., 2018. Evolution of high-Arctic glacial landforms during deglaciation. Geomorphology 311, 63–75.
Miller, H., Cotterill, C.J., Bradwell, T., 2014. Glacial and paraglacial history of the Troutbeck Valley, Cumbria, UK: integrating airborne LiDAR, multibeam bathymetry, and geological field mapping. Proc. Geol. Assoc. 125, 31–40.
Mills, S.C., Grab, S.W., Rea, B.R., Carr, S.J., Farrow, A., 2012. Shifting westerlies and precipitation patterns during the Late Pleistocene in southern Africa determined using glacier reconstruction and mass balance modelling. Quaternary Science Reviews 55, 145–159.
Mitchell, W.A., Riley, J.M., 2006. Drumlin map of the Western Pennines and southern Vale of Eden, Northern England. UK. J. Maps 2, 10–16.
Mollard, J.D., Janes, J.R., 1984. Airphoto Interpretation and the Canadian Landscape. Energy, Mines and Resources Canada, Ottawa.
Möller, P., Dowling, T.P.F., 2016. Streamlined subglacial bedforms on the Närke plain, south-central Sweden – Areal distribution, morphometrics, internal architecture and formation. Quat. Sci. Rev. 146, 182–215.
Möller, P., Dowling, T.P.F., 2018. Equifinality in glacial geomorphology: instability theory examined via ribbed moraine and drumlins in Sweden. GFF 140 (2), 106–135.
Morén, B., Heyman, J., Stroeven, A.P., 2011. Glacial geomorphology of the central Tibetan Plateau. J. Maps 7, 115–125.
Murray, A.B., Goldstein, E.B., Coco, G., 2014. The shape of patterns to come: from initial formation to long-term evolution. Earth Surf. Process. Land. 39, 62–70.
Napieralski, J., Hubbard, A., Li, Y.K., Harbor, J., Stroeven, A.P., Kleman, J., Alm, G., Jansson, K.N., 2007a. Towards a GIS assessment of numerical ice sheet model performance using geomorphological data. J. Glaciol. 53 (180), 71–83.
Napieralski, J., Harbor, J., Li, Y., 2007b. Glacial geomorphology and geographic information systems. Earth-Sci. Rev. 85, 1–22.
Näslund, J.O., Rodhe, L., Fastook, J.L., Holmlund, P., 2003. New ways of studying ice sheet flow directions and glacial erosion by computer modelling — examples from Fennoscandia. Quat. Sci. Rev. 22, 245–258.
Noh, M.J., Howat, I.M., 2015. Automated stereo-photogrammetric DEM generation at high latitudes: Surface Extraction from TIN-Based Search Minimization (SETSM) validation and demonstration over glaciated regions. GIScience Remote Sens. 52 (2), 198–217.
Norris, S.L., Margold, M., Froese, D.G., 2017. Glacial landforms of northwest Saskatchewan. J. Maps 13, 600–607.
Norris, S.L., Evans, D.J.A., Ó Cofaigh, C., 2018. Geomorphology and till architecture of terrestrial palaeo-ice streams of the southwest Laurentide Ice Sheet: A borehole stratigraphic approach. Quat. Sci. Rev. 186, 186–214.
Nuth, C., Kääb, A., 2011. Co-registration and bias corrections of satellite elevation data sets for quantifying glacier thickness change. The Cryosphere 5, 271–290.
Ó Cofaigh, C., 2012. Ice sheets viewed from the ocean: the contribution of marine science to understanding modern and past ice sheets. Phil. Trans. R. Soc. A 370 (1980), 5512–5539.
Ó Cofaigh, C., Evans, D.J.A., Smith, I.R., 2010. Large-scale reorganization and sedimentation of terrestrial ice streams during late Wisconsinan Laurentide Ice Sheet deglaciation. Geol. Soc. Am. Bull. 122, 743–756.
Ó Cofaigh, C., Dowdeswell, J.A., Jennings, A.E., Hogan, K.A., Kilfeather, A., Hiemstra, J.F., Noormets, R.M., Evans, J., McCarthy, D.J., Andrews, J.T., Lloyd, J.M., Moros, M., 2013. An extensive and dynamic ice sheet on the West Greenland shelf during the last glacial cycle. Geology 41 (2), 219–222.
Ojala, A.E.K., 2016. Appearance of De Geer moraines in southern and western Finland — Implications for reconstructing glacier retreat dynamics. Geomorphology 255, 16–25.
Ojala, A.E.K., Putkinen, N., Palmu, J.P., Nenonen, K., 2015. Characterization of De Geer moraines in Finland based on LiDAR DEM mapping. GFF 137 (4), 304–318.
Orkhonselenge, A., 2016. Glacial Geomorphology of Mt. Munkh Saridag in the Khuvsgul Mountain Range, Northern Mongolia. Géomorphologie: relief, processus, environnement 22 (4), 389–398.
Ottesen, D., Dowdeswell, J.A., 2006a. Assemblages of submarine landforms produced by tidewater glaciers in Svalbard. J. Geophys. Res. 111, F01016.
Ottesen, D., Dowdeswell, J.A., Rise, L., 2005. Submarine landforms and the reconstruction of fast-flowing ice streams within a large Quaternary ice sheet: the 2500 km long Norwegian-Svalbard margin (57 degrees – 80 degrees N). Geol. Soc. Am. Bull. 117 (7–8), 1033–1050.
Ottesen, D., Stokes, C.R., Rise, L., Olsen, L., 2008a. Ice-sheet dynamics and ice streaming along the coastal parts of northern Norway. Quat. Sci. Rev. 27, 922–940.
Ottesen, D., Dowdeswell, J.A., Benn, D.I., Kristensen, L., Christiansen, H.H., Christensen, O., Hansen, L., Lebesbye, E., Forwick, M., Vorren, T.O., 2008b. Submarine landforms characteristic of glacier surges in two Spitsbergen fjords. Quat. Sci. Rev. 27, 1583–1599.
Ottesen, D., Stokes, C.R., Bøe, R., Rise, L., Longva, O., Thorsnes, T., Olesen, O., Bugge, T., Lepland, A., Hestvik, O.B., 2016. Landform assemblages and sedimentary processes along the Norwegian Channel Ice Stream. Sediment. Geol. 338, 115–137.
Ottesen, D., Dowdeswell, J.A., Bellec, V.K., Bjarnadóttir, L.R., 2017. The geomorphic imprint of glacier surges into open-marine waters: Examples from eastern Svalbard. Mar. Geol. 392, 1–29.
Otto, J.-C., Smith, M.J., 2013. Section 2.6: Geomorphological mapping. In: Clarke, L. (Ed.), Geomorphological Techniques (Online Edition). British Society for Geomorphology, London ISSN: 2047-0371.
Owen, L.A., Finkel, R.C., Barnard, P.L., Haizhou, M., Asahi, K., Caffee, M.W., Derbyshire, E., 2005. Climatic and topographic controls on the style and timing of Late Quaternary glaciation throughout Tibet and the Himalaya defined by 10Be cosmogenic radionuclide surface exposure dating. Quat. Sci. Rev. 24 (12), 1391–1411.
Paron, P., Claessens, L., 2011. Makers and Users of Geomorphological Maps. In: Smith, M.J., Paron, P., Griffiths, J.S. (Eds.), Geomorphological Mapping: Methods and applications. Developments in Earth Surface Processes Vol. 15. Elsevier, Oxford, pp. 75–106.
Partsch, J., 1894. Die Vergletscherung des Riesengebirges zur Eiszeit. Forschungen zur Deutschen Landes- und Volkskunde VIII/2. pp. 103–194.
Patton, H., Hubbard, A., Andreassen, K., Auriac, A., Whitehouse, P.L., Stroeven, A.P., Shackleton, C., Winsborrow, M., Heyman, J., Hall, A.M., 2017a. Deglaciation of the Eurasian ice sheet complex. Quat. Sci. Rev. 169, 148–172.
Patton, H., Hubbard, A., Bradwell, T., Schomacker, A., 2017b. The configuration, sensitivity and rapid retreat of the Late Weichselian Icelandic ice sheet. Earth-Sci. Rev. 166, 223–245.
Pearce, D., Rea, B.R., Bradwell, T., McDougall, D., 2014. Glacial geomorphology of the Tweedsmuir Hills, Central Southern Uplands. Scotland. J. Maps 10 (3), 457–465.
Pearce, D.M., Mair, D.W.F., Rea, B.R., Lea, J.M., Schofield, J.E., Kamenos, N., Schoenrock, K., 2018. The glacial geomorphology of upper Godthåbsfjord (Nuup Kangerlua) in southwest Greenland. J. Maps 14, 45–55.
Penck, A., Brückner, E., 1901/1909. Die Alpen im Eiszeitalter. Tauchnitz, Leipzig.
Peterson, G., Johnson, M.D., Smith, C.A., 2017. Glacial geomorphology of the south Swedish uplands – focus on the spatial distribution of hummock tracts. J. Maps 13, 534–544.
Petrie, G., Price, R.J., 1966. Photogrammetric measurements of the ice wastage and morphological changes near the Casement Glacier. Alaska. Can. J. Earth Sci. 3, 827–840.
Phillips, E., Evans, D.J.A., Atkinson, N., Kendall, A., 2017. Structural architecture and glacitectonic evolution of the Mud Buttes cupola hill complex, southern Alberta. Canada. Quat. Sci. Rev. 164, 110–139.
Pike, R.J., 1988. The geometric signature: quantifying landslide-terrain types from digital elevation models. Math. Geol. 20, 491–511.
Pipaud, I., Loibl, D., Lehmkuhl, F., 2015. Evaluation of TanDEM-X elevation data for geomorphological mapping and interpretation in high mountain environments — A case study from SE Tibet, China. Geomorphology 246, 232–254.
Popper, K.R., 1972. Objective Knowledge. Oxford University Press, Oxford.

Prest, V.K., 1983. Canada's Heritage of Glacial Features. GSC Miscellaneous Report 28.
Prest, V.K., Grant, D.R., Rampton, V.N., 1968. Glacial map of Canada. Geological Survey of Canada, Map 1253A.
Priamonosov, A.P., Kuznetsova, E.J., Abaturova, I.V., 2000. National geological map of the Russian Federation, Map of Quaternary Formations, Polar-Ural series, map sheet Q-41-XII Kharp. 1. Ministry of Natural Resources of the Russian Federation, pp. 200000.
Price, R.J., 1961. The Deglaciation of the Upper Tweed Basin. Unpublished PhD thesis. University of Edinburgh.
Price, R.J., 1963. A glacial meltwater drainage system in Peebleshire. Scotland. Scott. Geogr. Mag. 79, 133–141.
Price, R.J., 1966. Eskers near the Casement Glacier. Alaska. Geogr. Ann. 48, 111–125.
Price, R.J., 1970. Moraines at Fjallsjökull. Iceland. Arctic Alp. Res. 2, 27–42.
Principato, S.M., Moyer, A.N., Hampsch, A.G., Ipsen, H.A., 2016. Using GIS and streamlined landforms to interpret palaeo-ice flow in northern Iceland. Boreas 45, 470–482.
Punkari, M., 1980. The ice lobes of the Scandinavian ice sheet during the deglaciation in Finland. Boreas 9 (4), 307–310.
Punkari, M., 1995. Glacial flow systems in the zone of confluence between the Scandinavian and Novaja Zemlya Ice Sheets. Quat. Sci. Rev. 14 (6), 589–603.
Putniņš, A., Henriksen, M., 2017. Reconstructing the flow pattern evolution in inner region of the Fennoscandian Ice Sheet by glacial landforms from Gausdal Vestfjell area, south-central Norway. Quat. Sci. Rev. 163, 56–71.
Rabus, B., Eineder, M., Roth, A., Bamler, R., 2003. The shuttle radar topography mission—a new class of digital elevation models acquired by spaceborne radar. ISPRS J. Photogramm. Remote Sens. 57 (4), 241–262.
Rączkowska, Z., Zwoliński, Z., 2015. Digital geomorphological map of Poland. Geogr. Pol. 88 (2), 205–210.
Raistrick, A., 1933. The glacial and post-glacial periods in West Yorkshire. Proc. Geol. Assoc. 44, 263–269.
Raisz, E.J., 1962. Principles of cartography. McGraw-Hill, New York 315 pp.
Rea, B.R., Whalley, W.B., Dixon, T.S., Gordon, J.E., 1999. Plateau icefields as contributing areas to valley glaciers and the potential impact on reconstructed ELAs: a case study from the Lyngen Alps, North Norway. Ann. Glaciol. 28, 97–102.
Reinardy, B.T.I., Leighton, I., Marx, P.J., 2013. Glacier thermal regime linked to processes of annual moraine formation at Midtdalsbreen, southern Norway. Boreas 42 (4), 896–911.
Reuther, A.U., Urdea, P., Geiger, C., Ivy-Ochs, S., Niller, H.P., Kubik, P.W., Heine, K., 2007. Late Pleistocene glacial chronology of the Pietrele Valley, Retezat Mountains, Southern Carpathians constrained by 10Be exposure ages and pedological investigations. Quat. Int. 164, 151–169.
Rippin, D.M., Pomfret, A., King, N., 2015. High resolution mapping of supra-glacial drainage pathways reveals link between microchannel drainage density, surface roughness and surface reflectance. Earth Surf. Proc. Land. 40 (10), 1279–1290.
Robb, C., Willis, I., Arnold, N., Guðmundsson, S., 2015. A semi-automated method for mapping glacial geomorphology tested at Breiðamerkurjökull. Iceland. Remote Sens. Environ. 163, 80–90.
Robinson, P., Dowdeswell, J.A., 2011. Submarine landforms and the behavior of a surging ice cap since the last glacial maximum: The open-marine setting of eastern Austfonna. Svalbard. Mar. Geol. 286 (1), 82–94.
Robinson, A.H., Morrison, J.L., Muehrcke, P.C., Kimerling, A.J., Guptill, S.C., 1995. Elements of cartography, 6th Edition. Wiley & Sons, Chichester 674 pp.
Rose, J., Smith, M.J., 2008. Glacial geomorphological maps of the Glasgow region, western central Scotland. J. Maps 4, 399–416.
Rupke, J., De Jong, M.G.G., 1983. Slope collapse destroying ice-marginal topography in the Walgau (Vorarlberg, Austria)- an example of the application of a 1:10000 geomorphological mapping system. Mater. Physiogeogr. 5, 33–41.
Ryan, J.C., Hubbard, A.L., Todd, J., Carr, J.R., Box, J.E., Christoffersen, P., Holt, T.O., Snooke, N., 2015. Repeat UAV photogrammetry to assess calving front dynamics at a large outlet glacier draining the Greenland Ice Sheet. The Cryosphere 9, 1–11.
Sagredo, E.A., Moreno, P.I., Villa-Martínez, R., Kaplan, M.R., Kubik, P.W., Stern, C.R., 2011. Fluctuations of the Última Esperanza ice lobe (52 S), Chilean Patagonia, during the last glacial maximum and termination 1. Geomorphology 125 (1), 92–108.
Saha, K., Wells, N.A., Munro-Stasiuk, M., 2011. An object-oriented approach to automated landform mapping: A case study of drumlins. Computers & Geosciences 37 (9), 1324–1336.
Sahlin, E.A.U., Glasser, N.F., 2008. A geomorphological map of Cadair Idris. Wales. J. Maps 4, 299–314.
Salcher, B.C., Hinsch, R., Wagreich, M., 2010. High-resolution mapping of glacial landforms in the North Alpine Foreland, Austria. Geomorphology 122, 283–293.
Schoeneich, P., 1993. Cartographie géomorphologique en Suisse, Institut de Géogrphie Lausanne. Travaux et recherches, Lausanne, pp. 1–13.
Schomacker, A., 2008. What controls dead-ice melting under different climate conditions? A discussion. Earth-Sci. Rev. 90, 103–113.
Schomacker, A., Kjaer, K.H., 2008. Quantification of dead-ice melting in ice-cored moraines at the high-Arctic glacier Holmströmbreen, Svalbard. Boreas 37, 211–225.
Schomacker, A., Benediktsson, Í.Ö., Ingólfsson, Ó., 2014. The Eyjabakkajökull glacial landsystem, Iceland: Geomorphic impact of multiple surges. Geomorphology 218, 98–107.
Seguinot, J., Rogozhina, I., Stroeven, A.P., Margold, M., Kleman, J., 2016. Numerical simulations of the Cordilleran ice sheet through the last glacial cycle. The Cryosphere 10, 639–664.
Shean, D.E., Alexandrov, O., Moratto, Z.M., Smith, B.E., Joughin, I.R., Porter, C., Morin, P., 2016. An automated, open-source pipeline for mass production of digital elevation models (DEMs) from very-high-resolution commercial stereo satellite imagery. ISPRS J. Photogramm. Remote Sens. 116, 101–117.
Sissons, J.B., 1967. The Evolution of Scotland's Scenery. Oliver & Boyd, Edinburgh 259 pp.
Sissons, J.B., 1977a. The Loch Lomond Readvance in the northern mainland of Scotland. In: Gray, J.M., Lowe, J.J. (Eds.), Studies in the Scottish Lateglacial Environment. Permagon Press, Oxford, pp. 45–60.
Sissons, J.B., 1977b. The Loch Lomond Readvance in southern Skye and some palaeoclimatic implications. Scott. J. Geol. 13, 23–36.
Sissons, J.B., 1979a. The limit of the Loch Lomond Advance in Glen Roy and vicinity. Scott. J. Geol. 15, 31–42.
Sissons, J.B., 1979b. The Loch Lomond advance in the Cairngorm Mountains. Scott. Geogr. Mag. 95, 66–82.
Smith, A.M., Murray, T., 2009. Bedform topography and basal conditions beneath a fast-flowing West Antarctic ice stream. Quat. Sci. Rev. 28 (7), 584–596.
Smith, G.R., Woodward, J.C., Heywood, D.I., Gibbard, P.L., 2000. Interpreting Pleistocene glacial features from SPOT HRV data using fuzzy techniques. Computers & Geosciences 26 (4), 479–490.
Smith, A.M., Murray, T., Nicholls, K.W., Makinson, K., Aðalgeirsdóttir, G., Behar, A.E., Vaughan, D.G., 2007. Rapid erosion, drumlin formation, and changing hydrology beneath an Antarctic ice stream. Geology 35 (2), 127–130.
Smith, M.J., Clark, C.D., 2005. Methods and visualisation of digital elevation models for landform mapping. Earth Surf. Process. Land. 30, 885–900.
Smith, M.J., Knight, J., 2011. Palaeoglaciology of the last Irish ice sheet reconstructed from striae evidence. Quat. Sci. Rev. 30 (1-2), 147–160.
Smith, M.J., Wise, S.M., 2007. Problems of bias in mapping linear landforms from satellite imagery. Int. J. Appl. Earth Obs. Geoinform. 9 (1), 65–78.
Smith, M.J., Rose, J., Booth, S., 2006. Geomorphological mapping of glacial landforms from remotely sensed data: An evaluation of the principal data sources and an assessment of their quality. Geomorphology 76, 148–165.
Smith, M.J., Griffiths, J., Paron, P. (Eds.), 2011. Geomorphological Mapping: Methods and Applications. Developments in Earth Surface Processes, Volume 15 Elsevier, Oxford 610 pp.
Smith, M.W., Carrivick, J.L., Quincey, D.J., 2016a. Structure from motion photogrammetry in physical geography. Prog. Phys. Geogr. 40 (2), 247–275.
Smith, M.J., Anders, N.S., Keesstra, S.D., 2016b. CLustre: semi-automated lineament clustering for palaeo-glacial reconstruction. Earth Surf. Process. Land. 41 (3), 364–377.
Sollas, W.J., 1896. A map to show the distribution of eskers in Ireland. The Sci. Trans. R. Dublin Soc. 5, 785–822.
Sollid, J.L., Andersen, S., Hamre, N., Kjeldsen, O., Salvigsen, O., Sturød, S., Tveitå, T., Wilhemsen, A., 1973. Deglaciation of Finnmark. North Norway. Norsk Geogr. Tidsskr. 27 (4), 233–325.
Spagnolo, M., Clark, C.D., Hughes, A.L.C., Dunlop, P., Stokes, C.R., 2010. The planar shape of drumlins. Sediment. Geol. 232, 119–129.
Spagnolo, M., Clark, C.D., Ely, J.C., Stokes, C.R., Anderson, J.B., Andreassen, K., Graham, A.G.C., King, E.C., 2014. Size, shape and spatial arrangement of megascale glacial lineations from a large and diverse dataset. Earth Surf. Process. Land. 39, 1432–1448.
Spagnolo, M., Phillips, E., Piotrowski, J.A., Rea, B.R., Clark, C.D., Stokes, C.R., Carr, S.J., Ely, J.C., Ribolini, A., Wysota, W., Szuman, I., 2016. Ice stream motion facilitated by a shallow-deforming and accreting bed. Nat. Commun. 7, 10723.
Spagnolo, M., Bartholomaus, T.C., Clark, C.D., Stokes, C.R., Atkinson, N., Dowdeswell, J.A., Ely, J.C., Graham, A.G.C., Hogan, K.A., King, E.C., Larter, R.D., Livingstone, S.J., Pritchard, H.D., 2017. The periodic topography of ice stream beds: Insights from the Fourier spectra of mega-scale glacial lineations. J. Geophys. Res.: Earth Surf. 122, 1355–1373.
Stansell, N.D., Polissar, P.J., Abbott, M.B., 2007. Last glacial maximum equilibrium-line altitude and paleo-temperature reconstructions for the Cordillera de Mérida, Venezuelan Andes. Quat. Res. 67, 115–127.
Stokes, C.R., 2002. Identification and mapping of palaeo-ice stream geomorphology from satellite imagery: implications for ice stream functioning and ice sheet dynamics. Int. J. Remote Sens. 23 (8), 1557–1563.
Stokes, C.R., 2018. Geomorphology under ice streams: moving from form to process. Earth Surf. Process. Land. 43, 85–123.
Stokes, C.R., Clark, C.D., 1999. Geomorphological criteria for identifying Pleistocene ice streams. Ann. Glaciol. 28 (1), 67–74.
Stokes, C.R., Clark, C.D., 2001. Palaeo-ice streams. Quat. Sci. Rev. 20 (13), 1437–1457.
Stokes, C.R., Clark, C.D., 2002. Are long subglacial bedforms indicative of fast ice flow? Boreas 31 (3), 239–249.
Stokes, C.R., Clark, C.D., 2003. The Dubawnt Lake palaeo-ice stream: evidence for dynamic ice sheet behaviour on the Canadian Shield and insights regarding the controls on ice-stream location and vigour. Boreas 32, 263–279.
Stokes, C.R., Tarasov, L., 2010. Ice streaming in the Laurentide Ice Sheet: A first comparison between data-calibrated numerical model output and geological evidence. Geophys. Res. Lett. 37, L01501.
Stokes, C.R., Clark, C.D., Storrar, R., 2009. Major changes in ice stream dynamics during deglaciation of the north-western margin of the Laurentide Ice Sheet. Quat. Sci. Rev. 28, 721–738.
Stokes, C.R., Spagnolo, M., Clark, C.D., Ó Cofaigh, C., Lian, O.B., Dunstone, R.B., 2013. Formation of mega-scale glacial lineations on the Dubawnt Lake Ice Stream bed: 1. size, shape and spacing from a large remote sensing dataset. Quat. Sci. Rev. 77, 190–209.
Stokes, C.R., Corner, G.D., Winsborrow, M.C.M., Husum, K., Andreassen, K., 2014. Asynchronous response of marine-terminating outlet glaciers during deglaciation of the Fennoscandian Ice Sheet. Geology 42, 455–458.
Stokes, C.R., Tarasov, L., Blomdin, R., Cronin, T.M., Fisher, T.G., Gyllencreutz, R., Hättestrand, C., Heyman, J., Hindmarsh, R.C.A., Hughes, A.L.C., Jakobsson, M., Kirchner, N., Livingstone, S.J., Margold, M., Murton, J.B., Noormets, R., Peltier, W.R.,

Peteet, D.M., Piper, D.J.W., Preusser, F., Renssen, H., Roberts, D.H., Roche, D.M., Saint-Ange, F., Stroeven, A.P., Teller, J.T., 2015. On the reconstruction of palaeo-ice sheets: Recent advances and future challenges. Quat. Sci. Rev. 125, 15–49.
Stokes, C.R., Margold, M., Creyts, T.T., 2016a. Ribbed bedforms on palaeo-ice stream beds resemble regular patterns of basal shear stress ('traction ribs') inferred from modern ice streams. J. Glaciol. 62, 696–713.
Stokes, C.R., Margold, M., Clark, C.D., Tarasov, L., 2016b. Ice stream activity scaled to ice sheet volume during Laurentide Ice Sheet deglaciation. Nature 530 (7590), 322–326.
Storrar, R.D., Livingstone, S.J., 2017. Glacial geomorphology of the northern Kivalliq region, Nunavut, Canada, with an emphasis on meltwater drainage systems. J. Maps 13, 153–164.
Storrar, R., Stokes, C.R., 2007. A Glacial geomorphological map of Victoria Island. Canadian Arctic. J. Maps 3, 191–210.
Storrar, R.D., Stokes, C.R., Evans, D.J.A., 2013. A map of large Canadian eskers from Landsat satellite imagery. J. Maps 9, 456–473.
Storrar, R.D., Stokes, C.R., Evans, D.J.A., 2014. Morphometry and pattern of a large sample (> 20,000) of Canadian eskers and implications for subglacial drainage beneath ice sheets. Quat. Sci. Rev. 105, 1–25.
Storrar, R.D., Jones, A., Evans, D.J.A., 2017. Small-scale topographically-controlled glacier flow switching in an expanding proglacial lake at Breiðamerkurjökull. SE Iceland. J. Glaciol. 63 (240), 745–750.
Streuff, K., Forwick, M., Szczuciński, W., Andreassen, K., Ó Cofaigh, C., 2015. Submarine landform assemblages and sedimentary processes related to glacier surging in Kongsfjorden. Svalbard 1 (1), 14 αrktos.
Stroeven, A.P., Fabel, D., Harbor, J., Hättestrand, C., Kleman, J., 2002a. Quantifying the erosional impact of the Fennoscandian ice sheet in the Torneträsk-Narvik corridor, northern Sweden, based on cosmogenic radionuclide data. Geogr. Ann. 84A, 275–287.
Stroeven, A.P., Fabel, D., Hättestrand, C., Harbor, J., 2002b. A relict landscape in the centre of Fennoscandian glaciation: Cosmogenic radionuclide evidence of tors preserved through multiple glacial cycles. Geomorphology 44, 145–154.
Stroeven, A.P., Harbor, J., Fabel, D., Kleman, J., Hättestrand, C., Elmore, D., Fink, D., Fredin, O., 2006. Slow, patchy landscape evolution in northern Sweden despite repeated ice-sheet glaciation. GSA Special Paper 398, 387–396.
Stroeven, A.P., Fabel, D., Harbor, J.M., Fink, D., Caffee, M.W., Dahlgren, T., 2011. Importance of sampling across an assemblage of glacial landforms for interpreting cosmogenic ages of deglaciation. Quat. Res. 76, 148–156.
Stroeven, A.P., Hättestrand, C., Heyman, J., Kleman, J., Morén, B.M., 2013. Glacial geomorphology of the Tian Shan. J. Maps 9 (4), 505–512.
Stroeven, A.P., Fabel, D., Margold, M., Clague, J.J., Xu, S., 2014. Investigating absolute chronologies of glacial advances in the NW sector of the Cordilleran Ice Sheet with terrestrial in situ cosmogenic nuclides. Quat. Sci. Rev. 92, 429–443.
Stroeven, A.P., Hättestrand, C., Kleman, J., Heyman, J., Fabel, D., Fredin, O., Goodfellow, B.W., Harbor, J.M., Jansen, J.D., Olsen, L., Caffee, M.W., Fink, D., Lundqvist, J., Rosqvist, G.C., Strömberg, B., Jansson, K.N., 2016. Deglaciation of Fennoscandia. Quat. Sci. Rev. 147, 91–121.
Sugden, D.E., 1970. Landforms of Deglaciation in the Cairngorm Mountains. Scotland. Trans. Inst. Br. Geogr. 51, 201–219.
Sugden, D.E., 1978. Glacial erosion by the Laurentide Ice Sheet. J. Glaciol. 20, 367–391.
Sugden, D.E., John, B.S., 1976. Glaciers and Landscape. Arnold, London 376 pp.
Thorp, P.W., 1986. A mountain icefield of Loch Lomond Stadial age, western Grampians, Scotland. Boreas 15, 83–97.
Tonkin, T.N., Midgley, N.G., Cook, S.J., Graham, D.J., 2016. Ice-cored moraine degradation mapped and quantified using an unmanned aerial vehicle: A case study from a polythermal glacier in Svalbard. Geomorphology 258, 1–10.
Trommelen, M.S., Ross, M., 2010. Subglacial landforms in northern Manitoba, Canada, based on remote sensing data. J. Maps 2010, 618–638.
Trommelen, M.S., Ross, M., 2014. Distribution and type of sticky spots at the centre of a deglacial streamlined lobe in northeastern Manitoba, Canada. Boreas 43, 557–576.
Trotter, F.M., 1929. The glaciation of the eastern Edenside, the Alston Block and the Carlisle Plain. Quart. J. Geol. Soc. Lond. 88, 549–607.
Turner, A.J., Woodward, J., Stokes, C.R., Ó Cofaigh, C., Dunning, S., 2014a. Glacial geomorphology of the Great Glen Region of Scotland. J. Maps 10, 159–178.
Turner, D., Lucieer, A., Wallace, L., 2014b. Direct georeferencing of ultrahigh-resolution UAV imagery. IEEE Trans. Geosci. Remote Sens. 52 (5), 2738–2745.
van der Bilt, W.G.M., Bakke, J., Balascio, N.L., 2016. Mapping sediment–landform assemblages to constrain lacustrine sedimentation in a glacier-fed lake catchment in northwest Spitsbergen. J. Maps 12 (5), 985–993.
Van Dorsser, J.J., Salomé, A.I., 1973. Different methods of detailed geomorphological mapping. In: K.N.A.G. Geografisch Tijdschrift VII, pp. 71–74.
Walker, D.A., Auerbach, N.A., Shippert, M.M., 1995. NDVI, biomass, and landscape evolution of glaciated terrain in northern Alaska. Polar Record 31 (177), 169–178.
Welch, R., 1966. A comparison of aerial films in the study of the Breiðamerkur glacier area, Iceland, The Photogramm. Rec. 5, 289–306.
Welch, R., 1967. The Application of Aerial Photography to the Study of a Glacial Area. University of Glasgow, Breiðamerkur, Iceland Unpublished PhD thesis.
Welch, R., 1968. Color aerial photography applied to the study of a glacial area. In: Smith, J.T. (Ed.), Manual of Color Aerial Photography. American Society of Photogrammetry and Remote Sensing, Falls Church, VA, pp. 400–401.
Westoby, M.J., Brasington, J., Glasser, N.F., Hambrey, M.J., Reynolds, J.M., 2012. 'Structure-from-Motion' photogrammetry: A low-cost, effective tool for geoscience applications. Geomorphology 179, 300–314.
Westoby, M.J., Glasser, N.F., Hambrey, M.J., Brasington, J., Reynolds, J.M., Hassan, M.A., 2014. Reconstructing historic Glacial Lake Outburst Floods through numerical modelling and geomorphological assessment: Extreme events in the Himalaya. Earth Surf. Process. Land. 39 (12), 1675–1692.
Westoby, M.J., Dunning, S.A., Woodward, J., Hein, A.S., Marrero, S.M., Winter, K., Sugden, D.E., 2016. Interannual surface evolution of an Antarctic blue-ice moraine using multi-temporal DEMs. Earth Surf. Dyn. 4, 515–529.
Wilson, S.B., 2005. Morphological analysis and mapping of Loch Lomond Stadial moraines using digital photogrammetry and geographical information systems. Unpublished PhD thesis. University of Glasgow 360 pp.
Winkler, S., 2018. Investigating Holocene mountain glaciations: a plea for the supremacy of glacial geomorphology when reconstructing glacier chronologies. Erdkunde in press.
Winsborrow, M.C.M., Andreassen, K., Corner, G.D., Laberg, J.S., 2010. Deglaciation of a marine-based ice sheet: Late Weichselian palaeo-ice dynamics and retreat in the southern Barents Sea reconstructed from onshore and offshore glacial geomorphology. Quat. Sci. Rev. 29 (3–4), 424–442.
Winsborrow, M.C.M., Stokes, C.R., Andreassen, K., 2012. Ice stream flow switching during deglaciation of the southwestern Barents Sea. Geol. Soc. Am. Bull. 124 (3–4), 275–290.
Wolf, P.R., DeWitt, B.A., Wilkinson, B.E., 2013. Elements of Photogrammetry with Application in GIS, Fourth Edition. McGraw-Hill Education.
Wright, W.B., 1912. The drumlin topography of south Donegal. Geol. Mag. 9, 153–159.
Wyshnytzky, C.E., 2017. On the mechanisms of minor moraine formation in high-mountain environments of the European Alps. Unpublished PhD thesis. Queen Mary University of London 329 pp.
Yu, P., Eyles, N., Sookhan, S., 2015. Automated drumlin shape and volume estimation using high resolution LiDAR imagery (Curvature Based Relief Separation): A test from the Wadena Drumlin Field, Minnesota. Geomorphology 246, 589–601.
Zasadni, J., Kłapyta, P., 2016. From valley to marginal glaciation in alpine-type relief: Lateglacial glacier advances in the Pięć Stawów Polskich/Roztoka Valley, High Tatra Mountains, Poland. Geomorphology 253, 406–424.
Zech, R., Abramowski, U., Glaser, B., Sosin, P., Kubik, P.W., Zech, W., 2005. Late Quaternary glacial and climate history of the Pamir Mountains derived from cosmogenic 10Be exposure ages. Quat. Res. 64 (2), 212–220.
Zemp, M., Frey, H., Gärtner-Roer, I., Nussbaumer, S.U., Hoelzle, M., Paul, F., Haeberli, W., Denzinger, F., Ahlstrøm, A.P., Anderson, B., Bajracharya, S., Baroni, C., Braun, L.N., Cáceres, B.E., Casassa, G., Cobos, G., Dávila, L.R., Delgado Granados, H., Demuth, M.N., Espizua, L., Fischer, A., Fujita, K., Gadek, B., Ghazanfar, A., Hagen, J.O., Holmlund, P., Karimi, N., Li, Z., Pelto, M., Pitte, P., Popovnin, V.V., Portocarrero, C.A., Prinz, R., Sangewar, C.V., Severskiy, I., Sigurðsson, O., Soruco, A., Usubaliev, R., Vincent, C., 2015. Historically unprecedented global glacier decline in the early 21st century. J. Glaciology 61, 745–762.